# MICRORNA DYSREGULATION FOLLOWING SPINAL CORD CONTUSION: IMPLICATIONS FOR NEURAL PLASTICY AND NEUROPATHIC PAIN

A Dissertation

by

ERIC ROSS STRICKLAND

Submitted to the Office of Graduate Studies of
Texas A&M University
in partial fulfillment of the requirements for the degree of

DOCTOR OF PHILOSOPHY

| | |
|---|---|
| Co-Chair of Committee, | Rajesh Miranda |
| Co-Chair of Committee, | James Grau |
| Committee Members, | Michelle Hook |
| | Mark Zoran |
| Intercollegiate Faculty Chair, | Craig Coates |

August 2013

Major Subject: Genetics

# ABSTRACT

Spinal cord injury (SCI) results in a number of devastating consequences, including loss of motor function, paralysis, and neuropathic pain. Concomitant peripheral tissue injury below the lesion site can result in uncontrollable nociception that sensitizes spinal neurons and promotes chronic pain. Additionally, drugs like morphine, though critical for pain management, elicit pro-inflammatory effects that exacerbate chronic pain symptoms. Currently, there is a lack of effective therapeutic mechanisms to promote regeneration at the lesion site, and a limited understanding of regulatory mechanisms that can be utilized to therapeutically manipulate spinal cord plasticity. MicroRNAs (miRNAs) constitute novel targets for therapeutic intervention to both promote repair and regeneration, and mitigate maladaptive plasticity that leads to neuropathic pain.

Microarray and qRT-PCR comparisons of contused and sham rat spinal cords at 4 and 14 days following SCI indicated that a total of 35 miRNAs were dysregulated, with miR1, miR124, and miR129 exhibiting significant down-regulation after SCI, and both miR21 and miR146a being transiently induced. Localized expression of miRNAs and cellular markers indicated that changes in miRNA regulation favor the emergence of neural stem cell niches and reversion of surviving neurons to a pre-neuronal phenotype. Additionally, both uncontrollable nociception and morphine administration resulted in further dysregulation of SCI-sensitive miRNAs, along with their mRNA targets. Morphine administration significantly induced expression of both miR21 and IL6R expression, indicating that morphine-induced miRNA dysregulation is involved in the

promotion of neuroinflammation that drives increased pain-sensitivity. Similarly, uncontrollable nociception significantly modulates expression of miR124, miR129, and miR146a, which inhibit cell cycle proteins and microglial activation, and dysregulation of these miRNAs, along with BDNF and IGF-1, likely contributes towards promotion of hypersensitivity in spinal neurons that underlies neuropathic pain. Consequently, SCI-sensitive miRNAs may constitute therapeutic targets for modulation of neuroinflammation and microglial activation in order to mitigate secondary injury, promote regeneration, and prevent maladaptive plasticity that drives neuropathic pain and exacerbation of chronic pain symptoms by morphine administration.

ACKNOWLEDGEMENTS

I would like to thank Dr. Rajesh Miranda for his continual patience and mentorship throughout the course of this research, and Dr. James Grau, Dr. Michelle Hook, and Dr. Mark Zoran for their consistent and valued guidance as members of my committee. I would also like to thank members of the Miranda, Grau, and Hook labs that were instrumental in my success. The support and friendship of Sridevi Balaraman, Rhonda Holgate, Benum Minavi, Jeremy Rawlings, Joseph Tingling, Pa-Chi Tsai, Sandra Galloway, Russell Huie, and Sarah Woller is greatly appreciated. Finally, thanks to my family for their endless support and encouragement: Mom, Dad, and Ryan.

TABLE OF CONTENTS

Page

Page

LIST OF FIGURES

LIST OF TABLES

Page

# 1. INTRODUCTION

## 1.1 Epidemiology and Pathophysiology of Central Nervous System Injury

The central nervous system (CNS) is highly vulnerable to injury, which can result in substantial cognitive and behavioral impairment. Acute insult to the brain, such as traumatic brain injury (TBI) and ischemic stroke, is one of the most common causes of disability and death in adults (Sosin et al., 1996; Ghajar, 2000; Langlois et al., 2006; Donnan et al., 2008; Feigin et al., 2010). In contrast, although it is a fairly uncommon cause of disability at an estimated 40 cases per million, spinal cord injury (SCI) commands a high socioeconomic cost out of proportion to its frequency (DeVivo, 1997; Jackson et al., 2004; Boswell et al., 2013). Stroke is responsible for 10-12% of all deaths in western countries and projected to be the fourth most common cause of disability-adjusted life-years (DALYs; the sum of life-years lost as a result of premature death and years lived with disability adjusted for severity) by 2030, but the vast majority of deaths occur in the elderly population with only 12% of stroke related deaths occurring in people less than 65 years of age (Bonita, 1992; Lopez et al., 2006; Donnan et al., 2008; Feigin et al., 2010). To the contrary, both TBI and SCI occur mostly in younger people, with the peak incidence of TBI between 15 and 24 years of age and the average age at injury for SCI patients ranging between 30 and 40 (Ghajar, 2000; Jackson et al., 2004; Feigin et al., 2010; Boswell et al., 2013). Whereas stroke prevalence is mostly tied to risk factors such as hypertension, diabetes, and smoking (Donnan et al., 2008; Feigin et al., 2010), the leading causes for TBI and SCI are motor vehicle

accidents, falls, and acts of violence (Ghajar, 2000; Jackson et al., 2004; Feigin et al., 2010; Cripps et al., 2011; Boswell et al., 2013). Moreover, injury results in the largest number of disability-adjusted life years lost, and as TBI and SCI tend to occur at a young age, the financial burden can be overwhelming (Murray and Lopez, 1997; Ghajar, 2000; Boswell et al., 2013). In particular, SCI can be financially crippling, as high quadriplegia sustained at age 50 can have lifetime expenses up to $2.4 million, whereas the same injury sustained at age 25 can cost an estimated $4.3 million (Boswell et al., 2013). As SCI shares many pathophysiological characteristics with stroke and TBI, cross-analyses of the mechanisms of injury progression and their impact on functional recovery can grant insight into possibilities for new therapeutic strategies to improve the quality of life following spinal cord trauma and significantly reduce its socioeconomic impact.

As an immune privileged organ, the central nervous system regulates influx of immune cells and mediators, such as T and B lymphocytes, from the vasculature through strict maintenance and modulation of the blood-brain barrier and blood-spinal cord barrier, but acute CNS injury disrupts proper blood-brain and blood-spinal cord barrier regulation triggering an inflammatory response (Perry, 1998; Jordan et al., 2008; Kaur and Ling, 2008; Pan and Kastin, 2008; Sandoval and Witt, 2008; Ankeny and Popovich, 2009; Schoknecht and Shalev, 2012). While inflammation is typically beneficial for an organism in response to injury or the presence of pathogens, prolonged inflammation in the CNS following injury can have detrimental effects that drive secondary injury, leading to additional neurodegeneration and substantially worse functional outcomes

(Jordan et al., 2008; Benowitz and Popovich, 2011; Smith, 2013). Brain and spinal cord inflammation consists of multiple components, including activation of microglia and astrocytes (Gomes-Leal et al., 2004; Lai and Todd, 2006; Jordan et al., 2008; Karimi-Abdolrezaee and Billakanti, 2012; Smith, 2013), formation of cytotoxic reactive oxygen species (ROS; Bains and Hall, 2012; Kahles and Brandes, 2012), and up-regulation of key inflammatory mediators such as cytokines and chemokines (Ghirnikar et al., 1998; Segal, 2005; Lai and Todd, 2006; Pan and Kastin, 2008; Das et al., 2012; Lambertsen et al., 2012; Smith et al., 2012), which allows infiltration of immune cells by increasing neurovascular permeability (Jordan et al., 2008; Kaur and Ling, 2008; Pan and Kastin, 2008; Sandoval and Witt, 2008; Ankeny and Popovich, 2009; Khatri et al., 2012; Oudega, 2012; Schoknecht and Shalev, 2012). In addition, expression of neurotrophins and other growth factors, such as IGF-1, play a key role in injury mitigation through restoration of vascular integrity and promotion of neural survival (Lindvall et al., 1994; Hicks et al., 1999; Dluzniewska et al., 2005; Sharma, 2005a; Wu, 2005; Allen and Dawbarn, 2006; Sharma, 2007a; Madathil et al., 2010).

While medical complications after ischemic stroke are the major cause of mortality (Slot et al., 2009; Kumar et al., 2010; Schoknecht and Shalev, 2012), preceding brain edema and hemorrhagic transformation due to blood-brain barrier dysfunction can affect outcomes with potentially serious short and long-term consequences (Balami et al., 2011). As such, early detection and mitigation of these neurological complications could substantially reduce stroke mortality and morbidity. Stroke is unique with regards to other acute CNS injuries in that blood-brain barrier dysfunction during the initial

phase of injury is solely driven by an energy failure due to a lack of glucose and oxygen through vascular occlusion, as opposed to the direct endothelial damage in the vasculature that often occurs immediately after traumatic injury (Khatri et al., 2012; Schoknecht and Shalev, 2012). Comparatively, blood-brain barrier dysfunction in TBI can also be delayed by several days, with subsequent edema formation accompanied by rises in intracranial pressure that mechanically impair blood flow, resulting in the development of an ischemic zone and secondary lesion progression (Rodriguez-Baeza et al., 2003; Shlosberg et al., 2010; Chodobski et al., 2011; Schoknecht and Shalev, 2012). Energy failure due to ischemic stroke triggers a cascade of processes that drive blood-brain barrier disruption, including depletion of adenosine triphosphate (ATP), a rise in intracellular potassium, lactic acidosis, and release of extracellular glutamate (Kulik et al., 2008; Khatri et al., 2012). The resulting ischemic environment results in increased blood-brain barrier permeability, reperfusion, and activation of astrocytes and microglia, which induces expression of pro-inflammatory cytokines (Khatri et al., 2012; Schoknecht and Shalev, 2012). Although the underlying molecular changes that lead to blood-brain barrier breakdown after TBI are not completely understood, the mechanisms involved mirror those following cerebral ischemia, including microglia and astrocyte activation, and production of both free radicals and inflammatory mediators (Shlosberg et al., 2010; Schoknecht and Shalev, 2012). In particular, interleukin-1-beta (IL-1β), interleukin-6 (IL-6), and tumor necrosis factor-α (TNF-α) are three of the most commonly studied cytokines up-regulated following both ischemic stroke and TBI, and they play an important role in the progression of neuroinflammation (Ghirnikar et al.,

1998; Jordan et al., 2008; Das et al., 2012; Lambertsen et al., 2012). In stroke, activated microglia and macrophages predominately produce TNF-α and IL-1β (Buttini et al., 1994; Davies et al., 1999; Lambertsen et al., 2005; Clausen et al., 2008; Lambertsen et al., 2012), while increased IL-6 expression is additionally observed in neurons (Suzuki et al., 1999; Suzuki et al., 2009; Lambertsen et al., 2012). Contrarily, IL-1β, IL-6, and TNF-α are all induced in activated astrocytes in addition to microglia and macrophages following TBI (Sawada et al., 1995; Ghirnikar et al., 1998; Das et al., 2012).

IL-1β is an important initiator of immune response, and its up-regulation promotes astrocyte proliferation and activation (Balasingam et al., 1994; Ghirnikar et al., 1998; John et al., 2004; Jordan et al., 2008). Increased IL-1β expression is associated with worse functional outcomes following both stroke and TBI, and its inhibition using a competitive receptor antagonist, neutralizing antibody, or mild immunosuppressant (minocycline) has been shown to significantly reduce infarct size and attenuate lesion volume, respectively (Yamasaki et al., 1995; Loddick and Rothwell, 1996; Boutin et al., 2001; Sanchez Mejia et al., 2001; Touzani et al., 2002; Bye et al., 2007; Ziebell and Morganti-Kossmann, 2010; Lambertsen et al., 2012). Likewise, TNF-α is a principle mediator of neuroinflammation, and its inhibition reduces both ischemic brain injury and improves neurological outcome in TBI through reduced blood-brain barrier dysfunction and brain edema (Shohami et al., 1997; Yang et al., 1998; Jordan et al., 2008; Ziebell and Morganti-Kossmann, 2010), while administration of recombinant TNF-α reverses the beneficial effects and worsens ischemic and traumatic brain damage (Barone et al., 1997; Shohami et al., 1997). However, TNF-α could also be neuroprotective, as TNF-α-

receptor deficient mice present larger ischemic infarcts than wild-type mice (Bruce et al., 1996; Jordan et al., 2008), pretreatment in ischemic, cerebral injury models through intracisternal administration of TNF-α significantly reduces infarct size and decreases microglial activation (Nawashiro et al., 1997), and mice deficient of TNF-α or its receptors have been shown to display exacerbated tissue and blood-brain barrier damage, as well as impaired neurological recovery after TBI (Scherbel et al., 1999; Sullivan et al., 1999; Ziebell and Morganti-Kossmann, 2010). Contrarily, while both IL-1β and TNF-α are primarily implicated in negative effects following brain injury, IL-6 can potentially exhibit beneficial or detrimental effects depending on the pathologic context, and it has both direct and indirect neurotrophic effects on neurons (Benveniste, 1998; Suzuki et al., 2009; Ziebell and Morganti-Kossmann, 2010). In the acute phase of ischemic injury, IL-6 promotes microglia and leukocyte activation and modulates acute inflammation by down-regulating the pro-inflammatory cytokines and up-regulating the anti-inflammatory molecules (Kharazmi et al., 1989; Chiang et al., 1994; Xing et al., 1998; Suzuki et al., 2009). Although increased plasma concentrations of IL-6 are associated with greater infarct volumes and worse functional outcomes in cerebral ischemia and with severe blood-brain barrier dysfunction in TBI (Kossmann et al., 1995; Castillo and Rodriguez, 2004; Smith et al., 2004; Jordan et al., 2008), enhanced production of IL-6 has been shown to be neuroprotective following cryolesion in a GFAP-IL-6 transgenic mouse model, and IL-6 deficiency resulted in increased oxidative stress, decreased cell survival, and delayed wound healing (Penkowa et al., 2000; Penkowa et al., 2003; Ziebell and Morganti-Kossmann, 2010).

In addition to cytokines, expression of neurotrophins and other growth factors are also modulated following CNS injury (Nieto-Sampedro et al., 1982; Hicks et al., 1997; Ghirnikar et al., 1998; Hicks et al., 1999; Lee et al., 2002; Lai and Todd, 2006). Neurotrophins, such as BDNF, nerve growth factor (NGF), and neurotrophin-3 (NT-3), are produced in the CNS by microglia, astrocytes, and neurons, and promote cell survival, growth, and differentiation effects by activating intracellular signal transduction pathways through interactions with specific high-affinity tyrosine kinase (trk) receptors (Meakin and Shooter, 1992; Barbacid, 1994; Elkabes et al., 1996; Miwa et al., 1997; Ghirnikar et al., 1998; Skaper and Walsh, 1998; Hicks et al., 1999). Although BDNF, the most abundantly expressed neurotrophin in the mature CNS (Hofer et al., 1990), has been shown to be neuroprotective in animal models of excitotoxicity, axotomy, and ischemia (Yan et al., 1992; Kindy, 1993; Beck et al., 1994; Cheng and Mattson, 1994; Tsukahara et al., 1994; Schabitz et al., 1997), neuroprotection does not appear to occur following TBI (Blaha et al., 2000). Conversely, NGF attenuated neuronal death in both TBI and ischemia (Shigeno et al., 1991; Sinson et al., 1995), suggesting that different types of CNS injury may require a specific compliment of neurotrophins to attenuate tissue damage and improve functional outcomes. Other growth factors produced by microglia also play a prominent role following CNS damage, such as transforming growth factor-beta (TGFβ) (Wiessner et al., 1993; Lehrmann et al., 1998; Zhu et al., 2000), basic fibroblast growth factor (bFGF; Shimojo et al., 1991; Li and Stephenson, 2002; Lai and Todd, 2006), and IGF-1 (Sandberg Nordqvist et al., 1996; Beilharz et al., 1998; Wildburger et al., 2001; Hwang et al., 2004;

Madathil et al., 2010). In particular, IGF-1 promotes neuronal survival, neurite outgrowth, maturation of oligodendrocytes, and myelination in the brain (D'Ercole et al., 1996), and it has neuroprotective effects after ischemic stroke and TBI (Lai and Todd, 2006; Madathil et al., 2010). Specifically, administration of IGF-1 reduced neuronal loss and infarct volume and increases glial proliferation following cerebral ischemia (Loddick and Rothwell, 1996; Guan et al., 2001; Liu et al., 2001; Cao et al., 2003), and both increased BDNF and NT-3 levels and improved motor and cognitive function after TBI (Kazanis et al., 2004; Saatman et al., 2006). Given that BDNF and IGF-1 are induced in both microglia and neurons following CNS injury and are functionally divergent from similarly microglia-derived pro-inflammatory cytokines like IL-1β and TNF-α (Hicks et al., 1999; Lee et al., 2002; Hwang et al., 2004; Lai and Todd, 2006; Jordan et al., 2008; Madathil et al., 2010; Ziebell and Morganti-Kossmann, 2010), optimizing therapeutic strategies for brain injury will require careful modulation of the microglia-activated balance between negating the detrimental effects of pro-inflammatory cytokine induction and maintaining the neuroprotection afforded by likewise induced growth factors.

Similar to ischemic stroke and TBI, maintenance of the blood-spinal cord barrier is necessary to ensure proper functionality of spinal nerve cells, glial cells, and axons, and dysregulation of the blood-spinal cord barrier following traumatic injury is critical to the development of spinal cord pathology and sensory-motor disruptions (Noble and Wrathall, 1989; Bilgen et al., 2002; Pan and Kastin, 2008; Sharma, 2008, 2011). Specifically, edema formation is an important driver of SCI pathology (Sharma, 2008,

2011), prominent within 2-5 min of injury and present as long as 15 days post-SCI (Nolan, 1969; Demediuk et al., 1987), dependent on the severity of the contusion injury (Noble and Wrathall, 1988, 1989; Sharma, 2005a, b), and associated with tissue damage at the lesion site (Schwab and Bartholdi, 1996; Sharma, 2011). Furthermore, inhibition of blood-spinal cord barrier disruption results in substantial neuroprotection (Sharma et al., 1993a, b; Sharma et al., 1993c; Sharma et al., 1995). Initiation of neuroinflammation by activated microglia additionally contributes to injury pathology, resulting in the axonal injury, demyelination, and delayed neuronal and glial cell death that drives secondary degeneration, and their inhibition reduces secondary injury (Giulian and Robertson, 1990; Blight, 1994; Popovich et al., 2002; Gomes-Leal et al., 2004). Activated microglia modulate astrogliosis (Ridet et al., 1997; Fitch et al., 1999) and produce pro-inflammatory cytokines, including IL-1β, IL-6, and TNF-α, which contribute to activation of astrocytes and other nearby microglia (Bartholdi and Schwab, 1997; Streit et al., 1998; Okada et al., 2004; Nakamura et al., 2005; Gris et al., 2007; Karimi-Abdolrezaee and Billakanti, 2012).

IL-1β induces astrocytic production of IL-6 and TNF-α as well as itself in a positive feedback loop (Chung and Benveniste, 1990; Norris et al., 1994; Wang et al., 2006), and treatment of contused spinal cord with IL-1 receptor antagonist at the lesion site has been shown to attenuate contusion-induced apoptosis (Nesic et al., 2001). However, IL-1β mediated activation of astrocytes also has several beneficial effects on the CNS microenvironment following injury, as it stimulates production of neuroprotective trophic and growth factors, such as fibroblast growth factor-2 (FGF-2),

NGF, and IGF-1, and contributes towards restoration of the blood-spinal cord barrier (Brenneman et al., 1995; Fitch et al., 1999; Mason et al., 2001; Albrecht et al., 2002; Liberto et al., 2004; Sofroniew, 2005; Wang et al., 2006; Sofroniew, 2009). Similarly, studies have shown dual neuroprotective and cytotoxic roles for TNF-α, where inhibition of TNF-α resulted in significantly improved functional recovery and reduction in blood-spinal cord barrier dysfunction and edema formation (Bethea et al., 1999; Bethea and Dietrich, 2002; Sharma et al., 2003; Sharma, 2010), but removal of TNF receptors reduced functional recovery and increased both apoptosis and lesion size due to a reduction in activation of the nuclear factor-kappaB (NF-kB) signaling pathway that led to an increase in the active form of the caspase-3 protein (Kim et al., 2001). The NF-kB transcription factor is a major regulator of immune and inflammatory responses, and its activation by TNF-α, along with IL-1β, drives astrogliosis following CNS injury (Yamamoto and Gaynor, 2001; Li and Verma, 2002; Zhang et al., 2009). Interestingly, selective inactivation of NF-kB in astrocytes is neuroprotective, resulting in dramatic improvement in functional recovery, reduced lesion volume, increased white matter sparing, and substantially decreased expression of pro-inflammatory cytokines and glial scar proteins (Brambilla et al., 2005). Because NF-kB activation in astrocytes also induces production of BDNF and NGF and ablation of reactive astrocytes compromises the reconstruction of the blood-spinal cord barrier after SCI (Zaheer et al., 2001; Faulkner et al., 2004), it is possible that the damaging effects incurred by removal of TNF receptors may be a result of the complete loss of both TNF and NF-kB signaling overly inhibiting astrogliosis, resulting in suppression of the beneficial production of

neurotrophins in both NF-kB-dependent and independent pathways and prevention of reactive astrocyte-mediated restoration of neurovascular integrity (Liberto et al., 2004; Zhang et al., 2009; Karimi-Abdolrezaee and Billakanti, 2012). While reactive astrocyte-mediated reconstruction of the blood-spinal cord barrier is essential for SCI repair (Fitch et al., 1999; Sofroniew, 2005, 2009; Karimi-Abdolrezaee and Billakanti, 2012), glial scar formation poses both physical and chemical barriers to axonal regeneration (McKeon et al., 1995; Silver and Miller, 2004; Busch and Silver, 2007) and prevents differentiation of both adult neuronal and oligodendrocyte precursor cells (Horky et al., 2006; Karimi-Abdolrezaee et al., 2006; Barnabe-Heider and Frisen, 2008; Karimi-Abdolrezaee et al., 2010; Siebert and Osterhout, 2011; Siebert et al., 2011). Correspondingly, induction of IL-6 in reactive astrocytes promotes production of glial scar proteins and a corresponding increase in glial scarring (Nakamura et al., 2005; Gris et al., 2007), while administration of anti-IL-6 antibodies attenuates glial scar formation, suppresses secondary injury through inhibition of neuroinflammation, and improves functional recovery (Okada et al., 2004).

Microglia and astrocyte activation also modulates expression of neurotrophins and growth factors following spinal cord trauma (Schwab and Bartholdi, 1996; Liberto et al., 2004; Sharma, 2005a, b, 2007a, 2011; Karimi-Abdolrezaee and Billakanti, 2012). Specifically, although expression of BDNF and IGF-1 is reduced at the lesion site during the early phases of SCI, both play an important role in injury pathology and exhibit therapeutic potential (Sharma et al., 1997; Sharma et al., 1998; Sharma et al., 2000a; Sharma et al., 2000b; Sharma, 2007a, 2011). Expression of both trkB and trkC receptors

is increased in neurons and astrocytes at the lesion site (Frisen et al., 1992), and BDNF, along with NT-3, is up-regulated in motor neurons and astrocytes rostral to the lesion (Uchida et al., 1998), suggesting that changes in BDNF/trkB signaling intensity and sensitivity varies spatially after SCI. In addition, IL-1β induced expression of IGF-1 in astrocytes is important for terminal differentiation of oligodendrocytes precursors and subsequent remyelination of axons following injury, and inhibited astrogliosis due to a lack of IL-1β signaling significantly impairs remyelination (Mason et al., 2001; Liberto et al., 2004). Furthermore, application of BDNF or IGF-1, either alone or in combination, within 30 min of SCI has been shown to significantly reduce blood-spinal cord barrier disruption, edema formation, NOS regulation, lesion size, and cell death (Novikova et al., 1996; Sharma et al., 1997; Jakeman et al., 1998; Sharma et al., 1998; Sharma, 2005a, b, 2006, 2007a, b, 2011). While these results are promising, the multifaceted state of the spinal cord microenvironment following traumatic injury suggests that more sophisticated therapeutic approaches may be needed to effectively coordinate inhibition of neuroinflammation and glial scar formation, rapid restoration of the blood-spinal cord barrier, and induction of trophic support in order to minimize secondary injury, promote regeneration, and facilitate robust functional recovery in human SCI patients.

### 1.2 Neuropathic Pain

Spinal cord injury can result in severely debilitating consequences, including loss of motor control, paralysis, and neuropathic pain. Chronic pain affects approximately two-

thirds of all SCI patients and can arise from nerve damage suffered with a concomitant peripheral tissue injury, in addition to damage to the spinal cord itself (Siddall and Loeser, 2001). Peripheral damage induces maladaptive spinal cord plasticity, consisting of sensitization of spinal neurons (Woolf and Wall, 1986; Sluka et al., 1997; Hains et al., 2003; Lampert et al., 2006), increased glial activity (Frei et al., 2000; Hains and Waxman, 2006; Detloff et al., 2008), and induced excitotoxicity and cell death (Liu et al., 1999; Beattie et al., 2002; Xu et al., 2004; Kuzhandaivel et al., 2011), by acting on nociceptive fibers as an uncontrollable source of over-excitation (Christensen and Hulsebosch, 1997; Ji et al., 2003; Yang et al., 2004), leading to development of neuropathic pain. In addition, uncontrollable nociceptive stimulation can severely undermine recovery of motor and sensory function. In adult rats, just 6 min of intermittent noxious stimulation impaired locomotor recovery, increased tissue loss, delayed the recovery of bladder function, and led to greater mortality and spasticity (Grau et al., 2004). Furthermore, whereas controllable stimulation promotes spinal learning (Crown et al., 2002), uncontrollable nociception inhibits adaptive spinal plasticity and increases allodynia (Ferguson et al., 2006). Intermittent noxious stimulation appears to mediate spinal plasticity mostly through down-regulation of BDNF and trkB (Gomez-Pinilla et al., 2007; Garraway et al., 2011), which cooperatively play an important role in modulation of neuronal plasticity, induction of axonal regeneration, and promotion of functional recovery following SCI (Xu et al., 1995; Patterson et al., 1996; McTigue et al., 1998; Kerr et al., 1999; Garraway et al., 2003; Boyce et al., 2007). Consequently, direct application of exogenous BDNF to the spinal

cord following injury could attenuate both uncontrollable nociception-induced maladaptive spinal plasticity and subsequent neuropathic pain symptoms.

One of the five first-line and most effective pharmalogical treatments for chronic pain after SCI is administration of opiate analgesics, such as morphine, with approximately one-third (33.3%) of all patients prescribed opiates reporting considerable improvement or elimination of pain (Dworkin et al., 2003; Widerstrom-Noga and Turk, 2003; McCarberg, 2004). While it was hypothesized that morphine could block the adverse effects of uncontrollable nociceptive stimulation applied below the level of injury, not only were these effects not attenuated, but a single dose of systemic morphine given on the day after spinal cord contusion exacerbated the effects of uncontrollable nociception, and rats treated with morphine and uncontrollable tailshock had a higher rate of mortality and displayed allodynic responses to innocuous sensory stimuli 3 weeks later (Hook et al., 2007). In addition, morphine treatment undermined recovery of sensory function and increased lesion size, independent of uncontrolled shock exposure. Similarly, administration of intrathecal morphine 24 hrs after contusion injury significantly attenuated the recovery of locomotor function, increased lesion size, decreased weight gain, and substantially increased mortality and autophagia (Hook et al., 2009). Morphine induced development of paradoxical pain symptoms has been attributed to immune responses (Watkins et al., 2005; Scholz and Woolf, 2007; Watkins et al., 2007), and prolonged morphine administration has been shown to activate microglia and astrocytes, leading to up-regulation of the pro-inflammatory cytokines IL-1β, IL-6, and TNF-α that block the analgesic effects of opioids (Gul et al., 2000; Song

and Zhao, 2001; Raghavendra et al., 2002; Szabo et al., 2002; Johnston et al., 2004; Cui et al., 2006; Tai et al., 2006). In particular, IL-1β has been shown to regulate a number of processes that propagate neuroexcitability and spinal sensitization, which in turn increases pain reactivity (Inoue et al., 1999; Viviani et al., 2003; Stellwagen et al., 2005; Tai et al., 2006; Prow and Irani, 2008). Furthermore, increased expression of IL-1β following morphine exposure, along with TNF-α, may exacerbate secondary injury by up-regulating expression of cytotoxic factors, such as inducible form of nitric oxide synthase, through activation of the astrocytic NF-kB pathway (Conti et al., 2007). Indeed, application of IL-1 receptor antagonist blocked the adverse effects of morphine on locomotor recovery and neuropathic pain (Hook et al., 2011). However, administration of the IL-1ra alone undermined functional recovery and increased tissue loss at the lesion site, suggesting that management of neuropathic pain and mitigation of morphine tolerance will require a more comprehensive and balanced approach to beneficially modulate microglia and astrocyte activation, production of pro-inflammatory cytokines, and regulation of neurotrophic signaling.

### 1.3 MicroRNA Overview and Dysregulation in CNS Injury

Effective therapeutic strategies that are capable of substantially improving functional outcomes and minimizing the impact of SCI by reducing cell death in the injury zone, promoting regeneration, and inhibiting the maladaptive spinal plasticity that drives neuropathic pain will require coordinated regulation of complex gene networks that mediate blood-spinal cord barrier disruption, activation of microglia and astrocyte,

induction of pro and anti-inflammatory cytokines, and glial scar formation. While altered gene expression has been shown to significantly contribute towards the pathogenesis of secondary SCI (Nesic et al., 2002; Bareyre and Schwab, 2003; De Biase et al., 2005), there is limited knowledge of regulatory networks that coordinate and control gene expression. MicroRNAs (miRNAs) are short, 18 to 25 nucleotide-long non-coding small RNAs that regulate gene expression by inhibiting protein translation or targeting mRNA transcripts for degradation (Alvarez-Garcia and Miska, 2005; Zamore and Haley, 2005). Individual miRNAs can simultaneously regulate several hundred mRNAs to affect specific biological processes related to cellular differentiation, growth, and apoptosis, as well as metabolic, immune, and inflammatory responses (Alvarez-Garcia and Miska, 2005; Stefani and Slack, 2008; Breving and Esquela-Kerscher, 2010).

MiRNA biogenesis begins in the nucleus with the transcription of miRNA genes, located in intergenic regions as well as in introns and exons of other genes, by Polymerase II, which yields a pri-miRNA precursor averaging hundreds to thousands of nucleotides in length (He and Hannon, 2004; Figure 1.1; Filipowicz et al., 2008; Breving and Esquela-Kerscher, 2010). In mammals, these pri-miRNAs are then processed by the Drosha-DGCR8 complex, consisting of the RNase-III type endonuclease Drosha and DiGeorge syndrome critical region gene 8 (DGCR8) protein, which recognizes stem-looped secondary structures of the pri-miRNA and excises them into approximately 70 nucleotide long, hairpin-shaped pre-miRNA precursors (Du and Zamore, 2005; Bushati and Cohen, 2007; Peters and Meister, 2007; Rana, 2007; Filipowicz et al., 2008). Pre-miRNAs are then exported out of the nucleus to the cytoplasm by exportin-5 and cleaved

by the endoribonuclease Dicer, complexed with TAR RNA binding protein (TRBP), to yield ~20 nucleotide miRNA duplexes. Typically, one strand is then selected to function as the mature miRNA, while the other is degraded, although occasionally both strands of the pre-miRNA become mature miRNAs (Du and Zamore, 2005; Bushati and Cohen, 2007; Peters and Meister, 2007; Rana, 2007; Filipowicz et al., 2008). Mature miRNAs are finally loaded onto miRNA-induced silencing complexes (miRISCs), of which Argonaute proteins play a key role. In animals, miRNAs interact with the 3' UTR of their target mRNAs through imperfect base pairing and according to experimentally and bioinformatically identified rules, with few exceptions (Doench and Sharp, 2004; Brennecke et al., 2005; Lewis et al., 2005; Grimson et al., 2007; Nielsen et al., 2007; Filipowicz et al., 2008). MiRNA-target base pairing must be perfect and contiguous for miRNA nucleotides 2 to 8 of the seed region to nucleate miRNA-mRNA association and establish efficient repression, base mismatches or bulges must be present in the central region of the miRNA-mRNA duplex, and there must be acceptable complementarity to the 3' end of the miRNA to stabilize the reaction (Brennecke et al., 2005; Grimson et al., 2007). In addition, multiple copies of miRNA binding sites are usually present in the target 3' UTR, and multiple sites for the same or different miRNAs are typically required for effective repression (Doench and Sharp, 2004; Brennecke et al., 2005; Lewis et al., 2005; Grimson et al., 2007; Nielsen et al., 2007; Filipowicz et al., 2008). Multiple binding sites can also synergistically when within 10-40 nucleotides of each other to enhance repression beyond their combined individual effects (Doench and Sharp, 2004; Grimson et al., 2007).

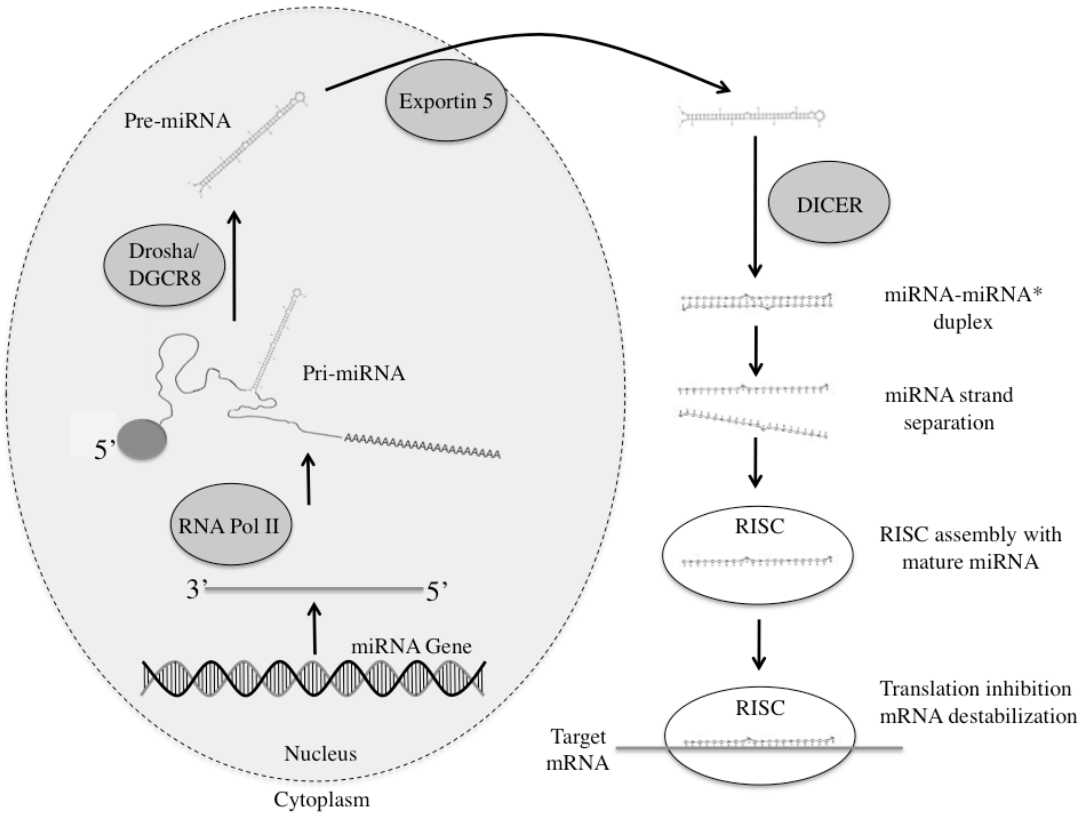


**Figure 1.** Schematic for the biogenesis of miRNAs. MiRNA genes are first transcribed in the nucleus by RNA Polymerase III into a pri-miRNA before the Drosha/DGCR8 complex processes them into ~70 nucleotide long pre-miRNAs. Pre-miRNAs are then transported from the nucleus into the cytoplasm by Exportin 5 and further processed into double stranded miRNA-miRNA* duplexes by the Dicer complex. Once the two duplex strands are separated, mature miRNA guide strands are preferentially loaded onto the RNA-induced silencing complex (RISC), and the assembled miRNA-RISC complex then targets complimentary seed regions of mRNA 3'UTRs for either suppression of translation or mRNA degradation.

MicroRNAs have been shown to be dysregulated in the CNS following stroke and traumatic brain injury (Lei et al., 2009; Redell et al., 2010; Saugstad, 2010; Liu et al., 2011; Rink and Khanna, 2011; Tan et al., 2011). Transient focal ischemia in adult rat brain results in dysregulation of 20 miRNAs predicted to target mRNAs known to mediate transcription, ionic homeostasis, neuroprotection, and inflammation (Dharap et al., 2009; Saugstad, 2010). Interestingly, miR146a, an anti-inflammatory miRNA that targets IL-6 and interleukin-1 receptor associated kinase-1 (IRAK-1), has exhibited biphasic expression following cerebral ischemia with acute down-regulation followed by substantial induction at 7 days following injury (Taganov et al., 2006; Bhaumik et al., 2009; Liu et al., 2010; Liu et al., 2011; Tan et al., 2011). In addition, expression of miR124a, a key promoter of neuronal differentiation, was significantly decreased in neural progenitor cells within the subventricular zone following focal cerebral ischemia (Liu et al., 2011). Similarly, robust miRNA dysregulation is observed following traumatic brain injury, and predicted targets of impacted miRNAs include proteins of signaling pathways induced by injury, including signal transduction, transcriptional regulation, proliferation, and differentiation (Redell et al., 2009; Saugstad, 2010). Of particular note, miR21 exhibits substantial transient up-regulation with peak expression approximately 3 days after TBI (Lei et al., 2009; Redell et al., 2011). As miR21 is known to be strongly anti-apoptotic and induce proliferation (Sathyan et al., 2007), it is possible that it plays an important role in the progression of neuroinflammation.

MicroRNAs are also dysregulated following spinal cord trauma (Liu et al., 2009; Nakanishi et al., 2010; Strickland et al., 2011; Yunta et al., 2012). Initial reports

indicated a time-dependent dysregulation of a number of miRNAs implicated in the inflammation, oxidation, and apoptosis that contribute towards the pathogenesis of SCI (Liu et al., 2009; Nakanishi et al., 2010). As will be discussed in detail in Section 2, we identified a subset of miRNAs, including brain trauma-sensitive miR124, miR21, and miR146a, that were significantly dysregulated following SCI and exhibited specific, coordinated changes in temporal and spatial expression patterns (Strickland et al., 2011). Because miR124 suppresses activation of microglia prior to SCI and both miR21 and miR146a are able to inhibit astrogliosis following injury (Ponomarev et al., 2011; Bhalala et al., 2012; Iyer et al., 2012; Willemen et al., 2012), dysregulation of these miRNAs, along with other SCI-sensitive miRNAs, may play an important role in mediating neuroinflammation, secondary injury, and neuropathic pain following spinal cord contusion.

# 2. MICRORNA DYSREGULATION FOLLOWING SPINAL CORD CONTUSION: IMPLICATIONS FOR NEURAL PLASTICITY AND REPAIR*

## 2.1 Overview

Spinal cord injury (SCI) is medically and socioeconomically debilitating. Currently, there is a paucity of effective therapies that promote regeneration at the injury site, and limited understanding of mechanisms that can be utilized to therapeutically manipulate spinal cord plasticity. MicroRNAs (miRNAs) constitute novel targets for therapeutic intervention to promote repair and regeneration. Microarray comparisons of the injury sites of contused and sham rat spinal cords, harvested 4 and 14 days following SCI, showed that 32 miRNAs, including miR124, miR129, and miR1, were significantly down-regulated, whereas SNORD2, a translation-initiation factor, was induced. Additionally, 3 miRNAs including miR21 were significantly induced, indicating adaptive induction of an anti-apoptotic response in the injured cord. Validation of miRNA expression by qRT-PCR and *in situ* hybridization assays revealed that the influence of SCI on miRNA expression persists up to 14 days and expands both anteriorly and caudally beyond the lesion site. Specifically, changes in miR129-2 and miR146a expression significantly explained the variability in initial injury severity, suggesting that these specific miRNAs may serve as biomarkers and therapeutic targets

*Reprinted with permission from "MicroRNA Dysregulation Following Spinal Cord Contusion: Implications for Neural Plasticity and Repair" by E.R. Strickland, M.A. Hook, S. Balaraman, J.R. Huie, J.W. Grau, and R.C. Miranda, 2011. *Neuroscience,* 186, 146-160, Copyright 2011 by Elsevier.

for SCI. Moreover, the pattern of miRNA changes coincided spatially and temporally with the appearance of SOX2, nestin, and REST immunoreactivity, suggesting that aberrant expression of these miRNAs may not only reflect the emergence of stem cell niches, but also the reemergence in surviving neurons of a pre-neuronal phenotype. Finally, bioinformatics analysis of validated miRNA-targeted genes indicates that miRNA dysregulation may explain apoptosis susceptibility and aberrant cell cycle associated with a loss of neuronal identity, which underlies the pathogenesis of secondary SCI.

## 2.2 Introduction

Current understanding of the mechanisms underlying spinal cord injury (SCI) is limited, and traditional therapeutic methods lack a molecular approach to prevent the loss of sensory function and paralysis. Effective rehabilitation will require a multifaceted therapeutic strategy that promotes tissue regeneration, reduces cell death in the secondary injury zone, and improves native function through behavioral training. To accomplish this, it is imperative to uncover the upstream genetic regulators responsible for coordinating the acute inflammatory and apoptotic responses driving secondary spinal cord injury, in addition to the chronic inflammation resulting from uncontrollable nociceptive stimulation, that impairs functional recovery through reduction of spinal cord plasticity (Grau et al., 2004; Grau et al., 2006; Hook et al., 2009). Therapeutic manipulation of these mechanisms, as well as other novel genetic and biochemical

pathways, could represent effective treatments for improving functional recovery, minimizing pathological damage, and attenuating neuropathic pain.

Other investigators have previously reported that altered gene expression significantly contributes to the pathogenesis of secondary SCI (Nesic et al., 2002; Bareyre and Schwab, 2003; De Biase et al., 2005), but there is limited knowledge of the regulatory networks that control gene expression. MiRNAs are short, ~22 nucleotide non-coding small RNAs that regulate gene expression by controlling protein translation or destabilizing mRNA transcripts (Alvarez-Garcia and Miska, 2005; Zamore and Haley, 2005). Individual miRNAs coordinate the expression of several hundred protein-coding genes, to affect a specific biological endpoint. In addition, many miRNAs exhibit remarkable phylogenetic similarities, and often complete evolutionary conservation (Lee et al., 2007), which is ideal for studying their effects and clinical relevance in animal models, such as *Rattus norvegicus*. Consequently, miRNAs may constitute one therapeutic target to alter the cellular proteome in the damaged spinal cord, to promote repair and regeneration. Initial reports on miRNA dysregulation following SCI have outlined expression changes in numerous miRNAs at time points ranging from 1 hr to 7 days; however, these analyses were strictly limited to the injury site, primarily focused on inflammatory and apoptotic mediated changes that dominate the early response to injury, and only reported localization patterns for miR124a and miR223 (Liu et al., 2009; Nakanishi et al., 2010).

The current study focused on a time course ranging from 24 hours to 14 days post-SCI, to evaluate the relationship between miRNA expression and functional

recovery following trauma. We also examined miRNA changes both rostral and caudal to the injury site, as significant changes in rostral/caudal gene expression have also been observed in response to a spinal cord contusion (De Biase et al., 2005). Likewise, we analyzed the functional roles of genes known to be regulated by significant miRNAs to determine the possible global effects of SCI-mediated miRNA dysregulation. Finally, we investigated the temporal relationship between miRNA profiles and expression patterns of biomarkers that indicate reemerging plasticity and loss of cellular identity following SCI.

## 2.3 Experimental Procedures

### *2.3.1 Subjects*

The subjects were male Sprague–Dawley rats (*Rattus norvegicus*) obtained from Harlan (Houston, TX). The rats were approximately 90-110 days old (300-350 g), and were individually housed in Plexiglas bins [45.7 (length) x 23.5 (width) x 20.3 (height) cm] with food and water continuously available. To facilitate access to the food and water, extra bedding was added to the bins after surgery and long mouse sipper tubes were used so that the rats could reach the water without rearing. Bladders were manually expressed in the morning (8-9:30 a.m.) and evening (6-7:30 p.m.) until subjects regained bladder control, which was operationally defined as three consecutive days with an empty bladder at the time of expression. Rats were maintained on a 12-hr light/dark cycle. All procedures described in these experiments were reviewed and approved by the Texas A&M University Laboratory Animal Care Committee.

*2.3.2 Surgery*

Subjects received a contusion injury using the Multicenter Animal Spinal Cord Injury Study (MASCIS) Impactor device (Gruner, 1992; Constantini and Young, 1994). Subjects were anesthetized with isoflurane (5%, gas). Once a stable level of anesthesia was achieved the inspired concentration of isoflurane was lowered to 2-3% and an area extending approximately 4.5 cm above and below the injury site was shaved and disinfected with iodine. A 7.0 cm incision was made over the spinal cord. Next, two incisions were made on either side of the vertebral column, extending about 3 cm rostral and caudal to the T12-T13 segment. The dorsal spinous processes at T12-T13 were removed (laminectomy), and the spinal tissue exposed. The dura remained intact. The vertebral column was fixed within the MASCIS device, and a moderate injury was produced by allowing the 10-g impactor (outfitted with a 2.5 mm tip) to drop 12.5 mm. T12-T13 level contusion models have been routinely used by members of our group to define spinal cord learning circuits and molecular mechanisms involved with recovery of function (e.g., (Ferguson et al., 2008; Brown et al., 2011; Hook et al., 2011)). Lesions at this level result in well-defined and replicable sensory-motor deficits, and we therefore chose to utilize contusion at this level to also examine changes in miRNA expression. Contusions at the T12-T13 level resulted in mean BBB (Basso, Beattie, and Bresnahan scale (Basso et al., 1995)) score of 2.75 +/- 0.49 (mean +/- SEM), indicating significant loss of locomotor function. There were no statistically significant differences in BBB scores between the various contusion groups. Sham controls received a laminectomy, but the cord was not contused with the MASCIS device. Following surgery, the wound

was closed using Michel clips. To help prevent infection, subjects were treated with 100,000 units/kg Pfizerpen (penicillin G potassium) immediately after surgery and again 2 days later. For the first 24 hours after surgery, rats were placed in a recovery room maintained at 26.6 °C. To compensate for fluid loss, subjects were given 2.5 ml of saline after surgery. Subjects were given about 20-24 hr to recover from surgery, and during recovery, additional saline was given to maintain hydration.

*2.3.3 Assessment of locomotor function*

Locomotor behavior was assessed for up to 14 days post-surgery using the BBB scale in an open enclosure (99 cm in diameter, 23 cm deep). Baseline motor function was assessed on the day following surgery. Because rodents often remain motionless (freeze) when introduced to a new apparatus, subjects were acclimated to the observation fields for 5 min per day, for 3 days prior to surgery. Each subject was placed in the open field, observed for 4 min, and scored for locomotor behavior using the procedure developed by Basso et al. (1995). Care was taken to ensure that the investigators' scoring behavior had high intra- and inter- observer reliability (all r's > 0.89), and that they were blind to the subject's experimental treatment.

*2.3.4 Isolation of RNA for microarray and qRT-PCR quantification*

Subjects were anesthetized 24 hrs, 4 days, or 14 days after injury and a 1 cm long segment of the spinal cord from the lesion center, as well as 1 cm rostral and caudal to the injury epicenter, was removed and flash-frozen in liquid nitrogen. Specimens were

crushed and RNA was isolated using the TRIzol (Invitrogen; Carlsbad, CA) protocol. MiRNA was then quantified using a Bioanalyzer 2100 (Agilent Technologies; Carmel, IN) and stored at -80 °C.

*2.3.5 MiRNA labeling and hybridization*

MiRNA expression of contused and sham spinal cords were compared using dual channel arrays on a HS 400 Pro hybridization platform (TECAN; Research Triangle Park, NC). Extracted miRNA from all sham controls were pooled in equal concentrations to eliminate outliers from control expression, and compared to each contused and sham sample individually. Dye swapping was utilized to eliminate bias, and a total of 12 arrays were hybridized according to the EXIQON miRCURY$^{TM}$ locked nucleic acid (LNA) microRNA Array Power Labeling kit protocol. After hybridization, arrays were scanned using a GenePix 400B scanner (Molecular Devices; Union City, CA), and the scanner gain and sensitivity was set so that the overall ratio of Cy3 to Cy5 intensity across the array was set at 1. Array features that were irrelevant to the analysis such as blank spots, Cy3 control features, and miRNA features for all species except rat, human, and mouse, were removed before statistical analyses. Data were exported to and analyzed for significance using GeneSifter software (Geospiza; Seattle, WA). Significantly expressed miRNAs were grouped according to fold change in expression and by genome clustering.

*2.3.6 Quantitative RT-PCR for miRNA*

Microarray data was validated with quantitative reverse transcription (qRT)-PCR for miRNAs, based on the protocol of the miRCURY$^{TM}$ LNA microRNA Universal RT-PCR system (EXIQON; Woburn, MA). RNA samples were converted to cDNA, and qRT-PCR was performed using a MyiQ$^{TM}$ Single-Color Real-Time PCR Detection System (Bio-Rad, Hercules, CA). Forward and reverse primers (EXIQON; Woburn, MA) for hsa-miR124, hsa-miR223, hsa-miR1, hsa-miR21, hsa-miR129-2, hsa-miR129-1, and hsa-miR146a, were used for PCR amplification, and real time data was normalized using U6 RNA. Relative miRNA expression was determined by calculating the mean difference between cycle threshold of the miRNA from the U6 small nuclear RNA ($U6_{SNB}$) normalized control for each sample [Δ cycle threshold (ΔCT)] within each sample group (samples with same miRNA ID, time, and condition parameters) and expressed as -ΔCT for relative change in expression. Sample means that were greater than ± 2 standard deviations from the mean ΔCT, or ± 3 standard deviations from the mean ΔCT after exclusion, were considered outliers and removed from the analysis. Of the 425 data points in 84 groups used in the analysis, only 17 data points were excluded according to this criteria, and no more than one data point in any individual experimental group was excluded. Fold change in miRNA expression was determined by calculating the difference between the mean ΔCTs of contused and sham sample groups at the same time point and spinal cord location (ΔΔCT), and expressed as fold-change ($2^{-\Delta\Delta CT}$).

*2.3.7 In situ hybridization & immunofluorescence analyses*

For immunofluorescence and *in situ* hybridization analyses, 24 hrs, 4 days or 14 days after injury subjects were deeply anesthetized with pentobarbital (100 mg/kg, i.p.), and perfused (intracardially) with 4% paraformaldehyde in 0.1 M saline buffer. A 1 cm long segment of the spinal cord was taken from the lesion center, as well as 1 cm rostral and caudal to the injury epicenter, and prepared for cryostat sectioning. The tissue was then sectioned to a thickness of 30 microns, in either a longitudinal or coronal orientation, and mounted onto suprafrost plus slides (VWR Scientific; West Chester, CA). *In situ* hybridization was conducted using biotin labeled LNA-modified oligonucleotide probes (EXIQON; Woburn, MA) according to the EXIQON instructions, followed by incubation with rhodamine avidin D for 1 hour at 4 °C. Slides were mounted and nuclear stained using VectaShield mounting medium with DAPI (Vector Labs; Burlingame, CA). Immunofluorescence was performed according to standard methodologies using monoclonal mouse anti-nestin, and polyclonal rabbit antibodies for glial fibrillary acidic protein (GFAP), RE1-silencing transcription factor (REST), sex determining region Y-box 2 (SOX2), and neurofilament (Abcam; Boston, MA). The secondary antibodies utilized included goat anti-mouse Alexafluor® 488 and goat anti-rabbit Alexafluor® 594 (Invitrogen; Eugene, CA). All primary and secondary antibodies were used at 1:200 and 1:300 dilutions, respectively. All photomicrography was conducted using an Olympus FSX100 microscope with imaging software (FSX-BSW v.2.01, Olympus), or on an Olympus BX60 microscope.

*2.3.8 Data analyses*

Microarray-derived data were analyzed by *t*-tests with Benjamini and Hochberg FDR corrections for multiple comparisons, using GeneSifter (Geospiza; Seattle, WA). All other data were analyzed using SPSS software version 18 (SPSS; Chicago, IL). MicroRNA expression, verified by qRT-PCR, was analyzed by multivariate analysis of variance (ANOVA) using Pillai's trace statistic, and further analyzed using *post hoc* univariate ANOVA and Fisher's least significant difference (f-LSD) test. Other data were analyzed using ANOVAs followed by post hoc f-LSD using planned comparisons. In all cases, the *priori* $\alpha$ value was set at 0.05. Data were expressed as mean ±SEM, as indicated in the figure legends.

The statistical relationship between injury severity and change in miRNA expression after SCI (the $R^2$, a goodness of fit) was determined using least squares regression analysis of explained variance, with BBB score at 24 hrs after surgery as the independent variable, and difference in cycle threshold change (-ΔΔCT; between contused subjects at 4 and up to 14 days post-SCI, and the mean of sham controls) as the dependent variable. Correlations between pairings of miRNAs were determined by Pearson's product-moment correlation (PPMC) using –ΔΔCT values of the paired miRNAs at 4 days post-SCI as separate independent variables. The *priori* $\alpha$ value was set at 0.05, and data were expressed as the difference in cycle threshold change of each contused subject relative to the mean cycle threshold change of sham controls (-ΔΔCT= $\Delta CT\ \bar{x}_{sham} - \Delta CT_{contused}$).

Bioinformatics were preformed using validated gene targets of selected miRNAs from the miRWALK online database (Dweep et al., 2011). Gene cross-referencing was performed using a Visual Basic/Microsoft Excel based bioinformatics macro script developed within our laboratory, available upon request. Results were generated into a table listing the miRNAs of interest in separate column headings, and the gene targets for each studied miRNA that were regulated by 2 or more of the 6 total investigated miRNAs were listed under the column heading corresponding to the regulating miRNAs. This list was indexed in alphabetical order by gene, with each gene having a unique table row, to cross-list all miRNAs targeting that specific gene. Each cross-referenced list was grouped according to common gene targets, with 2 groups being formed: one for miR1 and miR124, and a second for miR21 and miR146a. Each grouped list contained only those genes common between both constituent miRNAs, and analyzed for functional annotation in DAVID Bioinformatics Resources for functional annotation (Dennis et al., 2003; Huang da et al., 2009).

## 2.4 Results

### *2.4.1 Identification and quantification of significant changes in miRNA expression*

Initially, miRNA expression was quantitatively assessed in total RNA samples from animals harvested 4 and 14 days post SCI (5 contused and 5 sham animals each) using a miRNA microarray approach (for details, see Section 2.3.5). Microarray data were subjected to exploratory analyses using a 2-way ANOVA (SCI lesion condition x Time) with a Benjamini and Hochberg correction for multiple comparisons (False-discovery

rate (FDR)-set at a=0.1, fold-change cutoff, 1.8-fold). We identified 31 statistically significant, dysregulated small RNAs (30 miRNAs and 1 small nuclear RNA, SNORD2) that exhibited a significant main effect of SCI. Most miRNAs were down-regulated and despite an overall significant main effect of SCI, exhibited a greater decline at 14 days rather than at 4 days (e.g., miR124, miR129-2, miR129-1, Figure 2a). Conversely, the relatively few small RNAs that exhibited a statistically significant increase, tended to exhibit a greater increase at 4 days post SCI, compared to 14 days (e.g., miR21, SNORD2, Figure 2a). Despite this, hierarchical cluster analysis of the FDR-controlled, statistically significant small RNAs indicated that the 4 and 14-day sham controls clustered together within one linkage group, and SCI groups clustered together within a second linkage group, reaffirming the ANOVA-identified dominant main effect of SCI (Figure 2b, c). As a result, we collapsed the dimension of time and conducted *t*-tests with Benjamini and Hochberg FDR corrections to initially screen for SCI-regulated miRNAs (FDR-adjusted $\alpha = 0.05$, fold-change cutoff, 1.5-fold). Results indicated a group of 36 small non-coding RNAs that were significantly dysregulated following SCI, 4 up-regulated and 32 down-regulated.

Additional studies were confined to the 3 miRNAs (miR223, miR21, miR146a) exhibiting the greatest increase and 4 miRNAs (miR124, miR1, miR129-2, miR129-1) exhibiting the greatest decrease in expression, respectively. The expression of selected miRNAs post-SCI was further examined by qRT-PCR in order to validate microarray results, and expand the study to investigate expression changes present at 24 hrs and in regions 1 cm rostral and caudal to the injury site (Figure 3). Multivariate ANOVA of

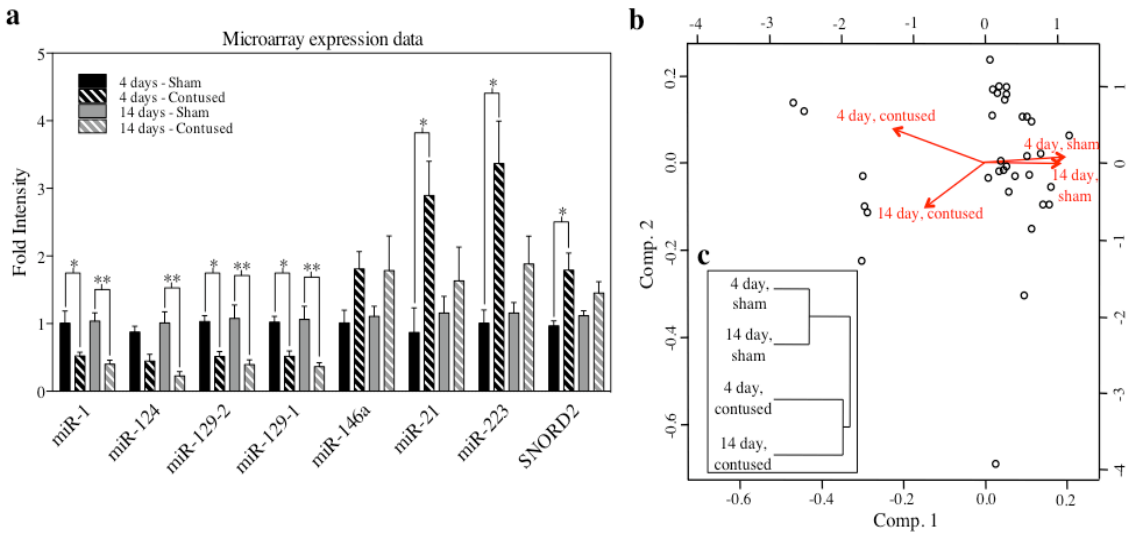


**Figure 2.** Analysis of microarray expression data indicates that SCI results in significant dysregulation of small RNAs. a, Bar graph depicting expression of significantly dysregulated miRNAs and other small RNAs (e.g. SNORD2) over time and experimental condition. The y-axis depicts fold change in intensity relative to a complex RNA target (a composite of equal RNA concentrations from all sham-lesioned animals at 4 and 14 days post-surgical manipulation). Data are expressed as ±SEM, with asterisks indicating statistical significance compared with sham controls (*$p < 0.05$, **$p < 0.01$). b,c, A hierarchical cluster dendogram of microarray data depicting principal component analysis (b), along with Euclidean distance and linkage (c), denotes that while both sham groups are similar to each other and both contused groups are likewise similar to each other, in terms of miRNA expression profiles, sham groups exhibited a low association with contused groups.

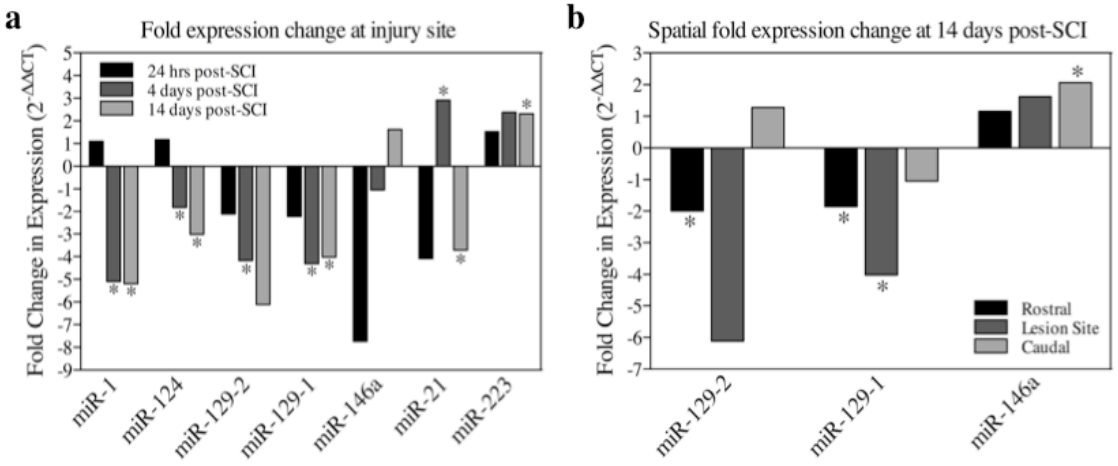


**Figure 3.** Bar graphs depicting qRT-PCR analysis of miRNA expression at the lesion site (a) and in regions rostral and caudal to the lesion (b) following SCI. a,b, The x-axis denotes miRNA of interest, and the y-axis denotes the fold expression change using the formula $2^{-\Delta\Delta CT}$, where ΔΔCT represents the mean difference of sham and contused ΔCT values. Animals received either a T12-T13 spinal contusion or laminectomy only (sham), and sacrificed at 24 hrs, 4 days, or 14 days post-surgery. The harvested cords were analyzed for miRNA expression within the injury site (a) and in spinal cord sections 1 cm rostral and caudal to the injury site (b). Data are expressed as a magnitude of change (a value of zero equates to no change between surgery conditions, positive values equate to increases in expression following SCI, and negative values vice versa), with asterisks indicating significance (f-LSD) compared with sham controls; *p* values are as indicated in the text.

qRT-PCR data indicated a significant interaction effect between surgery condition and time (Pillai's Trace Statistic, $F_{(10,26)} = 2.722$; $p<0.02$). In addition, *post hoc* univariate ANOVA indicated a significant main effect of surgery condition on miR124 and miR1 expression ($F_{(1,16)} = 6.774$, $p<0.02$ and $F_{(1,16)} = 7.319$, $p<0.02$, respectively), and a significant interaction effect between time and surgery condition on miR21 and miR146a expression ($F_{(2,16)} = 8.918$, $p<0.01$ and $F_{(2,16)} = 3.964$, $p<0.05$). Furthermore, *post hoc* least significant difference t-tests indicated that both miR124 and miR1 exhibited significant down-regulation at 4 days post-SCI ($p_{\text{miR124}}<0.005$ and $p_{\text{miR1}}<0.05$), as well as at 14 days ($p_{\text{miR124}}<0.01$ and $p_{\text{miR1}}<0.05$; Figure 3a). In contrast, miR21 was significantly up-regulated at 4 days and down-regulated at 14 days ($p<0.001$ and $p<0.01$, respectively). Interestingly, close examination of expression data for miR146a reveals that, although the interaction effect between time and condition results in a significant trend of increasing miR146a expression in contused subjects over the time course of 24 hrs to 14 days post-SCI (Student's 2-tailed *t*-test, $p<0.05$), none of the individual time points exhibited a significant change by surgery condition. The primary contributors to the significance of this trend are decreased miR146a expression at 24 hrs and increased expression at 14 days, relative to sham controls (Student's 2-tailed *t*-test, $p = 0.064$ and $p = 0.114$, respectively).

Conversely, not only did miR223 lack multivariate significance, but *post-hoc* univariate ANOVA also failed to indicate a significant main effect of spinal cord injury on miR223 expression ($F_{(2,16)} = 3.964$, $p<0.09$), although these data do suggest a trend towards significance. Preliminary microarray and qRT-PCR data (unpublished data)

indicated that miR223 was only significantly up-regulated at 4 days, but this could not be validated. Therefore, although miR223 showed significance at 14 days (Student's 2-tailed *t*-test, $p<0.02$; Figure 3a) in the qRT-PCR assay for this study, its inconsistence with previous observations, along with its high variability in expression between both individual specimens and separate assays, led us to exclude it from further analysis. Mature miR129-2 and miR129-1 transcripts share nearly identical sequence homology (a one nucleotide difference; they are 3' products formerly denoted as miR129-3p and miR129*, respectively) and exhibited similar expression patterns, so they were analyzed together as a separate group. The multivariate ANOVA revealed an overall significant main effect of spinal cord lesion (Pillai's Trace Statistic, $F_{(2,22)} = 5.374$; $p<0.02$). Furthermore, *post hoc* univariate ANOVA also indicated a significant main effect of condition for both miR129-2 and miR129-1 ($F_{(1,23)} = 8.721$, $p<0.01$ and $F_{(1,23)} = 9.097$, $p<0.01$, respectively). Student's 2-tailed t-tests of expression changes at individual time points confirmed significant down-regulation at 4 days for both miR129-2 and miR129-1 ($p<0.05$, for both), but only for miR129-1 at 14 days ($p<0.02$; Figure 3a). In addition, miR129-2 and miR129-1 both exhibited a significant decrease in expression in sections rostral to the injury site at 14 days post-SCI ($p<0.05$, for both; Figure 3b).

*2.4.2 Impact of injury severity on miRNA expression*

To explore the possibility that initial injury severity is predictive of dysregulated miRNA expression, locomotor function was routinely observed following surgery and scored using the Basso, Beattie, and Bresnahan (BBB) scale (Basso et al, 1995).

Regression analysis of explained variance revealed that 74.6% of the variation in the expression of miR129-2 (-ΔΔCT) on Days 4 and 14 was explained by the variation in initial BBB scores (logarithmic $R^2$=0.746, F(1,8)=23.437, $p$<0.001; Figure 4a), while 69.7% of the variation in the expression of miR146a on Day 14 was explained by variation in BBB score at 24 hrs ($R^2$=0.697, F(1,5)=8.585, $p$<0.05; Figure 4b). Although no other miRNAs were statistically related to injury severity, two instances of significant correlation between miRNAs were found. There was a statistically significant correlation between the expression of miR129-1 and miR129-2 (Pearson's $r$ = 0.851, $p$<0.05; Figure 4c), and between miR124 and miR21 (Pearson's $r$ = 0.897, $p$<0.05; Figure 4d), suggesting that these pairs of miRNAs may be co-regulated.

*2.4.3 MiRNA localization patterns and cellular identity following SCI*

Using *in situ* hybridization assays, we observed that miRNAs sensitive to spinal cord injury exhibit divergent temporal and spatial patterns. Initially, the possibility of false positives resulting from procedural abnormalities and high background was assessed using a scrambled miRNA (nonsense control), whose hybridization was acceptably minimal (i.e., at near background levels; Figure 5b, see insert), even within the lesion site. MiR124 expression at 4 days post-SCI in sham controls was largely confined to laminae VI-IX, with minimal expression in the dorsal horn (Figure 5a). At 14 days post-SCI, miR124 exhibited low expression within the injury site compared to the sham control, but was present in intact central grey matter tracts (Figure 5b, c), indicating a population of surviving neurons. Similarly, miR1 was down-regulated in grey matter at

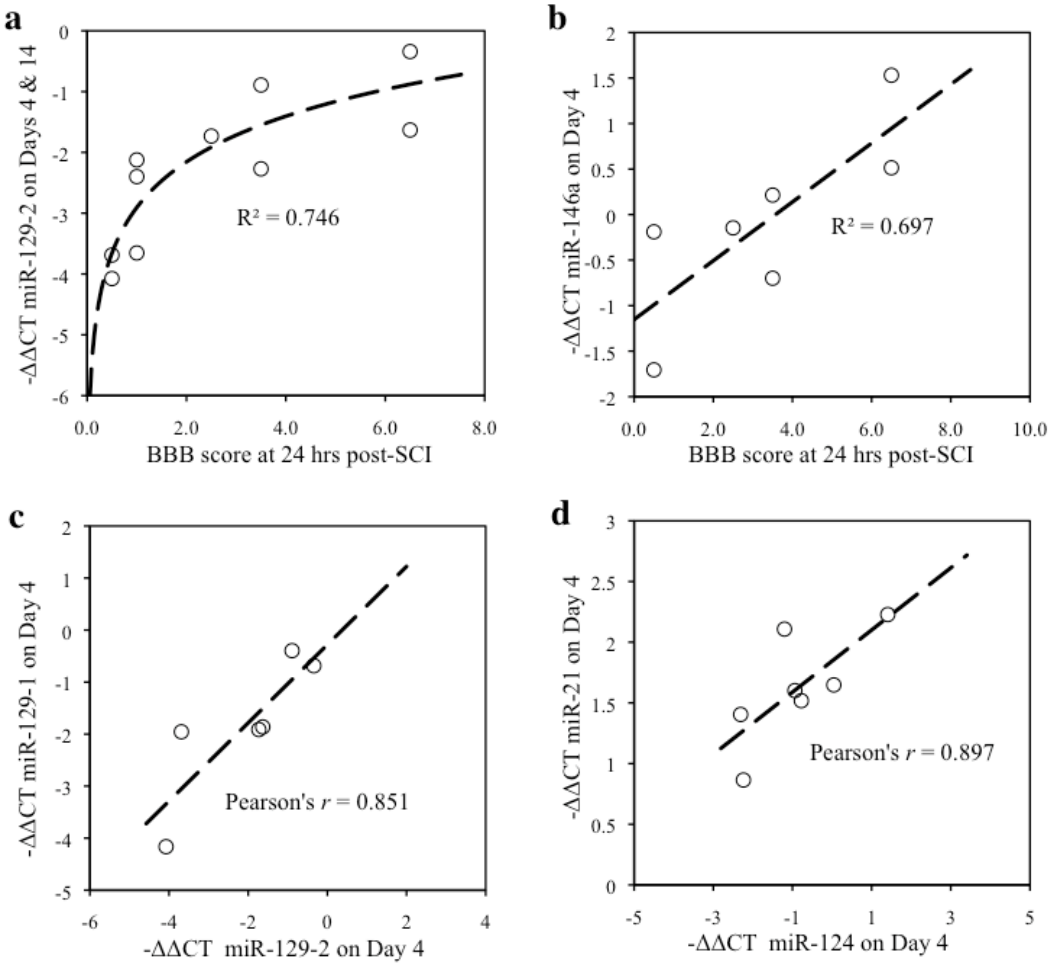


**Figure 4.** Regression analyses to assess the relationship between miRNA expression and initial injury severity. a,b, The x-axis represents the Basso, Beattie, and Bresnahan (BBB) score for baseline locomotor function, 24 hours following spinal cord contusion, and the y-axis depicts the difference in cycle threshold change (-ΔΔCT; a DDCT value of 1 indicates a 2-fold change in miRNA expression) between contused subjects and sham controls. Best-fit curves and correlation constants were generated using least squares regression analysis. Regression analysis indicates that 74.5% of the variation in the expression of miR129-2 (-ΔΔCT) on Days 4 and 14 is explained by the variation in BBB scores, 24 hours following SCI (Logarithmic regression $R^2$=0.746, F(1,8)=23.437, $p$<0.001; a), and 69.7% of the variation in miR146a on Day 4 is explained by variation in the BBB scores, 24 hours following SCI (Linear Regression $R^2$=0.697, F(1,4)=9.189, $p$<0.05; b). c,d, Correlation analyses also confirmed that miRNAs correlate with each other. The x-axis and y-axis each denote –ΔΔCT values for different miRNAs. Pearson's correlations indicated significant correlations between miR129-1 and miR129-2 (Pearson's $r$ = 0.851, $p$<0.05; c), and between miR124 and miR21 (Pearson's $r$ = 0.897, $p$<0.05; d), suggesting that these pairs of miRNAs may be co-regulated. Data are represented as the difference in cycle threshold change of each contused subject relative to the mean cycle threshold change of sham controls (-ΔΔCT= ΔCT $\overline{X}_{sham}$ - $\Delta CT_{contused}$).

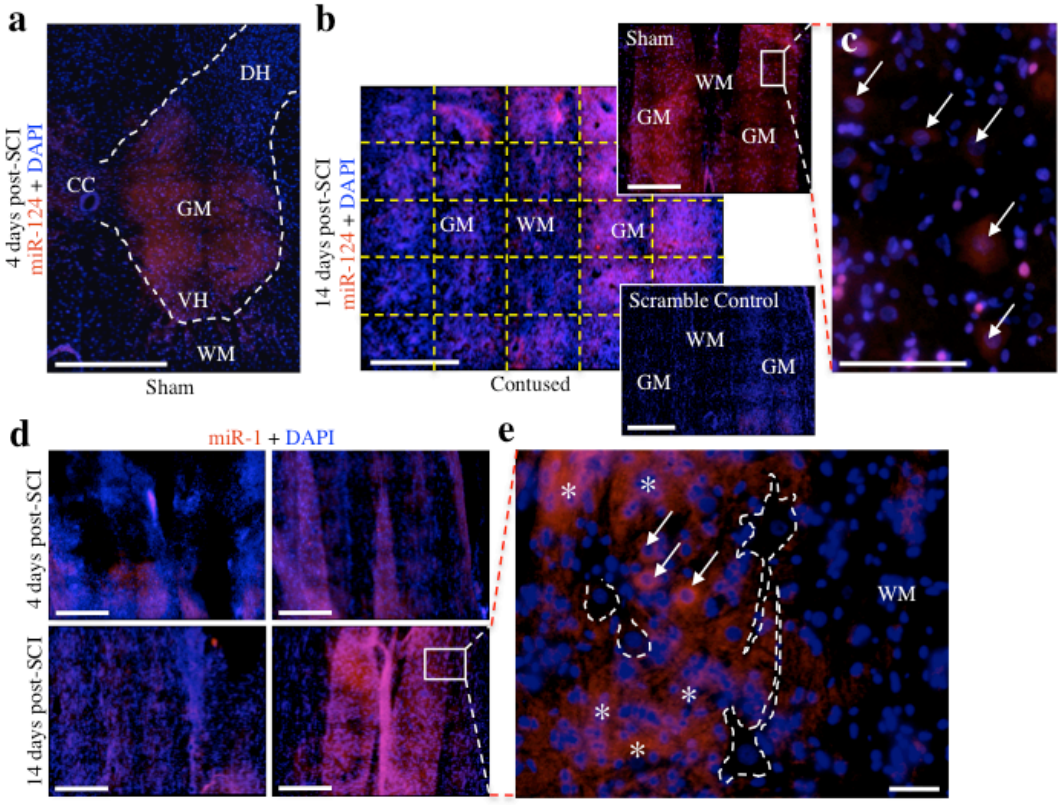


**Figure 5.** *In situ* hybridization analyses for miR124 and miR1 expression following SCI. a-e, Red fluorescence is indicative of miRNA expression, whereas blue fluorescence represents DAPI nuclear staining. Each micrograph is a composite of 25 separate micrographs per fluorescence channel at 20X magnification tiled together. a, Coronal localization of miR124 in sham controls was largely confined to laminae VI-IX of the grey matter, with minimal expression observed in the white matter. Dashed lines demarcate the grey matter boundaries. b, MiR124 exhibits reduced expression at the injury site of contused animals at 14 days post-SCI and localizes to grey matter tracts (hybridization pattern was similar at 4 days; data not shown). The scrambled miRNA control exhibited virtually undetectable levels of hybridization confirming the validity of the observed hybridization, as well as with other miRNA-targeted probes. Dashed yellow lines illustrate the orientation of the tiled micrographs stitched together to form one image. c, High magnification photomicrograph of sham control in (b) shows that miR124 localizes primarily to soma of large neuronal cells (indicated by arrows) in the grey matter of control animals. This neuronal hybridization is lost following SCI. d, MiR1 expression is reduced at the injury site of contused animals at both 4 and 14 days post-SCI and localizes to grey matter tracts. Expression in contused specimen was confined to peri-lesion tissue. e, High magnification photomicrograph of sham control in (d) indicates that miR1 expression is bound primarily to the neuropil with minimal expression in large neuronal cells. Arrows indicate cytoplasmic presence of miR1 in presumptive glial cells and asterisks denote miR1-rich areas of the neuropil. Dashed lines demarcate large, presumptive neuronal cells that do not express miR1. Abbreviations, central canal (CC), dorsal horn (DH), grey matter (GM), ventral horn (VH), and white matter (WH). Scale bars, 500 µm (a, b, d) and 50 µm (c, e).

the injury site of both 4 and 14 day specimens relative to sham controls, with expression being confined to peri-lesion tissue (Figure 5d). MiR1 expression localized primarily to the neuropil, and to the soma of small cells, while hybridization was absent in large neuronal-like cells (Figure 5e). Consistent with the qRT-PCR results, miR21 expression was decreased relative to controls at 14 days, but dramatically increased at 4 days (Figure 6a, b). Coincidentally, our laboratory previously reported that miR21 acts as an anti-apoptotic factor in fetal mouse cerebral cortex-derived progenitors (Sathyan et al., 2007), so the significant indication of heavy miR21 up-regulation at 4 days was of particular interest. In order to determine if this marked increase was due to a neural pro-survival response or from the presence of neural progenitors, immunofluorescence analysis for nestin (a neural progenitor factor) was performed immediately upon completion of the *in situ* hybridization protocol. Interestingly, expression of both nestin and miR21 increased substantially in central grey matter bands near the lesion site relative to sham controls, and exhibited a high degree of co-localization (Figure 6a). Coronal sections of the lesion site indicated that the increased miR21 expression observed in longitudinal sections extends throughout the grey matter, including both the dorsal and ventral horns, with low expression observed in the surrounding white matter (Figure 6b). Furthermore, expression of both miR21 and nestin was largely absent in peri-lesion tissue, suggesting that the sharp increase in miR21 expression, validated with qRT-PCR, was primarily bound to lesion-associated, immature neural cells (Figure 6a).

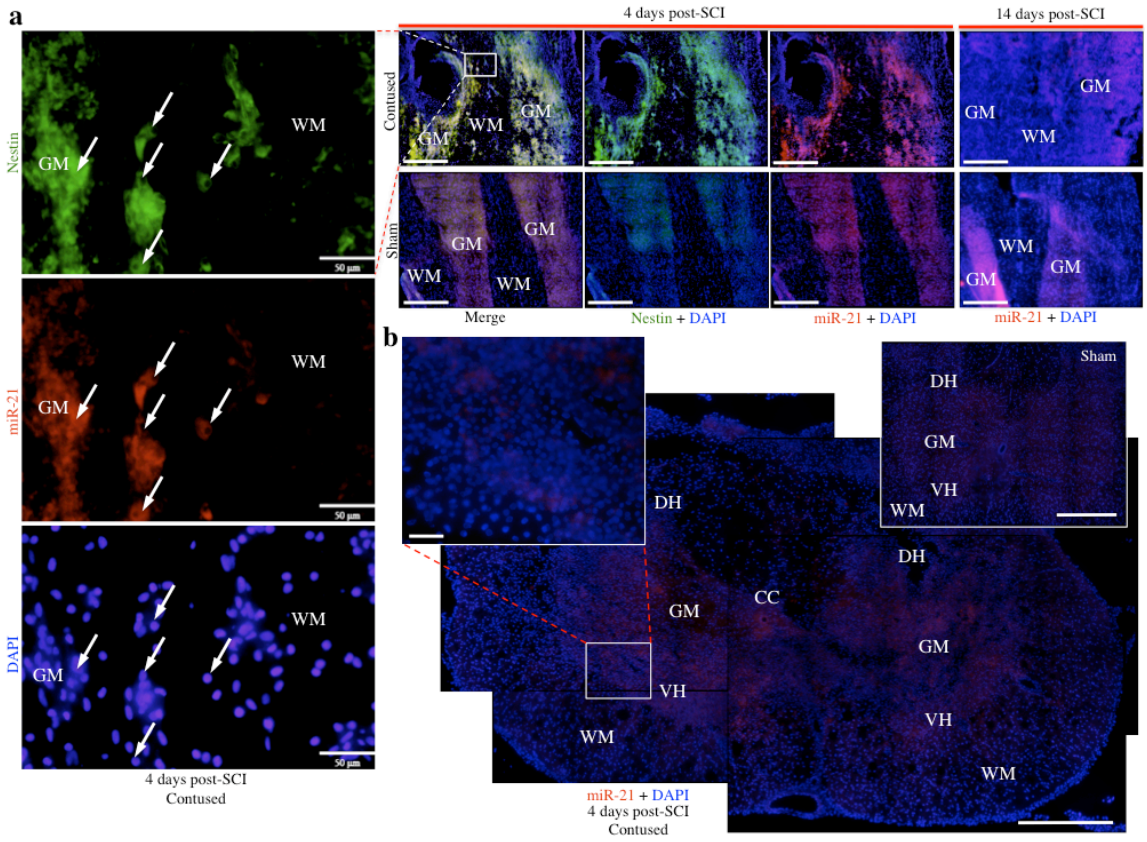


**Figure 6.** *In situ* hybridization analyses for miR21 expression at 4 and 14 days following SCI. a, Substantially increased expression of miR21 was observed within the grey matter at 4 days in contused animals and co-localized with nestin, indicated by yellow fluorescence (red = miR21; green = nestin). High magnification photomicrograph excerpts from the lesion site at 4 days show that nestin and miR21 co-localize to cells with small nuclei, and nestin appears globular as opposed to the fibrous morphology typically associated with astrocytes. Furthermore, miR21 is only observed within grey matter at the lesion site, with low peri-lesion expression. In contrast, decreased miR21 expression relative to sham animals was observed within grey matter tracts at the injury site 14 days post-SCI. b, MiR21 localizes throughout the grey matter tissue of coronal sections, including both the dorsal and ventral horns, with minimal expression in white matter. The coronal image of the lesion site is an overlaid composite of 4 coronal images of the same contused section, each containing 25 micrographs at 20X magnification stitched together per fluorescence channel, for an overall total of 200 micrographs stitched together to form one image (25 images per channel x 2 channels x 4 stitched coronal micrographs = 200 images). Abbreviations, central canal (CC), dorsal horn (DH), grey matter (GM), ventral horn (VH), and white matter (WH). Scale bars, 500 µm (a, b) and 50 µm (high magnification excerpts a, b).

The hybridization patterns for miR129-2 and miR129-1 at 4 days post-SCI were similar, comprised of high expression in cells near the lesion but low expression in peri-lesion tissue, particularly in white matter, relative to sham controls (Figure 7a, 6b). Specifically, in sham-lesioned control animals, expression of miR129-1 was observed within the cytoplasm of large neuronal-like cells (Figure 7c). In contrast, at 14 days post-lesion, miR129-1 expression was virtually undetectable within the lesion site, and was notably present only in peri-lesion grey matter tracts (Figure 7d). In addition, miR129-1 and miR129-2 were both negatively regulated in sections rostral to the injury site at 14 days, with expression primarily limited to grey matter tracts, and low expression throughout the white matter.

Subsequently, immunofluorescence analyses of biomarkers present at 14 days post-SCI was performed to correlate cellular identity after SCI with miRNA expression patterns. Following SCI, nestin expression was observed at the lesion site throughout the gray matter, including both the dorsal and ventral horns, which typically indicates either the presence of neural progenitor cells involved in the adaptive formation of new neurons, or reactive astrocytes contributing to glial scar formation (Gilyarov, 2008; Figure 8a-e). However, in contrast to the gray matter localization of nestin, glial fibrillary acidic protein (GFAP), an intermediate filament specific within the CNS to astrocytes and other glial cells, was primarily observed in the white matter following SCI, though nominal expression was observed in grey matter as well (Figure 8f-h). Although there was notable presence of reactive astrocytes (nestin+/GFAP+), the lesion site also contained large networks of nestin+/GFAP- cells containing neuronal

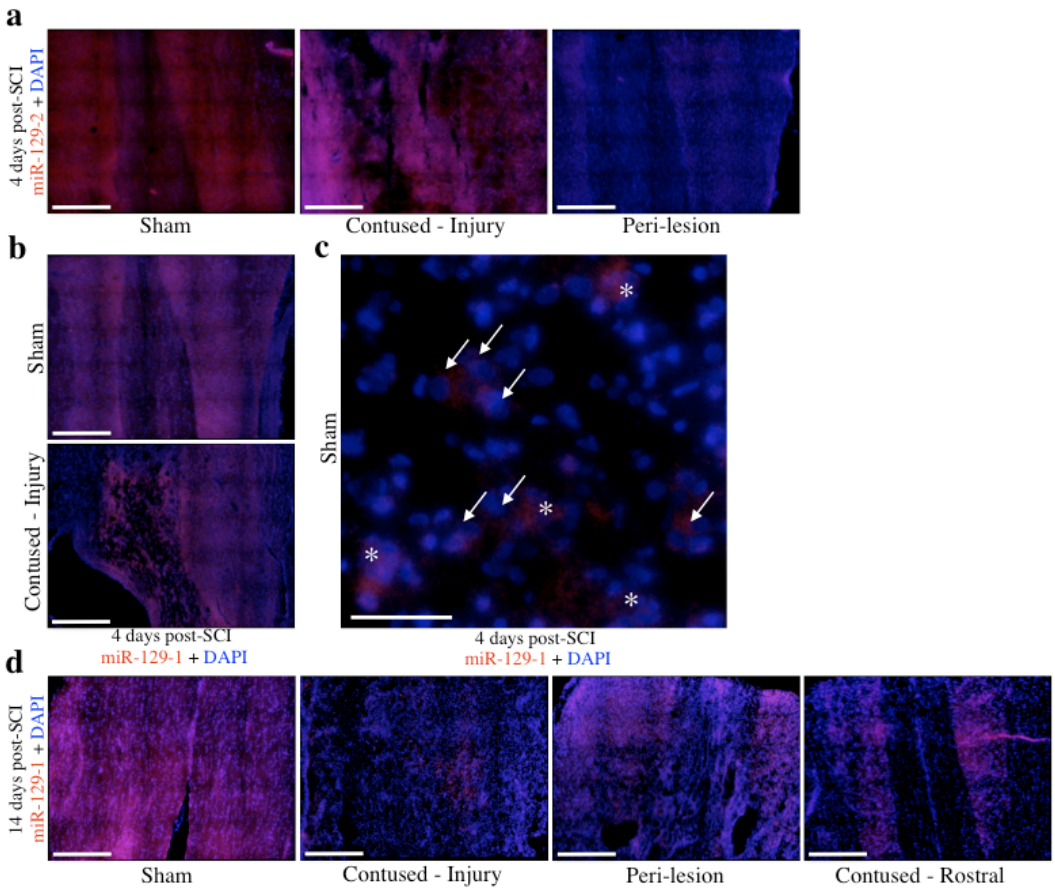


**Figure 7.** *In situ* hybridization for miR129-2 and 129-1 at statistically significant time points following SCI as determined from qRT-PCR. a-d, Red fluorescence is indicative of miRNA expression, whereas blue represents nuclear (DAPI) fluorescence. a, Decreased expression of miR129-2 was observed at 4 days in peri-lesion tissue of contused animals, but expression was present within the lesion site itself. b, Similarly, miR129-1 followed the same localization pattern at 4 days with expression being bound to lesion-associated cells only. c, High magnification micrograph of sham control at 4 days post-SCI shows both cytoplasmic and nuclear labeling of miR129-1 in the neuropil and large neuronal cells, indicated by asterisks and arrows, respectively. d, Conversely, expression at 14 days post-SCI was low within the lesion itself and localized predominately with peri-lesion grey matter at the rostral and caudal sectional extremes, with decreased expression also observed in tissue 1cm rostral to the lesion site. Scale bars, 500 µm (a, b, d) and 50 µm (c).

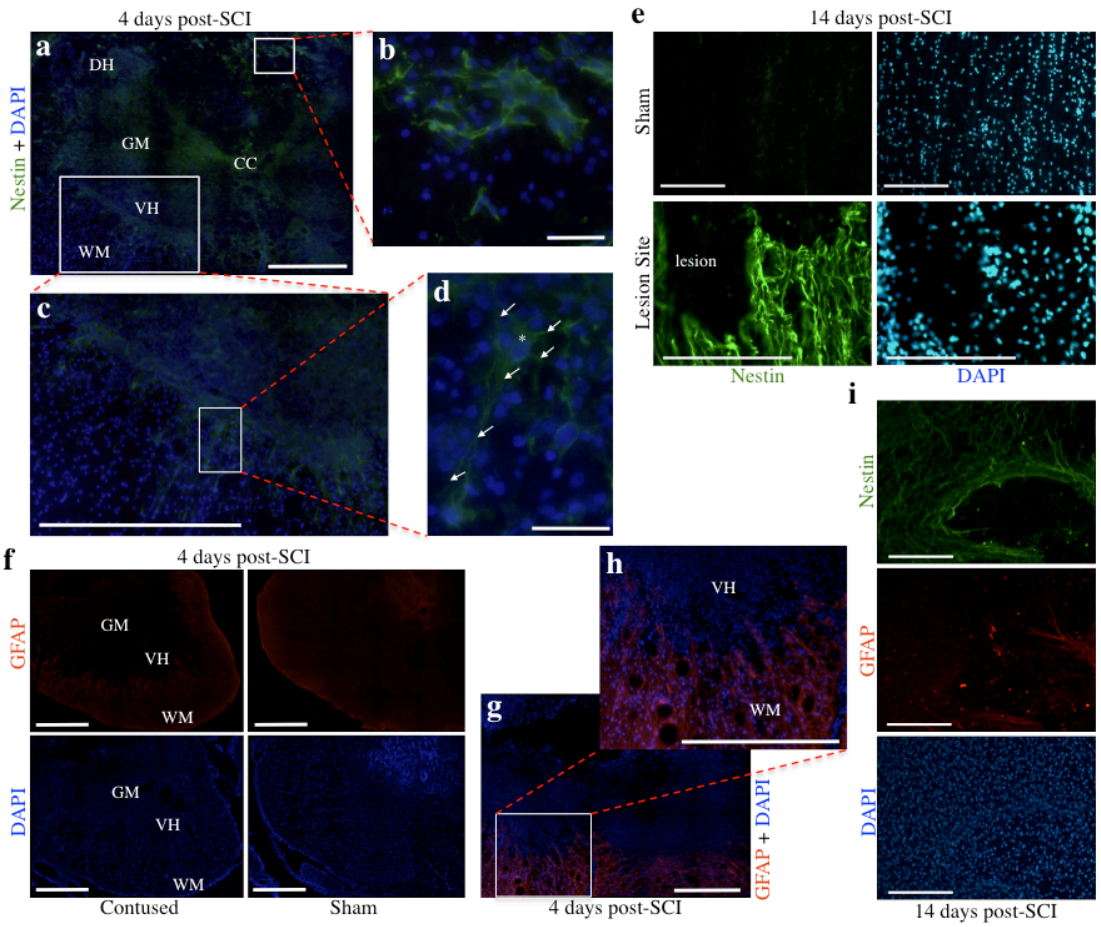


**Figure 8.** Expression of biomarkers for neural differentiation is consistent with the emergence of neuronal immaturity in addition to reactive astrocytes. a-e, Nestin expression is increased in contused specimens both 4 and 14 days after SCI. a, Increased nestin expression was observed throughout the grey matter, and in both the dorsal and ventral horns, in coronal sections of contused animals 4 days following injury. b-d, High magnification micrographs show nestin fiber tracts associated with small glial cells in the white matter/remnants of the dorsal horn (b), nestin positive cells along the interface between the ventral horn and white matter (c), and a large, nestin positive neuronal cell projecting into the white matter from the ventral horn (d). Arrows label nestin-labeled processes of the neuron, and an asterisk denotes the large nucleus; note the triangular shaped cell body and long axonal process. e, At 14 days post-surgery, contused specimens illustrated a higher level of nestin expression than that observed at 4 days, relative to sham controls. f-i, In addition to nestin, contused specimens also exhibited an increase in GFAP (f), but expression was largely confined to white matter (g, h) and GFAP and nestin did not co-localize exclusively. i, Large numbers of nestin+/GFAP- cells with long processes were observed within the lesion site, indicative of neuronal immaturity rather than reactive astrocytosis. Abbreviations, central canal (CC), dorsal horn (DH), grey matter (GM), ventral horn (VH), and white matter (WH). Scale bars, 500 µm (a, c, f-h), 200 µm (e, i) and 50 µm (b, d).

morphologies such as long axonal-like processes and large nuclei (Figure 8i), whereas sham controls exhibited minimal nestin expression (Figure 8e). In addition, REST, a transcription factor present in neural progenitor cells and indirectly inhibited through a negative feedback loop by miR124 to induce neuronal fate (Visvanathan et al., 2007), was up-regulated in and adjacent to the lesion site, but not in sham controls (Figure 9a-d). Furthermore, expression of neurofilament was localized to fibers running proximal and parallel to nestin-positive processes, but did not display co-localization (Figure 10a), indicative that the nestin-positive cells are not mature neurons (Figlewicz et al., 1988; Lagace et al., 2007). To address the possibility that the nestin+/GFAP- regions are active sites for adult neurogenesis following SCI, tissue was immunostained for nestin and the transcription factor SOX2, a positive regulator of nestin during neurogenesis that is expressed in stem and progenitor cells (Jin et al., 2009). Interestingly, at 4 days, SOX2 expression was observed throughout the grey matter, including both the ventral and dorsal horns (Figure 10b), specifically in two groups of cells within the lesion site: within clusters of small, immature cells that were also nestin-positive (indicating activation of stem cell niches within the lesion site; Figure 10d), and within nuclei of large neuronal cells (Figure 10c, e). The expression of Sox2 in the latter cell population, while not co-localized with nestin (Figure 10f), was nevertheless consistent with the disappearance of miR124 (Figure 5b) and the appearance of REST (Figure 9a-d), and supports a hypothesis that neurons within the lesion site transiently revert to a more immature phenotype. In contrast, substantially lower levels of SOX2 were observed

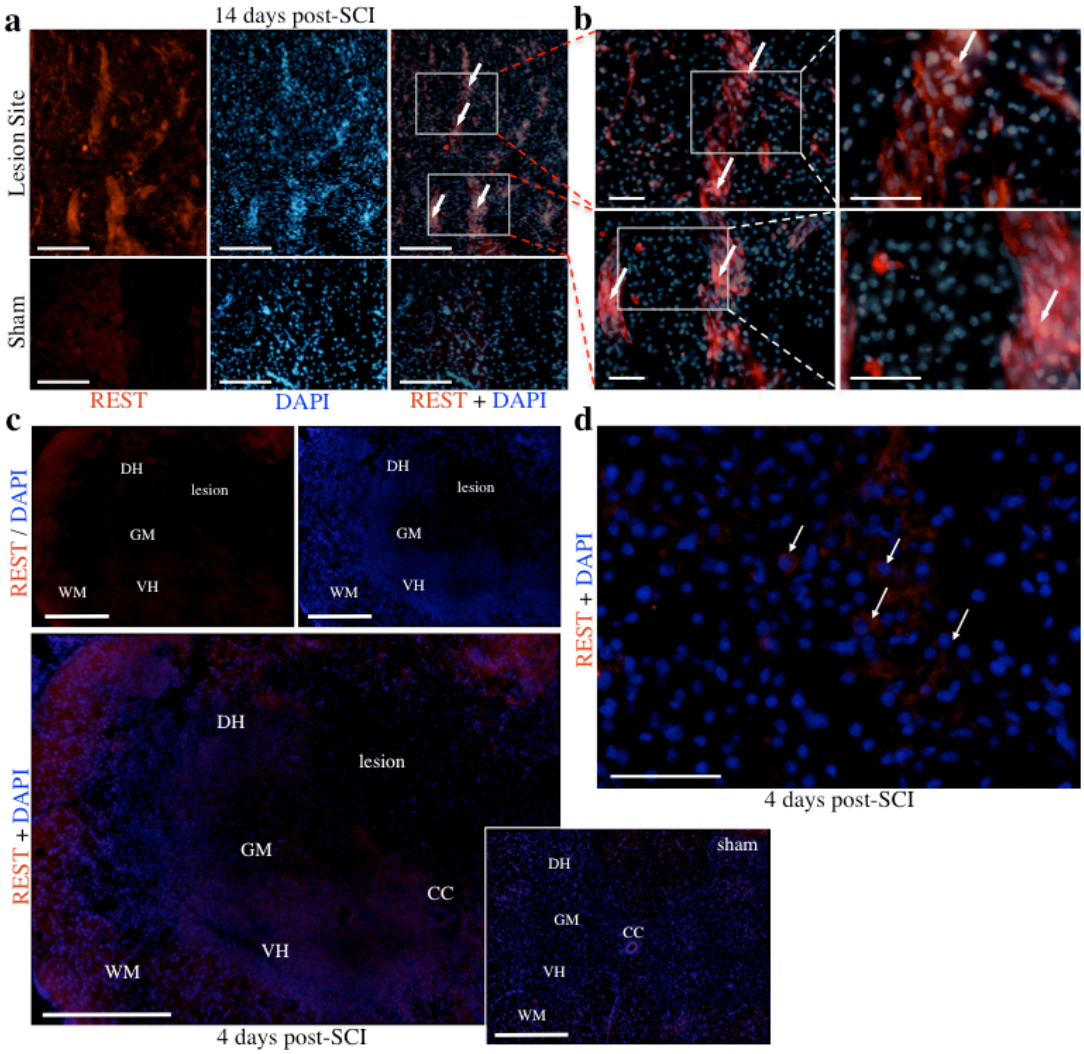


**Figure 9.** Expression of REST is increased following SCI. a, REST expression at 14 days was increased in cells within and adjacent to the lesion site, but not in sham controls. b, Boxed in sections from (a) are shown in higher magnification in adjacent panels (20X and 40X, respectively). c, Expression of REST at 4 days increased within both white and grey matter of coronal sections, including the dorsal and ventral horns. d, High magnification micrograph shows cytoplasmic REST expression in large neuronal cells (indicated by arrows) of a contused specimen 4 days post-SCI. Abbreviations, central canal (CC), dorsal horn (DH), grey matter (GM), ventral horn (VH), and white matter (WH). Scale bars, 500 μm (c), 200 μm (a) and 50 μm (b, d).

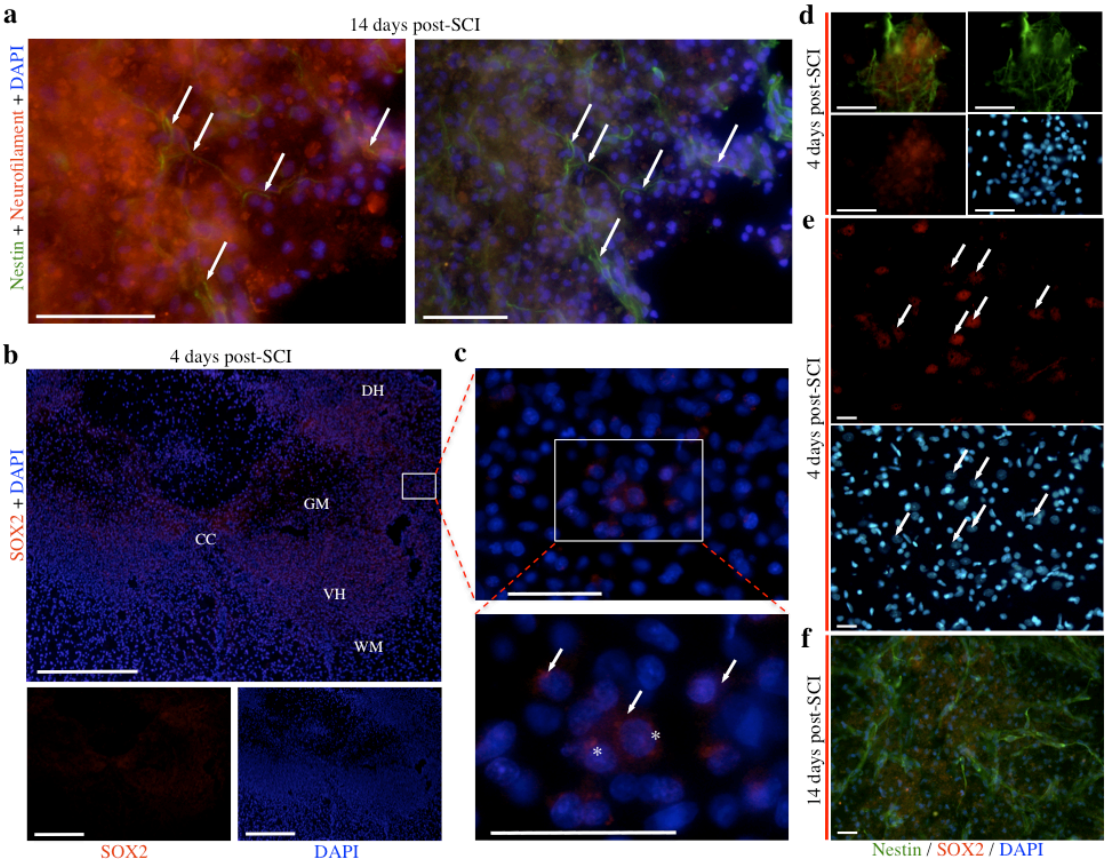


**Figure 10.** Expression of SOX2 is increased following SCI. a, Nestin and neurofilament fiber tracts run parallel to one another, but do not co-localize, indicating that nestin+ cells are not mature neurons. The globular appearance of red immunofluorescence is indicative of neurofilament depolymerization within injured neurons at the lesion site. Arrows point to nestin immunoreactive fibers within the lesion site perforating through a region of grey matter containing damaged neurons labeled with globular neurofilament-like immunofluorescence. b-e, Localization of SOX2 at 4 days post-SCI. SOX2 was observed throughout the grey matter in coronal sections, including both the dorsal and ventral horns (b), and high magnification micrographs illustrate both cytoplasmic and nuclear labeling within large neuronal cells, indicated by arrows and asterisks, respectively (c). SOX2 (red) co-localizes to small clusters of nestin positive cells (green) within the lesion site (d), indicating emergence of neural progenitor cells following SCI. SOX2 expression (red, arrows) is also observed in nestin-negative neuronal cells in the peri-lesion region (e). f, At 14 days post-SCI, low levels of SOX2 expression are observed following injury, and SOX2 does not co-localize with nestin, suggesting that these nestin-positive cells are further differentiated towards their neuronal lineage. Abbreviations, central canal (CC), dorsal horn (DH), grey matter (GM), ventral horn (VH), and white matter (WH). Scale bars: 500 μm (b) and 50 μm (a, c-f).

at 14 days, along with increased nestin expression, and co-localization with nestin was negligible (Figure 10g).

*2.4.4 Bioinformatics analyses of miRNA targets*

To determine the functional significance of miRNA expression changes, validated gene targets of miRNAs were obtained from miRWALK (Dweep et al., 2011) and cross-referenced to determine gene targets common between multiple miRNAs. These lists were then grouped into two categories, those that were common targets of miR1 and miR124, and a second group containing common targets of miR21 and miR146a. The resulting gene lists were then analyzed using the DAVID Bioinformatics Resources for functional annotation (Dennis et al., 2003; Huang da et al., 2009; Table 1).

Quantitative RT-PCR data indicated that both miR1 and miR124 were down-regulated at 4 and 14 days, and initial bioinformatics showed that they target similar types of genes, so they were grouped together for functional analysis. Functional annotation revealed that both miRNAs are inhibitors gene networks that promote transcription and translation (for significant Gene Ontologies, see Table 1), and their down-regulation results in an increase in protein synthesis that contributes to the initiation of cell cycle, induction of apoptosis, and response to inflammation. Interestingly, inhibition of these miRNAs also promotes cell motility, which is indicative of the emergence of immature cells and, in conjunction with cell cycle initiation, reaffirms the immunofluorescence observations that neurons at the injury site appear to be shifting to a pre-neuronal state.

**Table 1.** Statistical annotation of miRNA function. Gene targets of SCI-sensitive miRNAs, were identified using miRWALK (Dweep et al., 2011). This analysis was limited to miRNA gene targets that were identified from the published literature and cross-referenced for gene targets shared by two or more SCI-sensitive miRNAs. The cross-referenced lists were grouped according to similarity, and functional annotation by Gene Ontology Term (Ashburner et al., 2000) was performed in two groups, one for miR1 and miR124, and another for miR21 and miR146a common targets (Dennis et al., 2003; Huang da et al., 2009). Enriched Gene Ontologies were retained when the Benjamini corrected Fisher Exact *t*-test *p*-value was less than 0.05.

| **Gene Ontology ID ~ functional term** | **Gene Count** | **Benjamini *p*-value** |
|---|---|---|
| ***miR-1 and miR-124 common targets*** | | |
| GO:0006357~regulation of transcription from RNA polymerase II promoter | 17 | 1.72E-02 |
| GO:0006928~cell motion | 12 | 4.70E-02 |
| GO:0010608~posttranscriptional regulation of gene expression | 8 | 4.66E-02 |
| GO:0022402~cell cycle process | 13 | 4.67E-02 |
| GO:0032268~regulation of cellular protein metabolic process | 17 | 6.03E-04 |
| GO:0042981~regulation of apoptosis | 17 | 3.67E-02 |
| GO:0043065~positive regulation of apoptosis | 12 | 3.61E-02 |
| GO:0045449~regulation of transcription | 35 | 4.29E-02 |
| GO:0048545~response to steroid hormone stimulus | 9 | 1.61E-02 |
| h_tnfr1Pathway:TNFR1 Signaling Pathway | 7 | 8.39E-04 |
| ***miR-21 and miR-146a common targets*** | | |
| GO:0008284~positive regulation of cell proliferation | 6 | 6.94E-03 |
| GO:0008285~negative regulation of cell proliferation | 6 | 4.28E-03 |
| GO:0009628~response to abiotic stimulus (radiation, UV) | 8 | 8.54E-05 |
| GO:0032268~regulation of cellular protein metabolic process | 7 | 1.69E-03 |
| GO:0033554~cellular response to stress | 6 | 2.26E-02 |
| GO:0042127~regulation of cell proliferation | 11 | 2.69E-05 |
| GO:0042981~regulation of apoptosis | 10 | 1.11E-04 |
| GO:0043065~positive regulation of apoptosis | 9 | 2.71E-05 |
| GO:0043066~negative regulation of apoptosis | 6 | 4.20E-03 |
| GO:0044451~nucleoplasm part | 7 | 1.53E-02 |
| GO:0045449~regulation of transcription | 12 | 1.29E-02 |
| hsa04010:MAPK signaling pathway | 7 | 3.81E-03 |

MiR21 and miR146a were both transiently induced following SCI and also had similar validated gene target profiles, so they were analyzed together as a second functional group. Functional annotation illustrates that miR21 and miR146a act primarily to inhibit cell proliferation and apoptosis through the regulation of transcription and translation. In addition, due to their association within the same annotation cluster, it is possible that the primary method by which these two miRNAs regulate cell proliferation is through the inhibition of gene ontology groups including the MAPK signaling and nucleoplasm production pathways (Table 1).

Finally, analysis was not performed for miR129-2 and miR129-1 because validated targets have not been published, and the analysis of predicted targets did not produce statistically significant Gene Ontologies. Further study may be needed to determine valid gene targets of the miR129 family, or to functionally analyze validated targets as they become available in published literature.

## 2.5 Discussion

Spinal cord injury dramatically alters the cellular landscape of impacted tissue through the activation of inflammatory pathways, which ultimately cause further insult by contributing to the pathogenesis of secondary SCI, instead of protective mediation. The resulting loss of cellular plasticity, especially in the presence of uncontrollable nociceptive stimuli, impairs therapeutic efforts to improve functional recovery (Grau et al., 2006; Hook et al., 2009). Because microRNAs are capable of regulating hundreds of genes simultaneously, either post-transcriptionally or through promoter interaction (Li et

al., 2006; Breving and Esquela-Kerscher, 2010), it is likely that they play a major role in the induction of these maladaptive processes following SCI, and could therefore become attractive candidates for drug targets in therapeutic intervention for spinal cord injury.

In the current study we investigated the regulation of microRNAs after SCI. Specifically, we identified 7 miRNAs using microarray analysis that were significantly altered within 4 to 14 days after SCI (223, 21, and 146a positively and 1, 124, 129-2, and 129-1 negatively). Additionally, one other non-coding small RNA, SNORD2, an ATP-dependent helicase important for ribosome-associated translation initiation (Sudo et al., 1995; Hernandez and Vazquez-Pianzola, 2005), was also significantly induced within the lesion site. These data collectively suggest that cellular adaptation to injury involves simultaneous inhibition and initiation of translation resulting in a shift in protein expression profiles in the injury site.

Using both qRT-PCR and *in situ* hybridization analyses, we were able to validate the differential SCI-related expression of all the above miRNAs except for miR223. In contrast to recent reports by Nakanishi et al. (2010), who found that miR223 expression was significantly induced early following injury (6-12 hours, post SCI), we observed that at best, miR223 was induced as a later component (14 days post-SCI) of injury. While we do not as yet understand the source of these temporal variations in miR223 expression, miR223 has recently been implicated in myeloid cell differentiation and may play a role in inflammation (Johnnidis et al., 2008; Pedersen and David, 2008; Tsitsiou and Lindsay, 2009). Consequently, miR223 expression could represent a signature for infiltration of immune cells into the injury site.

Additionally, we found that miR21 was initially induced and then suppressed at the lesion site. Suppression of miR21 has been shown to cause apoptosis in both cortical progenitor cells and gliomas (Corsten et al., 2007; Sathyan et al., 2007; Krichevsky and Gabriely, 2009), so the observed up-regulation of miR21 at 4 days, in conjunction with the simultaneous re-expression of nestin, would suggest a protective role in promoting cell survival and neural progenitor cell integration at the lesion site. While miR21 was transiently increased following SCI, miR146a exhibited a more prolonged increase up to 14 days post SCI. Accumulating evidence indicates that miR146a acts not only as an anti-inflammatory mediator because it inhibits the translation of a number of cytokines and chemokines, including IL-6, IL-8, IL-1β and TNF-α (Taganov et al., 2006; Li et al., 2010a), but also as a pro-growth miRNA, as evidenced by its promotion of cell proliferation in hepatocellular carcinoma (Xu et al., 2008). Indeed, a functional analysis of validated (published) gene targets of SCI-sensitive miRNAs (miRWALK) indicates that both miR21 and miR146a inhibit expression of genes that repress cell proliferation and promote apoptosis. It is therefore possible that miR146a compensates for the decline in miR21, and in doing so, supports cell and tissue growth following SCI, in addition to reducing overall inflammation at the injury site.

We also observed that miR129-2 and miR129-1 were significantly suppressed at 4 days post-SCI, and that this suppression spread rostrally beyond the lesion site at 14 days. Recent evidence shows that the miR129 family inhibits the G1/S phase-specific regulator CDK6, and consequently, miR129 suppression allows post-mitotic, G1 phase-arrested cells to proliferate (Wu et al., 2010). Such aberrant cell cycle entry could

ultimately lead to significant neuronal death (Di Giovanni et al., 2003; Herrup and Yang, 2007). This maladaptive proliferation caused by miR129 down-regulation is contradictory to the pro-growth proliferation induced by increased levels of miR21 and miR146a, which collectively illustrates that the balance between miRNAs like miR21, miR146a, and miR129 may well play a critical role in neuronal survival following SCI.

Interestingly, miR146a and miR129-2 exhibited divergent expression patterns (miR146a was up-regulated and miR129-2 was suppressed) following SCI, when compared to sham control cohorts. However, within the cohort of SCI animals themselves, the initial severity of the lesion was inversely related to later expression of both miRNAs. A less severe injury, as measured by the BBB score on day 1 post-SCI, was associated with increased expression of both miR146a and 129-2 at 4 and up to 14 days later. Moreover, the initial severity of the injury could explain a large and significant proportion of the variability in miRNA expression (63% and 75% for miR146a and miR129-2 respectively), suggesting that these miRNAs in turn may serve as effective therapeutic targets or proxy measures for the severity of an injury. Importantly, expression of none of the other SCI-regulated miRNAs were related to the severity of the injury, suggesting that most other miRNAs respond to injury in a more or less "all or none" manner.

We also observed that following SCI, both miR1 and miR124, best known for their critical role in maintaining the differentiation states of cells and tissues, exhibited a persistent and significant decline. MicroRNA-124, thought to be a neuronal-specific miRNA, drives ectoderm differentiation towards a neuronal lineage through a negative

feedback loop that inhibits REST-mediated repression of neuronal genes, while simultaneously down-regulating non-neuronal genes (Visvanathan et al., 2007). In contrast, miR1 is best known for its capacity to drive mesoderm differentiation into either skeletal or cardiac muscle fates by silencing non-muscle genes (Chen et al., 2006; Ivey et al., 2008; Williams et al., 2009), although this miRNA is also expressed in neural tissue like the brain and spinal cord (Mishima et al., 2007), as well as in the retina, where its expression is altered in several models of retinal neurodegeneration (Loscher et al., 2008). The steep decrease in miR124 expression in the lesion site of contused animals, specifically within the grey matter bands and within the large presumptive motor-neuronal cells, could be partly attributed to the high degree of neuronal death resulting from the primary injury (Nakanishi et al., 2010). However, SOX2 and REST were both up-regulated in large motorneurons that had lost miR124 expression in regions proximal to the lesion site, suggesting that cellular de-differentiation, aside from death, underlies the observed decrease in miR124. Thus, a likely synergistic effect of the concurrent suppression of both miR1 and miR124 would be the transient emergence of a cellular environment highly favorable for plasticity and neural fate reprogramming. However, any early increase in neuronal plasticity at the lesion site, mediated by miR124/miR1 suppression, may ultimately synergize with the pro-apoptotic, pro-cell cycle effects of suppressing miR21/miR129 at 14 days to cause cell cycle failure and induction of apoptosis in surviving post-mitotic neurons.

The lesioned spinal cord exhibits additional evidence for cellular plasticity in the form of activated stem cell niches. While some nestin-positive cells co-localize with

GFAP, indicating the presence of reactive astrocytes, other networks of nestin-positive cells did not exhibit such co-localization. Moreover, within the lesion site, we also observed clusters of nestin-positive cells that also express SOX2, a stem cell-associated transcription factor that controls nestin expression in neural progenitor cells of the CNS to promote differentiation (Jin et al., 2009). The presence of SOX2+/nestin+ and nestin+/GFAP-cells within the lesion site, 4-days post-lesion, suggests the specific activation of stem cell niches and the emergence of cells that exhibit a neuronal progenitor identity. At 14 days post-lesion, nestin-positive cells within the lesion site no longer expressed SOX2 suggesting that these cells had progressed further towards a neural identity.

## 2.6 Conclusions

Our evidence shows that SCI results in a very specific and limited profile of miRNA changes, and that these changes evolve in a coordinated manner over a period of time following the injury. Interestingly, most changes are limited to the lesion site with very limited miRNA dysregulation observed in regions anterior or caudal to the injury site. Over a prolonged period (14 days), only three miRNAs also exhibited spatial dysregulation. MiR129-1 and 129-2 were suppressed in regions anterior to the injury site, whereas miR146a was increased caudal to the injury site. Interestingly, both miR129-2 and miR146a also exhibit a strong potential to be proxy markers for the initial severity of spinal cord injury. These data collectively suggest that global changes in miRNA-driven control of protein-coding gene networks remain largely confined to the

lesion site, with minimal initial adaptations within the surrounding non-injured tissue. It remains to be determined whether other miRNA adaptations appear over time in specific afferent or efferent targets of projections from within the lesion site, including cortical, thalamic or lower motor-neuron targets.

A statistical analysis of the gene ontology classifications of published mRNA targets associated with the miRNAs aberrantly expressed following SCI yields a cohesive picture of miRNA involvement favoring a loss of neuronal identity and the emergence of neuronal progenitors within the lesion site. Such a hypothesis is well supported by the induced expression SOX2 and nestin within probable stem cell niches. It is additionally supported by the expression of both SOX2 and the suppressor of neuronal identity, REST, along with the loss of miR124 within surviving, presumptive motorneurons within the lesion site. In the latter case, this loss of neuronal identity may well be a factor in the induction of apoptosis driving secondary SCI, but could also represent a target of opportunity for therapeutic intervention in the immediate aftermath of SCI. De-differentiating neurons and activated stem cell niches may be subjected to reprogramming, possibly using the complement of miRNAs that are dysregulated following SCI itself. Further functional analyses will be required to explore the therapeutic and regenerative potential of manipulating levels of these SCI-sensitive miRNAs, in the immediate and prolonged time period following an injury, to minimize secondary injury and enhance functional recovery.

# 3. THE ASSOCIATION BETWEEN SCI-SENSITIVE MIRNAS AND PAIN SENSITIVITY, AND THEIR REGULATION BY MORPHINE

## 3.1 Overview

Increased pain sensitivity is a common sequel to spinal cord injury (SCI). Moreover, drugs like morphine, though critical for pain management, elicit pro-inflammatory effects that exacerbate chronic pain symptoms. Previous reports showed that SCI results in the induction and suppression of several microRNAs (miRNAs), both at the site of injury, as well as in segments of the spinal cord distal to the injury site. We hypothesized that morphine would modulate the expression of these miRNAs, and that expression of these SCI-sensitive miRNAs may predict adaptation of distal nociceptive circuitry following SCI. Our data indicated that expression of miR1, miR124, and miR129-2 at the injury site predicted the nociceptive response mediated by spinal regions distal to the lesion site, suggesting a molecular mechanism for the interaction of SCI with adaptation of functionally intact distal sensorimotor circuitry. Moreover, the SCI-induced miRNA, miR21 was induced by subsequent morphine administration, representing an alternate, and hitherto unidentified, maladaptive response to morphine exposure. Contrary to predictions, mRNA for the pro-inflammatory interleukin-6 receptor (IL6R), an identified miR21 target, was also induced following SCI, indicating dissociation between miRNA and target gene expression. Moreover, IL6R mRNA expression was inversely correlated with locomotor function suggesting that inflammation is a predictor of decreased spinal cord function. Collectively, our data indicate that miR21 and other SCI-sensitive

miRNAs may constitute therapeutic targets, not only for improving functional recovery following SCI, but also for attenuating the effects of SCI on pain sensitivity.

## 3.2 Introduction

The effects of spinal cord injury (SCI) can be severely debilitating, especially the chronic presence of neuropathic pain that affects close to two-thirds of all spinal cord-injured patients (Siddall and Loeser, 2001; Anderson, 2004). One of the primary treatments for chronic pain following SCI is administration of opiate analgesics such as morphine, which are also given during the acute phase of spinal injury for pain mitigation (Dworkin et al., 2003; McCarberg, 2004). However, administration of morphine in the acute phase of a spinal contusion injury in rats has been shown to significantly attenuate locomotor function and increase expression of chronic pain symptoms (Hook et al., 2007; Hook et al., 2009). The increased chronic pain associated with morphine administration has been attributed to the activation of astrocytes and microglia by morphine and inhibition of analgesic effects by increased expression of pro-inflammatory cytokines TNFα, IL-1β, and IL-6 (Song and Zhao, 2001; Raghavendra et al., 2002; Johnston et al., 2004; Cui et al., 2006; Tai et al., 2006). Accordingly, the application of an interleukin-1 receptor antagonist prior to intrathecal morphine prevents the maladaptive effects of morphine on neuropathic pain and functional recovery (Hook et al., 2011).

While these results are promising, there is limited knowledge of the remodeling of pain neuro-circuitry and the activation of potentially maladaptive gene regulatory

networks following morphine treatment in SCI. MiRNAs are short, 18 to 25 nucleotide-long non-coding small RNAs that play an important regulatory role in gene expression by inhibiting protein translation or targeting mRNA transcripts for degradation (Alvarez-Garcia and Miska, 2005; Zamore and Haley, 2005). Individual miRNAs are able to coordinate gene networks to affect a specific cellular endpoint by simultaneously controlling expression of several hundred mRNAs. Furthermore, miRNAs have been implicated in physiological processes relevant to neuropathic pain, including innate immune responses involved in wound inflammation (Williams et al., 2008; Roy and Sen, 2011) and the regulation of inflammation in response to morphine treatment in human monocyte-derived macrophages (Dave and Khalili, 2010).

MiRNAs are also dysregulated following SCI (Liu et al., 2009; Nakanishi et al., 2010; Strickland et al., 2011; Yunta et al., 2012). We previously reported that miR124, miR129, and miR1 were significantly down-regulated following spinal cord contusion, while both miR21 and miR146a were transiently induced, and changes in miR146a and miR129-2 expression significantly explained the variability in injury severity (Strickland et al., 2011). We hypothesized that the temporal expression of miR146a, miR21, and other SCI-sensitive miRNAs may be further dysregulated following administration of morphine in the acute phase of a spinal contusion injury. Such dysregulation could constitute an important role in both inflammation and the progression of neuropathic pain during the chronic phase of injury. Moreover, these miRNAs may contribute towards the regulation of the nociceptive circuitry and chronic effects of morphine exposure. To assess these possibilities, the current study investigated the relationship

between SCI-sensitive miRNA expression and morphine administration, evaluated at 2 and 15 days post-SCI to explore the effects of acute morphine treatment in both the acute and chronic phases of SCI. In addition, we also investigated the relationship between miRNA expression and the variance in baseline and morphine-attenuated pain sensitivity following SCI.

## 3.3 Experimental Procedures

### *3.3.1 Subjects*

All of the experiments were reviewed and approved by the institutional animal care committee at Texas A&M University and all NIH guidelines for the care and use of animal subjects were followed. Male Sprague–Dawley rats (*Rattus norvegicus*) obtained from Harlan (Houston, TX) at approximately 90-110 days old (300-350 g) were individually housed in Plexiglas bins [45.7 (length) x 23.5 (width) x 20.3 (height) cm] with food and water continuously available. To facilitate access to the food and water, extra bedding was added to the bins after surgery and long mouse sipper tubes were used so that the rats could reach the water without rearing. Subjects were weighed on the same days that they were assessed for locomotor function, and were checked daily for signs of autophagia and spasticity. A subject was classified as having spasticity if the limb was in an extended, fixed position and was resistant to movement. Bladders were manually expressed in the morning (8:00-9:30 hrs) and evening (18:00-19:30 hrs) until subjects regained bladder control, which was operationally defined as three consecutive

days with an empty bladder at the time of expression. The rats were maintained on a 12 hr light/dark cycle and tested during the last 6 hrs of the light cycle.

*3.3.2 Surgery*

Subjects were anesthetized with isoflurane (5%, gas). Once a stable level of anesthesia was achieved, the inspired concentration of isoflurane was lowered to 2-3% and an area extending approximately 4.5 cm above and below the injury site was shaved and disinfected with iodine. A 7.0 cm incision was made over the spinal cord. Next, two incisions were made on either side of the vertebral column, extending about 3 cm rostral and caudal to the T12-T13 segment. The dorsal spinous processes at T12-T13 were removed (laminectomy), and the spinal tissue exposed. The dura remained intact. For the contusion injury, the vertebral column was fixed within the MASCIS device (Gruner, 1992; Constantini and Young, 1994) and a moderate injury was produced by allowing the 10 g impactor (outfitted with a 2.5 mm tip) to drop 12.5 mm. Sham controls received a laminectomy, but the cord was not contused with the MASCIS device. Following surgery, the wound was closed with Michel clips. T12-T13 level contusion models have been routinely used by members of our group to define spinal cord learning circuits and molecular mechanisms involved with recovery of function (Ferguson et al., 2008; Brown et al., 2011; Hook et al., 2011). Lesions at this level result in well-defined and replicable sensory-motor deficits, and we therefore chose to utilize contusion at this level to also examine changes in miRNA expression.

An intrathecal cannula was also inserted into the subarachnoid space immediately after the contusion injury. For this procedure, a 15 cm long polyethylene (PE-10) cannula, fitted with a 0.23 mm (diameter) stainless steel wire (SWGX-090, Small Parts), was threaded 2 cm under the vertebrae immediately caudal to the injury site. The cannula tip terminated over the S2-S3 spinal segments, so that morphine was delivered to the lumbosacral regions mediating hind-paw pain reactivity. To prevent cannula movement, the exposed end of the tubing was secured to the vertebrae rostral to the injury using an adhesive (Cyanoacrylate). The wire was then pulled from the tubing and the wound was closed using Michel clips.

To help prevent infection, subjects were treated with 100,000 units/kg Pfizerpen (penicillin G potassium) immediately after surgery and again 2 days later. For the first 24 hrs after surgery, rats were placed in a recovery room maintained at 26.6 $^{0}$ C. To compensate for fluid loss, subjects were given 2.5 ml of saline after surgery. Michel clips were removed 14 days after surgery.

*3.3.3 Drug administration*

After baseline assessments of locomotor and sensory function, rats were assigned to a morphine or vehicle treatment group. Twenty-four hours or 14 days after injury, the rats were given an intrathecal infusion of morphine sulfate (90 μg i.t., Mallinckrodt, Hazelwood, MI) dissolved in 2 μL of distilled water. This dose of morphine was chosen based on previous studies that demonstrated that this high dose is required to achieve strong anti-nociception and block behavioral reactivity to nociceptive stimulation after

SCI, as well as being detrimental to long-term recovery of locomotor function (Hook et al., 2009; Hook et al., 2011). Control subjects were treated with 2 μL of vehicle. These drug injections were followed by a 10 μL injection of saline, to flush the catheter. Locomotor ability was assessed with the BBB scale prior to and after drug treatment. This behavioral index was used to ensure that injury severity was balanced across groups prior to drug treatment.

*3.3.4 Assessment of locomotor function*

Locomotor behavior was assessed using the Basso, Beattie and Bresnahan (BBB) scale (Basso et al., 1995), in an open enclosure (99 cm diameter, 23 cm deep). This 21-point scale is used as an index of hindlimb functioning after a spinal injury. Using this scale, no movement of the hindlimbs (ankle, knee or hip) is designated a score of 0, and intermediate milestones include slight movement of one joint (1), extensive movement of all three joints (7), occasional weight supported stepping in the absence of coordination (10), and consistent weight supported stepping with consistent FL-HL coordination (14). Higher scores reflect consistent limb coordination and improved fine motor skill. Baseline motor function was assessed on the day following injury and prior to drug treatment. Because rodents often freeze when first introduced to a new apparatus, subjects were acclimated to the observation fields for 5 min per day for 3 days prior to surgery. Each subject was placed in the open field and observed for 4 min. Care was taken to ensure that the investigators' scoring behavior had high intra- and inter-observer

reliability (all r's > 0.89) and that they were blind to the subject's experimental treatment.

*3.3.5 Sensory reactivity*

For the assessment of morphine efficacy, nociceptive reactivity was assessed immediately before and 30 minutes after intrathecal morphine administration. Thermal reactivity was assessed using radiant heat in the tail-flick test. Subjects were placed in the restraining tubes with their tail positioned in a 0.5 cm deep groove, cut into an aluminum block, and allowed to acclimate to the apparatus (IITC Inc., Life Science, CA) and testing room for 15 min. The testing room was maintained at 26.5˚C. Thermal thresholds were then assessed. Thermal reactivity was tested using a halogen light that was focused onto the rat's tail. Prior to testing the temperature of the light, focused on the tail, was set to elicit a baseline tail-flick response in 3-4 sec (average). This pre-set temperature was maintained across all subjects. In testing, the latency to flick the tail away from the radiant heat source (light) was recorded. If a subject failed to respond, the test trial was automatically terminated after 8 s of heat exposure. Two tests occurred at 2-minute intervals, and the second test's tail-flick latencies were recorded. To confirm that subjects did not respond in the absence of the stimuli, blank trials were also performed. A 'false alarm' was recorded if subjects made a motor or vocalization response during the blank tests. The blank trials were performed 1 min before or after each sensory test (in a counterbalanced fashion). No false alarms were recorded.

*3.3.6 Isolation of RNA for qRT-PCR*

Subjects were euthanized (100 mg/kg of pentobarbital, i.p.) 24 hrs after drug treatment. A 5 mm segment of spinal cord from the injury site, hearts, and carotid arteries were collected, snap frozen in liquid nitrogen, and stored at –80 °C until further analysis. Specimens were crushed and RNA was isolated using the TRIzol (Invitrogen; Carlsbad, CA) protocol. Total RNA was then quantified using a NanoDrop 2000 Spectrophotometer (Thermo Scientific; Wilmington, DE) and stored at -80 °C.

*3.3.7 Quantitative RT-PCR*

MiRNA expression data was measured with quantitative reverse transcription (qRT)-PCR for miRNAs, based on the protocol of the miRCURY$^{TM}$ LNA microRNA Universal RT-PCR system (EXIQON; Woburn, MA). RNA samples were converted to cDNA, and qRT-PCR was performed using a 7900HT Fast Real-Time PCR System (Applied Biosystems, Foster City, CA). Forward and reverse primers (EXIQON; Woburn, MA) for hsa-miR124, hsa-miR1, hsa-miR21, hsa-miR129-2, and hsa-miR146a were used for PCR amplification, and real time data was normalized using U6 RNA. Similarly, messenger RNA (mRNA) expression of IL-6 receptor (IL6R) was measured using qRT-PCR for mRNAs, based on the protocol for PerfeCTa® SYBR® Green SuperMix with ROX™ (Quanta Biosciences; Gaithersburg, MD). RNA samples were converted to cDNA using qScript™ cDNA SuperMix (Quanta Biosciences; Gaithersburg, MD), and qRT-PCR was performed using a 7900HT Fast Real-Time PCR System (Applied Biosystems, Foster City, CA). Forward and reverse primers (Integrated DNA

Technologies; Coralville, IA) for IL-6R were used for PCR amplification, and real time data was normalized using glyceraldehyde 3-phosphate dehydrogenase (GAPDH). Relative miRNA and mRNA expression was determined by calculating the mean difference between cycle threshold of either the miRNA from the U6 small nuclear RNA ($U6_{SNB}$) normalized control, or the IL6R mRNA from the GAPDH normalized control for each sample [Δ cycle threshold (ΔCT)] within each sample group (samples with same miRNA ID, time, and condition parameters) and expressed as -ΔCT for relative change in expression. Sample means that were greater than ± 2 standard deviations from the mean ΔCT, or ± 3 standard deviations from the mean ΔCT after exclusion, were considered outliers and removed from the analysis. Of the 218 data points in 36 groups used in the analysis, only 14 data points were excluded according to this criteria, and no more than one data point in any individual experimental group was excluded. Fold change in miRNA/mRNA expression was determined by calculating the difference between the mean ΔCTs of sham, morphine, and vehicle sample groups at the same time point (-ΔΔCT), and expressed as a baseline-corrected percentage of fold-change ($[2^{-\Delta\Delta CT}-1]*100$).

*3.3.8 Data analysis*

All data were analyzed using SPSS software version 18 (SPSS; Chicago, IL). MicroRNA expression, verified by qRT-PCR, was analyzed by multivariate analysis of variance (ANOVA) using Pillai's trace statistic, and further analyzed using *post hoc* univariate ANOVA and Fisher's least significant difference (f-LSD) test. Other data

were analyzed using ANOVAs followed by *post hoc* f-LSD using planned comparisons. In all cases, the *a priori* α value was set at 0.05. Data were expressed as mean ±SEM, as indicated in the figure legends.

Correlations between initial injury severity and either miRNA or IL6R mRNA expression, and between tail-flick latency and either miRNA or IL6R mRNA expression, were determined by Pearson's product-moment correlation (PPMC) using –ΔCT values of either the miRNAs or IL6R, initial BBB scores, day 13 BBB scores, and tail-flick latency as separate independent variables. All partial correlations were controlled for time only. The *a priori* α value was set at 0.05, and data were expressed as the mean difference in cycle threshold change of either each miRNA relative to the cycle threshold of U6 controls ($-\Delta CT = CT_{U6} - CT_{miRNA}$) or IL6R expression relative to the cycle threshold of GAPDH controls ($-\Delta CT = CT_{GAPDH} - CT_{IL6R}$).

## 3.4 Results

### *3.4.1 Quantification of morphine-induced changes in miRNA expression*

We previously reported that miR1, miR21, miR124, miR129-2, and miR146a were significantly dysregulated following spinal cord contusion (Strickland et al., 2011). To determine whether morphine treatment further dysregulates SCI-sensitive miRNAs, their expression was examined by qRT-PCR in sham controls and in response to vehicle and morphine treatment following contusion, at either 2 or 15 days post-SCI. Multivariate ANOVA of qRT-PCR data indicated a significant main effect of time (Pillai's Trace Statistic, $F_{(5,19)}=21.094$; $p<0.005$) and treatment ($F_{(10,40)}=3.742$; $p<0.005$), and a

significant interaction effect between time and treatment ($F_{(10,40)}$=6.478; $p$<0.005). *Post hoc* univariate ANOVAs indicated a main effect of treatment on miR21, miR129-2, and miR146a ($F_{(2,23)}$=65.038; $p$<0.005, $F_{(2,23)}$=17.265; $p$<0.005, and $F_{(2,23)}$=16.163; $p$<0.005, respectively), and a significant interaction effect of time and treatment on miR21 and miR146a expression ($F_{(2,23)}$=8.229; $p$<0.005 and $F_{(2,23)}$=10.055; $p$<0.005, respectively). In addition, *post hoc* least significant difference (LSD) *t*-tests indicated that both miR21 and miR146a expression is increased following spinal cord trauma, irrespective of morphine treatment ($p_{miR21}$<0.001 and $p_{miR146a}$<0.001; Figure 11a, b). In contrast, miR129-2 expression was down-regulated following both morphine and vehicle administration ($p_{miR129\text{-}2}$<0.001 and $p_{miR129\text{-}2}$<0.001, respectively), and there was no change in the expression of either miR1 or miR124 (Figure 11a, b). *Post hoc* planned comparisons indicated that there was a significant increase in expression of miR21 in response to morphine treatment relative to vehicle at 15 days post-SCI (Student's two-tailed *t*-test, $p$<0.05; Figure 11c, d). In addition, Pearson's product-moment correlations indicated a statistically significant correlation between miR21 expression and time (Pearson's $r$=0.61, $p$<0.005). Controlling for time, partial correlation analysis showed that miR21 expression was significantly correlated with the expression of miR1, miR124, and miR146a (Pearson's $r$=0.51, $p$<0.03, Pearson's $r$=0.58, $p$<0.01, and Pearson's $r$=0.83, $p$<0.001, respectively).

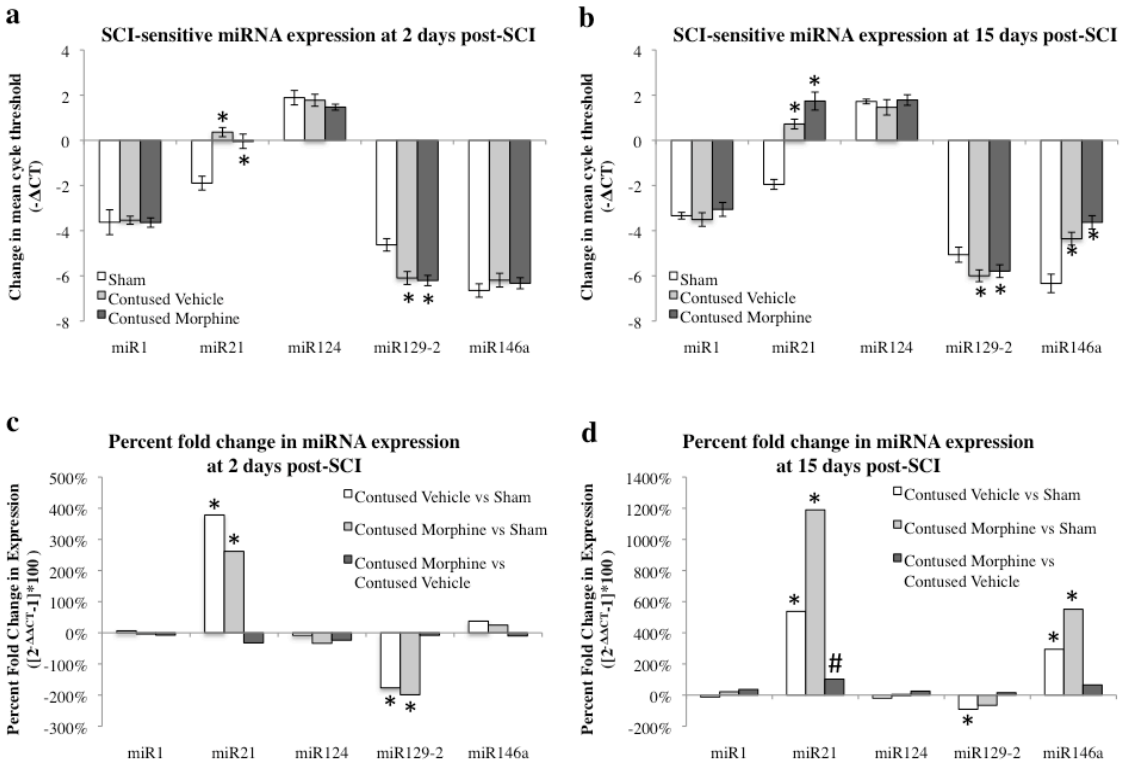


**Figure 11.** Bar graphs depicting qRT-PCR analysis of miRNA expression of miR1, miR21, miR124, miR129-2, and miR146a at the lesion site for sham animals and after administration of either morphine or vehicle in contused animals at either 2 (a, c) or 15 (b, d) days post-SCI. (a-b) The x-axis denotes miRNA of interest, and the y-axis denotes the mean change in cycle threshold, where ΔCT represents the mean difference of miRNA and U6 control ΔCT values. Animals received either a laminectomy only (sham) or a T12-T13 spinal contusion followed by administration of vehicle or morphine 24 hrs later, and sacrificed at 2 or 15 days post-surgery for harvesting of the cords. Data are expressed relative to U6 controls (a value of zero equates to no difference in expression between the miRNA and U6, positive values equate to higher miRNA expression, and negative values vice versa), with asterisks indicating significance (f-LSD) compared with sham controls; *p* values are as indicated in the text. (c-d) The x-axis denotes miRNA of interest, and the y-axis denotes the baseline-corrected percentage of fold expression change of miRNA using the formula $(2^{-\Delta\Delta CT}-1)*100$, where ΔΔCT represents the mean difference of contused vehicle and sham, contused morphine and sham, or contused morphine and contused vehicle ΔCT values. Data are expressed as a percentage of change (a value of zero equates to no change between surgery conditions), with asterisks indicating significance (f-LSD) compared with sham controls and hash tags indicating significance (f-LSD) compared with contused vehicle controls; *p* values are as indicated in the text.

*3.4.2 Impact of injury severity and functional recovery on miRNA expression*

We previously observed a significant relationship between the expression of both miR129-2 and miR146a and injury severity, as indicated by initial BBB scores following surgery. Accordingly, we assessed whether this relationship would be replicated by the new data set. Indeed, there was a statistically significant correlation between BBB scores at 24 hours post-SCI and the expression of both miR129-2 and miR146a across both time points (Pearson's $r$=0.66, $p$<0.001 and Pearson's $r$=-0.55, $p$<0.001, respectively; Figure 12a, b). Contrary to our previous findings, we also found a statistically significant correlation between the expression of miR21 and initial BBB scores (Pearson's $r$=-0.88, $p$<0.001; Figure 12c). Additionally, we analyzed the relationship between recovery of function, as indicated by Day 13 BBB scores, and miRNA expression at 15 days post-SCI. Similar to initial injury severity, there were statistically significant correlations between BBB scores at 13 days post-SCI and expression of miR129-2, miR146a, and miR21 (Pearson's $r$=0.50, $p$<0.05, Pearson's $r$=-0.70, $p$<0.001, and Pearson's $r$=-0.80, $p$<0.001, respectively; Figure 13a-c).

*3.4.3 Relationship between SCI-sensitive miRNA expression and sensory reactivity*

In order to assess the possibility that pain sensitivity is associated with the expression of SCI-sensitive miRNAs, thermal thresholds were measured by the tail flick-latency test, following SCI, both before and after treatment of morphine. Accordingly, there were statistically significant correlations between baseline tail-flick latency and expression of miR1, miR124, and miR129-2 regardless of time point (Pearson's $r$=0.41, $p$<0.05,

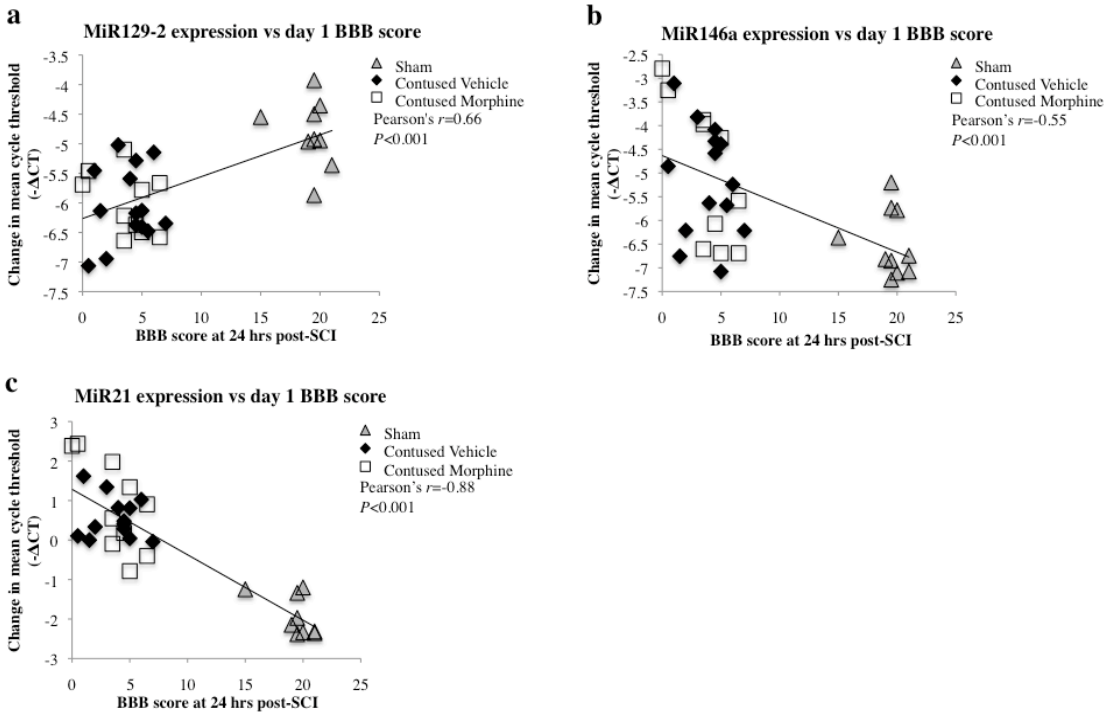


**Figure 12.** Correlation analysis to assess the relationship between miRNA expression and initial injury severity. (a-c) The x-axis represents the Basso, Beattie, and Bresnahan (BBB) score for baseline locomotor function, 24 hours following spinal cord contusion, and the y-axis depicts the mean difference in cycle threshold change (-ΔCT) between miRNA expression at both 2 and 15 days post-SCI and U6 controls. Pearson's product-moment correlations indicated a significant correlation between miR129-2 (a), miR146a (b), and miR21 (c), and initial BBB score (Pearson's $r$=0.66, $P$<0.001, Pearson's $r$=-0.55, $P$<0.001, and Pearson's $r$=-0.88, $P$<0.001, respectively). Data are represented as the mean change in cycle threshold of miRNA expression relative to U6 controls (-ΔCT= $CT_{U6}$ - $CT_{miRNA}$).

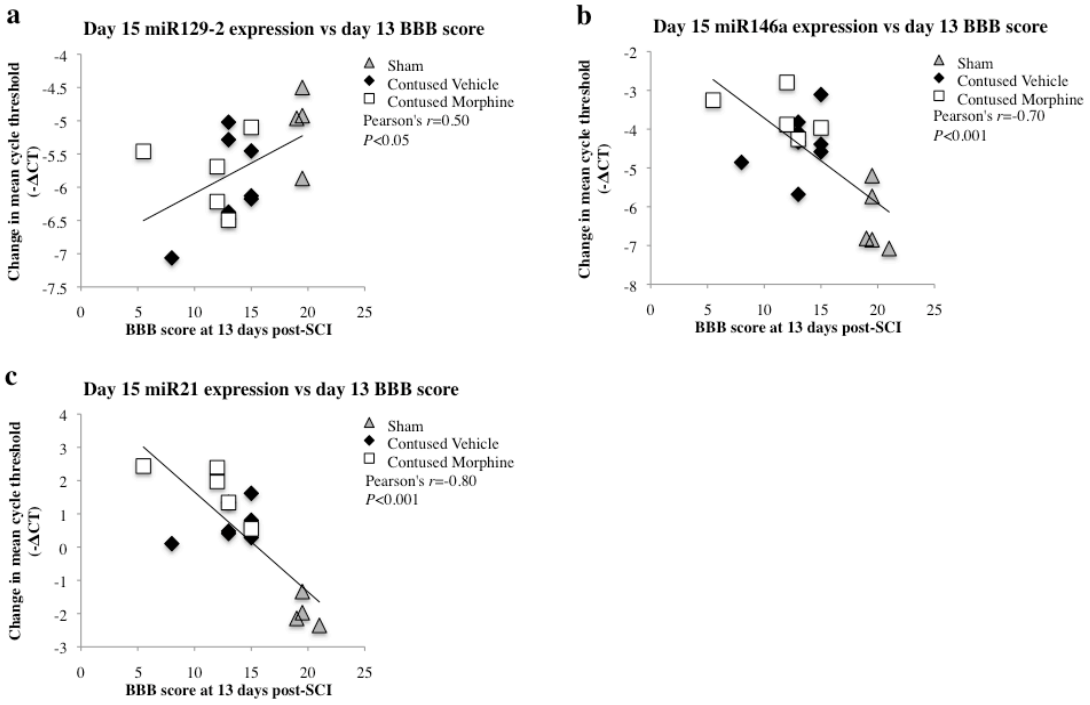


**Figure 13.** Correlation analysis to assess the relationship between miRNA expression and functional recovery. (a-c) The x-axis represents the BBB score for locomotor function recorded 13 days following spinal cord contusion, and the y-axis depicts the mean difference in cycle threshold change (-ΔCT) between miRNA expression at 15 days post-SCI and U6 controls. Pearson's product-moment correlations indicated a significant correlation between miR129-2 (a), miR146a (b), and miR21 (c), and Day 13 BBB score (Pearson's $r$=0.50, $P$<0.05, Pearson's $r$=-0.70, $P$<0.001, and Pearson's $r$=-0.80, $P$<0.001, respectively). Data are represented as the mean change in cycle threshold of miRNA expression relative to U6 controls (-ΔCT= $CT_{U6}$ - $CT_{miRNA}$).

Pearson's $r$=0.43, $p$<0.05, and Pearson's $r$=0.41, $p$<0.05, respectively; Figure 14a-c), and as predicted these correlations were abolished following morphine administration.

*3.4.4 Expression of miR-1 in vascular tissues following SCI*

We previously observed a significant decrease in miR1 expression following spinal cord contusion (Strickland et al., 2011), but did not find a significant change in expression following SCI and administration of the tail-flick test. Given the positive correlation of miR1 expression with sensory reactivity and the capability of miR1 to inhibit angiogenesis (Stahlhut et al., 2012), added to the fact that miR1 is heavily expressed in the cardiovascular system (Fichtlscherer et al., 2011; Jakob and Landmesser, 2012), it is possible that the change in expression of miR1 at the injury site may represent a broader response of vascular and cardiac tissues to SCI. We therefore assessed miR-1 expression in heart and carotid arterial tissue. Quantitative RT-PCR indicated that there was not a significant change in miR1 expression in either of these tissues following SCI (Figure 15), suggesting that the changes in miR-1 expression previously observed (Strickland et al., 2011) are localized within the injury site rather than due to adaptive changes in the peripheral vascular system.

*3.4.5 MiRNA regulation of pain neuro-circuitry associated cytokines*

As miR21 is further dysregulated following morphine administration, we assessed the extent to which changes in miR21 expression were associated with alterations in known cytokine mRNA targets. MiR21 has previously been shown to regulate the interleukin-6

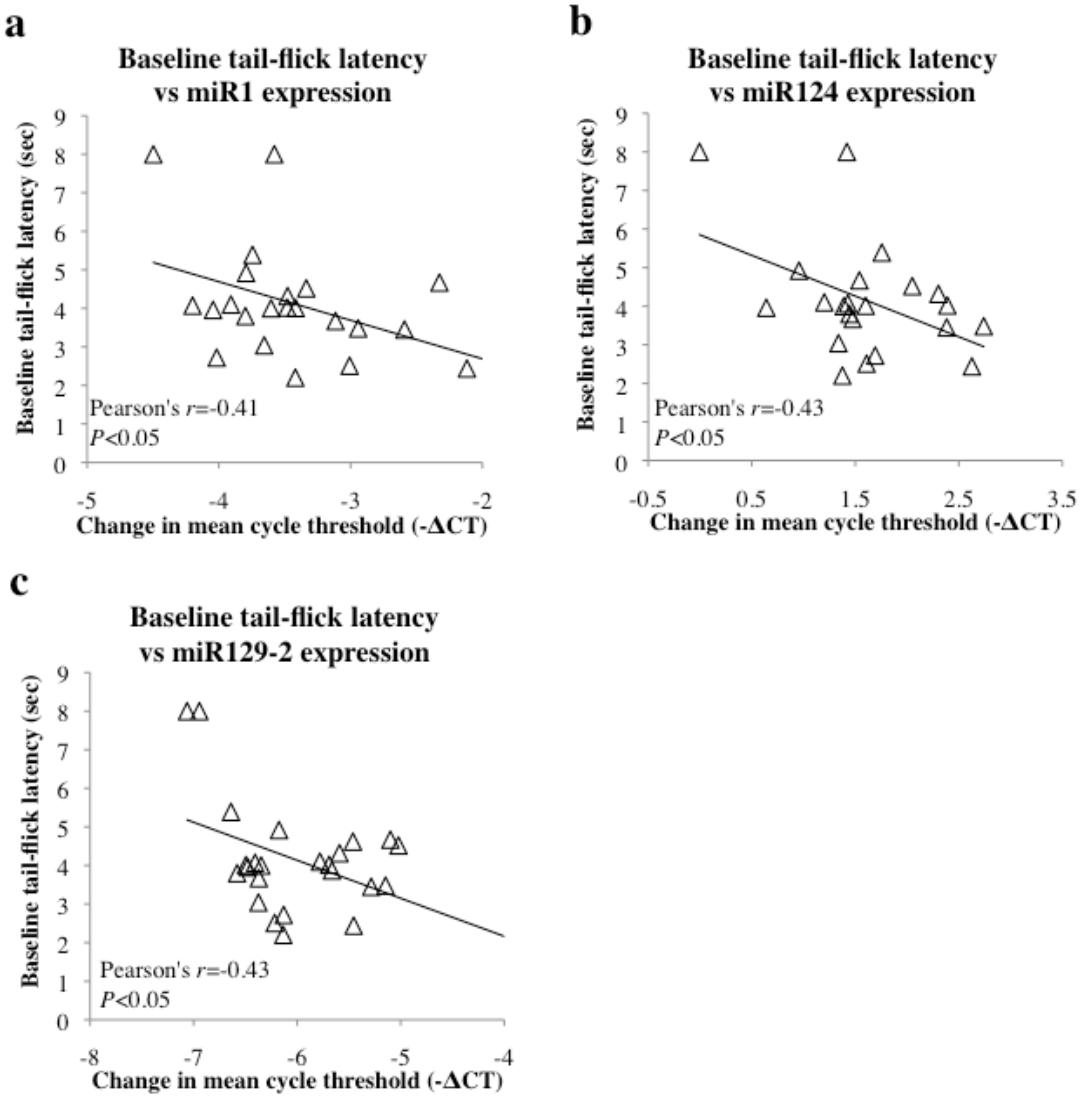


**Figure 14.** Correlation analyses to assess the relationship between miRNA expression and sensory reactivity following SCI. (a-c) The x-axis represents the mean difference in cycle threshold change (-ΔCT) between miRNA expression at both 2 and 15 days post-SCI and U6 controls, and the y-axis depicts the baseline tail-flick latency for pain sensitivity assessed 24 hours following spinal cord contusion and prior to morphine or vehicle administration. Pearson's correlations indicated a significant correlation between miR1 (a), miR124 (b), and miR129-2 (c) and baseline tail-flick latency (Pearson's $r$=-0.41, $P$<0.05, Pearson's $r$=-0.43, $P$<0.05, and Pearson's $r$=-0.41, $P$<0.05, respectively), but no significant correlations were found following vehicle or morphine administration. Data are represented as the mean change in cycle threshold of miRNA expression relative to U6 controls (-ΔCT= $CT_{U6}$ - $CT_{miRNA}$).

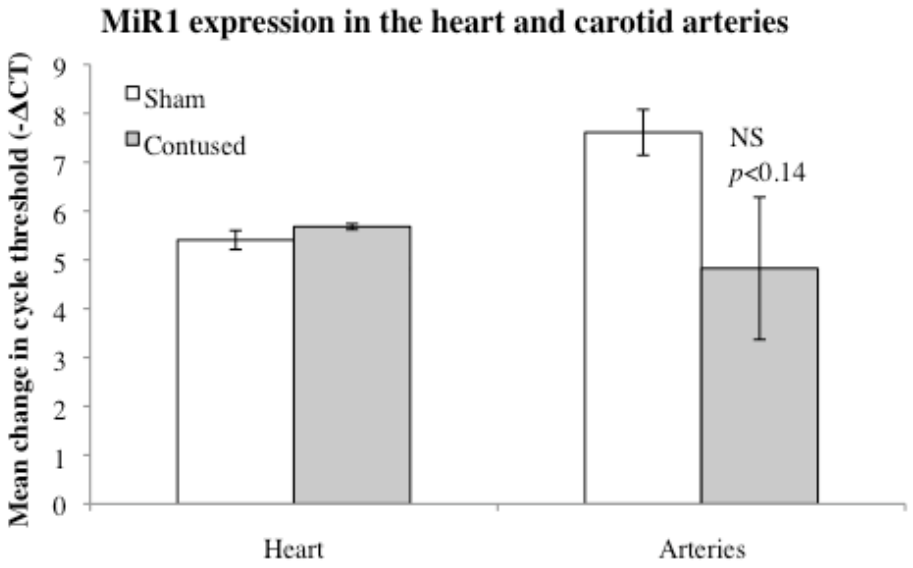


**Figure 15.** Bar graph depicting qRT-PCR analysis of miR1 expression in hearts and carotid arteries following SCI. The x-axis denotes tissue of interest, and the y-axis denotes the mean change in cycle threshold, where ΔCT represents the mean difference of miR1 and U6 control ΔCT values. Animals received either a laminectomy only (sham) or a T12-T13 spinal contusion, and were sacrificed 24 hrs post-surgery for harvesting of the cords. Data are expressed as measure of expression relative to U6 controls (a value of zero equates to no difference in expression between miR1 and U6, positive values equate to a higher expression of miR1, and negative values vice versa), and indicate that there was no significant change in miR1 expression between contused and sham groups, both in heart and carotid artery tissue ($p<0.17$ and $p<0.14$, respectively).

receptor, IL6R (Frankel et al., 2008). To determine if IL6R was additionally dysregulated by alteration of pain neuro-circuitry, the expression of mRNA transcripts for IL6R was examined by qRT-PCR in sham controls and in response to vehicle and morphine treatment following contusion injury. An ANOVA revealed a main effect of both time and treatment on IL6R mRNA ($F_{(1,28)}$=4.533; $p$<0.05, and $F_{(2,28)}$=10.881; $p$<0.01, respectively), and *post hoc* LSD *t*-tests indicated that IL6R expression is increased following spinal cord trauma, irrespective of morphine treatment ($p_{\text{Contused Vehicle vs. Sham}}$<0.0001 and $p_{\text{Contused Morphine vs. Sham}}$<0.001; Figure 16a, b). In addition, there were significant correlations between IL6R mRNA expression and miR21, miR124, miR129-2, and miR146a (Pearson's $r$=0.63, $p$<0.001, Pearson's $r$=-0.38, $p$<0.05, Pearson's $r$=-0.59, $p$<0.001, and Pearson's $r$=0.57, $p$<0.001, respectively). Partial correlations controlling for the effects of time also indicated that the expression of IL6R mRNA was significantly correlated with expression of both miR124 and miR146a (Pearson's $r$=-0.54, $p$<0.05, and Pearson's $r$=0.47, $p$<0.05, respectively). Furthermore, IL6R expression was predictive of nociceptive sensitivity, as there was a statistically significant correlation between baseline tail-flick latency and IL6R expression across both time points (Pearson's $r$=-0.585, $p$<0.01; Figure 17a), and this correlation was abolished following morphine administration. Finally, there was a statistically significant correlation between BBB scores at 24 hours post-SCI and IL6R expression, indicating that variation in initial injury severity is predictive of variation in IL6R expression (Pearson's $r$=0.656, $p$<0.01; Figure 17b), but there was not a significant correlation between day 13 BBB scores and IL6R mRNA expression ($p$=0.49).

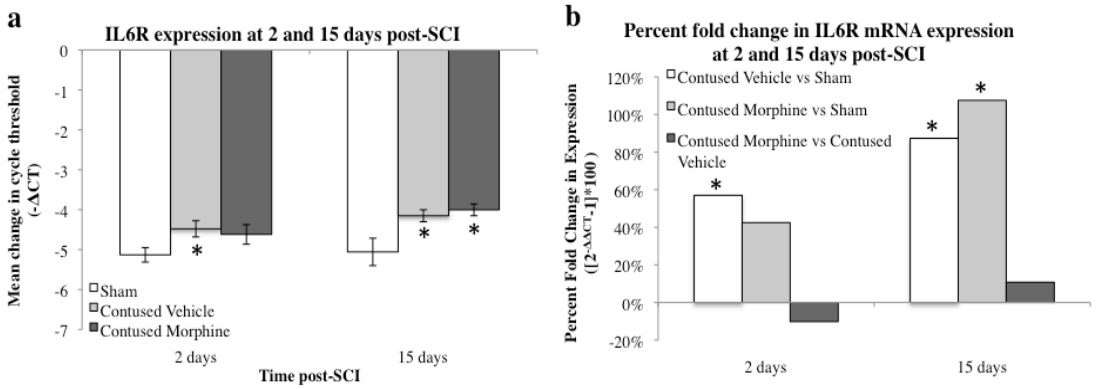


**Figure 16.** Bar graphs depicting qRT-PCR analysis of mRNA expression of IL6R at the lesion site for sham animals and after administration of either morphine or vehicle in contused animals at 2 and 15 days post-SCI. (a) The x-axis denotes time following surgery, and the y-axis denotes the mean change in cycle threshold, where ΔCT represents the mean difference of mRNA and GAPDH control ΔCT values. Animals received either a laminectomy only (sham) or a T12-T13 spinal contusion followed by administration of vehicle or morphine 24 hrs later, and sacrificed at 2 or 15 days post-surgery for harvesting of the cords. Data are expressed relative to GAPDH controls (a value of zero equates to no difference in expression between the miRNA and GAPDH, positive values equate to higher miRNA expression, and negative values vice versa), with asterisks indicating significance (f-LSD) compared with sham controls; *p* values are as indicated in the text. (b) The x-axis denotes time after surgery, and the y-axis denotes the baseline-corrected percentage of fold expression change of IL6R mRNA using the formula $(2^{-\Delta\Delta CT}-1)*100$, where ΔΔCT represents the mean difference of contused vehicle and sham, contused morphine and sham, or contused morphine and contused vehicle ΔCT values. Data are expressed as a percentage of change (a value of zero equates to no change between surgery conditions), with asterisks indicating significance (f-LSD) compared with sham controls and hash tags indicating significance (f-LSD) compared with contused vehicle controls; *p* values are as indicated in the text.

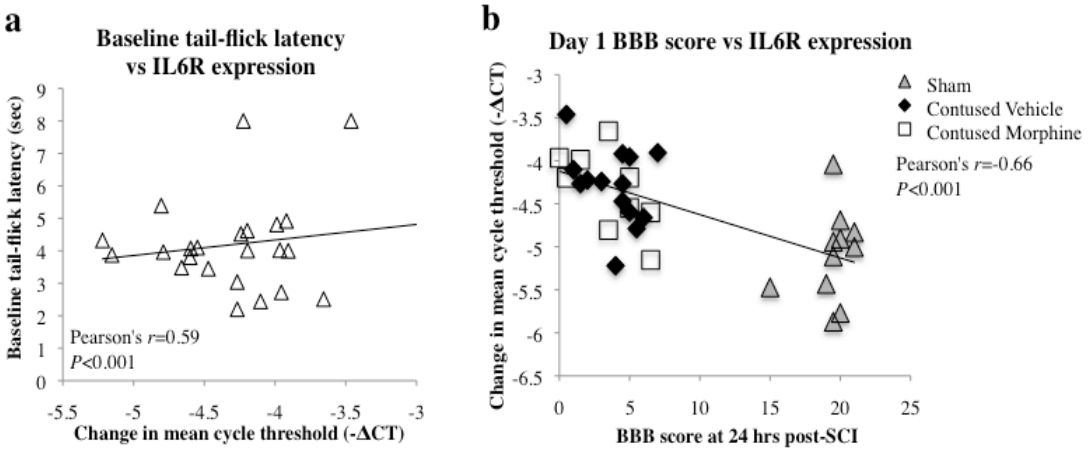


**Figure 17.** Correlation analyses to assess the relationship between IL6R mRNA expression and sensory reactivity following SCI. (a) The x-axis represents the mean difference in cycle threshold change (-ΔCT) between mRNA expression at both 2 and 15 days post-SCI and GAPDH controls, and the y-axis depicts the baseline tail-flick latency for pain sensitivity at 24 hours following spinal cord contusion and prior to morphine or vehicle administration. Pearson's product-moment correlations indicated a significant correlation between IL6R and baseline tail-flick latency (Pearson's $r$=0.59, $P$<0.01), but no significant correlations were found following vehicle or morphine administration. Data are represented as the mean change in cycle threshold of mRNA expression relative to GAPDH controls (-ΔCT= $CT_{GAPDH}$ - $CT_{IL6R}$). (b) The x-axis represents the BBB score for baseline locomotor function, 24 hours following spinal cord contusion, and the y-axis depicts the mean difference in cycle threshold change (-ΔCT) between IL6R mRNA expression at both 2 and 15 days post-SCI and GAPDH controls. Pearson's product-moment correlations indicated a significant correlation between IL6R expression and initial BBB score (Pearson's $r$=-0.66, $P$<0.01). Data are represented as the mean change in cycle threshold of miR21 expression relative to GAPDH controls (-ΔCT= $CT_{GAPDH}$ - $CT_{IL6R}$).

## 3.5 Discussion

Morphine treatment plays an important role in pain mitigation in both the acute and chronic phase of spinal cord trauma. However, its deleterious effects on functional recovery and exacerbation of chronic pain systems, through activation of innate immune responses, provide a substantial challenge towards clinical efforts to minimize the short and long term effects of SCI (Dworkin et al., 2003; McCarberg, 2004; Watkins et al., 2005; Hook et al., 2007; Scholz and Woolf, 2007; Watkins et al., 2007; Hook et al., 2009; Hook et al., 2011). Given their dysregulation following SCI and ability to coordinate the expression of large gene networks, it is likely that miRNAs are involved in SCI-induced remodeling of nociceptive circuitry, and consequently, the effects of opiates like morphine on this circuitry. Therapeutic manipulation of these miRNAs could attenuate the maladaptive effects of acute morphine administration on both the acute and chronic phases of SCI by suppressing activation of inflammation and inhibiting the synaptic remodeling that increases both neuropathic pain and morphine tolerance.

In the current study, we investigated the regulation of SCI-sensitive miRNAs following morphine treatment. Specifically, we replicated our previous observation that miR129-2 is decreased following spinal cord contusion, while miR21 and miR146a were induced, irrespective of morphine treatment (Strickland et al., 2011). Interestingly, in this study, neither miR1 nor miR124 were significantly altered in SCI animals. One possible explanation that merits further investigation is that the measurement of pain sensitivity itself exposed SCI animals to nociceptive stimuli, which may have

normalized miR1 and miR124 expression. This possibility is supported by reports showing that peripheral inflammation, which is also known to trigger nociception, results in persistent elevation in miR1 in the dorsal horn of the spinal cord (Kusuda et al., 2011). Additionally, both miR1 and miR124 are predicted to play a central role in the late phase gene repression associated with long-term potentiation-dependent neuronal plasticity (Ryan et al., 2012), and therefore, the normalization of these miRNAs may be important for activation of neural circuitry associated with pain as well.

We found that morphine exposure significantly induced miR21 expression and resulted in a near-significant increase in miR146a expression 15 days after SCI. This is the first evidence for the potential involvement of miRNAs and consequently, miRNA-regulated gene networks, as mediators of morphine's effects on plasticity in the spinal cord following SCI. In addition, changes in expression of miR21 were significantly explained by the variance in expression of miR1, miR124, and miR146a, suggesting that these miRNAs may be co-regulated. Moreover, while the expression of miR21 and miR146a was significantly correlated with locomotor behavioral performance following SCI, their expression did not predict pain sensitivity. Consequently, the induction of these miRNAs by morphine is unlikely to be related to the analgesic actions of morphine, but rather, to its pro-inflammatory actions. Several lines of evidence support this hypothesis. Firstly, the expression of both miR146a and miR21 is induced by pro-inflammatory cytokines (Taganov et al., 2006; Loffler et al., 2007; O'Connell et al., 2007; Tili et al., 2007; Nakasa et al., 2008), and reciprocally, both miRNAs target mRNA transcripts of pro-inflammatory cytokines or their receptors (Frankel et al., 2008;

Nahid et al., 2009; Li et al., 2010a). Secondly, both miR21 and miR146a play an important role in the innate immune response (Taganov et al., 2006; Moschos et al., 2007; Nahid et al., 2009; Li et al., 2010a; Li et al., 2010b), because increased expression of both miR21 and miR146a negatively regulates innate immune signaling. Finally, miR21 and miR146a have been found to be highly expressed in activated astrocytes, and their over expression results in attenuation of astrocytic hypertrophy and suppression of the astrocyte-mediated inflammation response, respectively (Bhalala et al., 2012; Iyer et al., 2012). As a result, it is more likely that these miRNAs serve as a component of morphine-induced inflammation rather than being involved in the morphine-triggered signaling cascade driving analgesia.

Interestingly, we observed that although the interleukin receptor IL6R was dysregulated following SCI, it was not additionally dysregulated by morphine administration. Moreover, contrary to our prediction, the transcript for IL6R, the identified miR21 target, was persistently up-regulated following SCI, suggesting a dissociation between miRNA and target gene networks following SCI, as has been observed in other models of neural damage (Pappalardo et al., 2013). Indeed, changes in expression of IL6R were significantly explained by the variance in miR21, miR124, miR129-2, and miR146a, suggesting that regulation of IL6R involves a network of miRNAs rather than any single miRNA. We also observed that variations in IL6R mRNA expression explained a statistically significantly portion of the variance in initial injury severity, suggesting that decreased expression of IL6R, and presumably lower levels of inflammation, was associated with a less severe initial injury. Indeed, this

relationship is likely to be causal in nature, because application of an anti-IL6R antibody immediately after injury has been shown to significantly decrease tissue damage, increase axonal regeneration, and improve functional recovery (Mukaino et al., 2010). Finally, since variability in IL6R mRNA expression also explained a statistically significant proportion of the variability in pain sensitivity (58.5%), it is possible that IL6R also plays a significant role in remodeling inflammation-driven pain neuro-circuitry following SCI and opiate exposure.

We were able to reaffirm our previous finding that expression changes of both miR129-2 and miR146a were significantly explained by the variance of initial injury severity (Strickland et al., 2011). In addition, we found that fluctuations in miR21 expression were significantly explained by the variance in BBB scores 24 hours post-SCI, and that changes in miR129-2, miR146a, and miR21 were also significantly explained by the variance in functional recovery at 13 days post-SCI. Similar to miR146a, miR21 is a negative regulator of inflammation, but it also has anti-apoptotic activity (Sathyan et al., 2007; Roy and Sen, 2011). As such, its up-regulated expression may result in increased neuronal survival following SCI by inhibiting inflammation and cell death, factors which are likely to result in better locomotor function and higher initial BBB scores. One therapeutically relevant prediction from these data that merits further investigation is that application of miR21 or miR146a mimetics prior to or concurrent with morphine administration in the acute phase of SCI may attenuate opioid mediated inflammation, and could also reduce apoptosis (protecting the potential for recovery) in this early phase of injury.

Finally, we observed that miRNA expression at the injury site explained a significant proportion of the sensitivity to nociceptive stimuli, i.e., the response of sensorimotor circuitry distal to the injury site. Not surprisingly, these correlations between pain sensitivity and miRNA expression were abrogated by morphine administration, due to the analgesic effects of morphine. While these correlations do not necessarily imply causality, they do advance the possibility that there is a degree of molecular integration between the injury site and more caudal, but anatomically intact neuro-circuitry. A mechanism for cross-talk between miRNAs at the injury site and caudal neuro-circuitry is unclear at this time, but the possibility that these interactions serve an adaptive function is intriguing, and needs further investigation.

## 3.6 Conclusion

Our evidence shows that acute morphine administration results in a very specific and limited profile of changes in SCI-sensitive miRNA expression during the chronic phase of injury. Interestingly, expression changes are confined to miRNAs, like miR21, that are both induced by and inhibitors of pro-inflammatory cytokines, suggesting that morphine may potentially interfere with miRNA-mediated negative feedback pathways. Like miR21, IL6R mRNA was persistently up-regulated after SCI, and its expression negatively correlated with initial injury severity, suggesting that IL6R and miR21 may be a coordinately regulated, adaptive response to SCI. Furthermore, miR1, miR124, and miR129-2 expression at the injury site appears to play a substantial role in the regulation of distal nociceptive signaling pathways. Collectively, these data suggest that SCI-

sensitive miRNAs constitute an important component of emerging pain-sensitivity and inflammation, and consequently, these miRNAs could serve as therapeutic targets following SCI.

# 4. REGULATORY EFFECTS OF INTERMITTENT NOXIOUS STIMULATION ON SPINAL CORD INJURY-SENSITIVE MICRORNAS AND THEIR PRESUMPTIVE TARGETS FOLLOWING SPINAL CORD CONTUSION

## 4.1 Overview

Chronic pain is a common consequence of spinal cord injury (SCI), and uncontrollable nociception due to peripheral tissue damage below the level of the lesion site can sensitize spinal neurons and lead to the development of neuropathic pain. Previous studies indicated that SCI results in the induction and suppression of several microRNAs (miRNAs) at both the site of lesion, and in regions distal to the injury site. We hypothesized that SCI-sensitive miRNAs would also be dysregulated by uncontrollable nociception, and that their expression may regulate gene targets important for the progression of maladaptive plasticity and hypersensitivity. Our data indicated that intermittent noxious stimulation decreased expression of miR124 in dorsal tissue during the acute phase of injury and induced expression of miR129-2 in dorsal tissue and miR1 in ventral tissue during the chronic phase of injury, suggesting that uncontrollable nociception distal to the injury site can affect specific regulatory changes in gene networks within sensorimotor circuitry of the lesion site. We also found that uncontrollable nociception significantly down-regulated brain-derived neurotrophic factor (BDNF) expression 24 hrs after uncontrollable tailshock, and that expression of insulin growth factor-1 (IGF-1) was significantly induced at both 24 hrs and 7 days. Expression changes in IGF-1 mRNA expression were significantly explained by the

variance in miR124, miR21, and miR146a, while changes in BDNF mRNA expression were significantly explained by the variance in miR21 and miR124 expression, suggesting that both BDNF and IGF-1 regulation involves a network of miRNAs. Contrary to predictions, changes in neither BDNF nor IGF-1 expression, identified targets of miR1, were associated with variances in miR1 expression, indicating dissociation between miRNA and target gene expression. Collectively, these data suggest that SCI-sensitive miRNAs may constitute therapeutic targets for attenuating increased glial activation and progression of neuropathic pain after SCI.

## 4.2 Introduction

Spinal cord injury (SCI) can cause a variety of debilitating consequences, including a loss of motor control, paralysis, and pain. Uncontrollable nociception associated with concomitant peripheral tissue injury following SCI is particularly problematic, as the noxious stimulation results in increased glial activity (Frei et al., 2000; Hains and Waxman, 2006; Detloff et al., 2008) and sensitization of spinal neurons (Hains et al., 2003; Lampert et al., 2006) that drives maladaptive spinal plasticity, impaired behavioral recovery, pain hypersensitivity, excito-toxicity, and cell death (Liu et al., 1999; Beattie et al., 2002; Xu et al., 2004; Kuzhandaivel et al., 2011). Accordingly, we previously reported that intermittent noxious stimulation delayed the recovery of bladder function, led to greater mortality and spasticity, and increased tissue loss at the injury site in adult rats (Grau et al., 2004). In addition, we found that nociceptive stimulation at 24 hrs resulted in decreased brain-derived neurotrophic factor (BDNF)-tropomyosin-receptor

kinase (TrkB) signaling (Gomez-Pinilla et al., 2007; Garraway et al., 2011), and this signaling pathway has been shown to play a key role in modulating neuronal plasticity, promoting axonal regeneration, and improving functional recovery following SCI (Xu et al., 1995; Patterson et al., 1996; McTigue et al., 1998; Kerr et al., 1999; Garraway et al., 2003; Boyce et al., 2007).

Despite the importance of uncontrollable nociception to recovery from SCI, there is limited knowledge of the effects of nociception on mechanisms that may ultimately influence neurotrophic signaling pathways and functional recovery. Our previous data showing that a network of miRNAs was altered following SCI suggested a hypothesis that these molecules may also be sensitive to nociceptive stimuli following SCI, resulting in activation of potentially mal-adaptive gene networks. MiRNAs are short, 18 to 25 nucleotide-long non-coding small RNAs that play an important regulatory role in gene expression by inhibiting protein translation or targeting mRNA transcripts for degradation (Alvarez-Garcia and Miska, 2005; Zamore and Haley, 2005). Individual miRNAs are able to coordinate gene networks to affect a specific cellular endpoint by simultaneously controlling expression of several hundred mRNAs. Additionally, not only have miRNAs been shown to play a major role in neurodegenerative diseases (Kim et al., 2007; Hebert et al., 2008; Hebert and De Strooper, 2009; Numakawa et al., 2011), but they also regulate BDNF expression in the brain (Mellios et al., 2008) and inhibit its expression in neurodegenerative disease states like Alzheimer's disease (Lee et al., 2012).

We and other groups have previously shown that SCI is followed by dysregulated miRNA expression (Liu et al., 2009; Nakanishi et al., 2010; Strickland et al., 2011). Our previous study showed that miR1, miR124, and miR129 were significantly down-regulated following spinal cord contusion, with miR146a and miR21 transiently induced (Strickland et al., 2011). In addition, changes in both miR129-2 and miR-146a expression significantly explained the variability in injury severity. Interestingly, miR1, a member of the miR1/miR206 family has been shown to regulate important growth-promoting neurotrophic factors like BDNF (Lewis et al., 2003; Lee et al., 2012) and insulin growth factor-1 (IGF-1; Yu et al., 2008; Li et al., 2012). Moreover, increased expression of IGF-1 has been associated with increased spasticity of skeletal muscle following SCI (Gorgey and Gater, 2012). Consequently, miR1 and other SCI-sensitive miRNAs may be further dysregulated following intermittent noxious stimulation, and play an important role in regulating critical gene networks involved in the maladaptive spinal cord plasticity that results in hypersensitivity and impaired functional recovery. To assess these possibilities, the current study investigated the relationship between SCI-sensitive miRNA expression and intermittent noxious stimulation at 1 hour, 24 hours, and 7 days post-SCI. Likewise, we also assessed the relationship between the expression of miRNAs sensitive to intermittent noxious stimulation and that of their mRNA targets.

## 4.3 Experimental Procedures

### *4.3.1 Subjects*

The subjects were male Sprague–Dawley rats (*Rattus norvegicus*) obtained from Harlan (Houston, TX). The rats were approximately 90-110 days old (350-400 g), individually housed in Plexiglas bins [45.7 (length) x 23.5 (width) x 20.3 (height) cm] with food and water continuously available, and maintained on a 12 hour light/dark cycle. All behavioral testing was performed during the light cycle. To facilitate access to the food and water, extra bedding was added to the bins after surgery and long mouse sipper tubes were used so that the rats could reach the water without rearing. All of the experiments were reviewed and approved by the institutional animal care committee at Texas A&M University and all NIH guidelines for the care and use of animal subjects were followed.

### *4.3.2 Surgery*

Subjects were anesthetized with isoflurane (5%, gas). Once a stable level of anesthesia was achieved, the concentration of isoflurane was lowered to 2-3%. An area extending approximately 4.5 cm above and below the injury site was shaved and disinfected with iodine, and a 7.0 cm incision was made over the spinal cord. Next, two incisions were made on either side of the vertebral column, extending about 3 cm rostral and caudal to the T12-T13 segment. The dorsal spinous processes at T12-T13 were removed (laminectomy), and the spinal tissue exposed. The dura remained intact. For the contusion injury, the vertebral column was fixed within the MASCIS device (Gruner,

1992; Constantini and Young, 1994), and a moderate injury was produced by allowing the 10 g impactor (outfitted with a 2.5 mm tip) to drop 12.5 mm. Sham controls received a laminectomy, but the cord was not contused with the MASCIS device. Following surgery, the wound was closed with Michel clips. T12-T13 level contusion models have been routinely used by members of our group to define spinal cord learning circuits and molecular mechanisms involved with recovery of function (Ferguson et al., 2008; Brown et al., 2011; Hook et al., 2011). Lesions at this level result in well-defined and replicable sensory-motor deficits, and we therefore chose to utilize contusion at this level to also examine changes in miRNA expression.

To help prevent infection, subjects were treated with 100,000 units/kg Pfizerpen (penicillin G potassium) immediately after surgery and again 2 days later. For the first 24 hours after surgery, rats were placed in a recovery room maintained at 26.6 $^{0}$ C. To compensate for fluid loss, subjects were given 2.5 ml of saline after surgery. Bladders were manually expressed twice daily (morning and evening) until the animals had empty bladders for three consecutive days, at the times of expressing.

*4.3.3 Uncontrollable intermittent noxious stimulation*

Intermittent shock to the tail was applied to subjects as previously described (Garraway et al., 2011). Subjects were treated with electrical stimulation 24 hours after surgery (modified from Washburn et al., 2007), and were loosely restrained in Plexiglas tubes also as previously described (Crown et al., 2002; Grau et al., 2004). Electrical stimulation was applied to the tail using an electrode gel (Harvard Apparatus, Holliston,

MA, USA) and attached 2 cm from the tip of the tail with Orthaleic tape. Leads from the fuse clip were attached to a BRS/LVE shock generator (Model SG-903), and intermittent constant current 1.5 mA, AC (60 Hz) electrical stimulus was applied through the electrodes. Rats treated with uncontrollable intermittent stimulation received 180, 80-ms tail shocks on a variable time schedule with a mean inter-stimulus interval of 2 seconds (range 0.2-3.8 s). Unshocked subjects were placed in the restraining tubes for an equal amount of time as shock subjects, had the electrodes attached, but did not receive the electrical stimuli.

*4.3.4 RNA extraction and qRT-PCR*

Animals were sacrificed at 1 hr, 24 hrs, or 7 days following SCI/unshocked ($SCI_{unshock}$) or SCI/shock-exposed ($SCI_{shock}$) treatment. All subjects were deeply anesthetized with pentobarbital (50 mg/kg), and 1 cm of spinal cord around the lesion epicenter was rapidly removed. To determine the spatial (dorsal-ventral) changes in the expression of miRNAs and genes of interest, the spinal cord tissue was further sectioned to yield dorsal and ventral portions in the 24 hrs and 7 days after treatment groups. The cord was processed for the extraction of total RNA (RNeasy Mini Kit; Qiagen, Valencia, CA, USA), quantified using a NanoDrop 2000 Spectrophotometer (Thermo Scientific; Wilmington, DE), and stored at -80 °C.

MiRNA expression data was measured with quantitative reverse transcription (qRT)-PCR for miRNAs, based on the protocol of the miRCURY$^{TM}$ LNA microRNA Universal RT-PCR system (EXIQON; Woburn, MA). RNA samples were converted to

cDNA, and qRT-PCR was performed using a 7900HT Fast Real-Time PCR System (Applied Biosystems, Foster City, CA). Forward and reverse primers (EXIQON; Woburn, MA) for hsa-miR124, hsa-miR1, hsa-miR21, hsa-miR129-2, and hsa-miR146a were used for PCR amplification, and real time data was normalized using U6 RNA. Similarly, messenger RNA (mRNA) expression of brain-derived neurotrophic factor (BDNF) and insulin growth factor-1 (IGF-1) was measured using qRT-PCR for mRNAs, based on the protocol for PerfeCTa® SYBR® Green SuperMix with ROX™ (Quanta Biosciences; Gaithersburg, MD). RNA samples were converted to cDNA using qScript™ cDNA SuperMix (Quanta Biosciences; Gaithersburg, MD), and qRT-PCR was performed using a 7900HT Fast Real-Time PCR System (Applied Biosystems, Foster City, CA). Forward and reverse primers (Integrated DNA Technologies; Coralville, IA) for BDNF and IGF-1 were used for PCR amplification, and real time data was normalized using glyceraldehyde 3-phosphate dehydrogenase (GAPDH). Relative miRNA and mRNA expression was determined by calculating the mean difference between cycle threshold of either the miRNA from the U6 small nuclear RNA ($U6_{SNB}$) normalized control, or the BDNF/IGF-1 mRNA from the GAPDH normalized control for each sample [Δ cycle threshold (ΔCT)] within each sample group (samples with same miRNA ID, time, and condition parameters) and expressed as -ΔCT for relative change in expression. Sample means that were greater than ± 2 standard deviations from the mean ΔCT, or ± 3 standard deviations from the mean ΔCT after exclusion, were considered outliers and removed from the analysis. Of the 560 data points in 105 groups used in the analysis, only 30 data points were excluded according to this criteria, and no

more than one data point in any individual experimental group was excluded. Fold change in miRNA/mRNA expression was determined by calculating the difference between the mean ΔCTs of sham, SCI/unshocked ($SCI_{unshock}$), and SCI/shock-exposed ($SCI_{shock}$) sample groups at the same time point (-ΔΔCT), and expressed as a baseline-corrected percentage of fold-change ($[2^{-\Delta\Delta CT}-1]*100$).

*4.3.5 Data analysis*

All data were analyzed using SPSS software version 18 (SPSS; Chicago, IL). MicroRNA expression, verified by qRT-PCR, was analyzed by multivariate analysis of variance (ANOVA) using Pillai's trace statistic, and further analyzed using *post hoc* univariate ANOVA and Fisher's least significant difference (f-LSD) test. Other data were analyzed using ANOVAs followed by *post hoc* f-LSD using planned comparisons. In all cases, the *a priori* α value was set at 0.05. Data were expressed as mean ±SEM, as indicated in the figure legends.

## 4.4 Results

*4.4.1 Quantification of shock-induced changes in miRNA expression*

**4.4.1.1 Uncontrollable nociception had no significant effect on SCI-sensitive miRNAs 1 hr following treatment**

We previously reported that miR1, miR21, miR124, miR129-2, and miR146a were significantly dysregulated following spinal cord contusion (Strickland et al., 2011). To determine whether uncontrollable intermittent noxious stimulation further dysregulates

SCI-sensitive miRNAs, their expression was determined by qRT-PCR in sham controls and in contused animals following either no shock exposure ($SCI_{unshock}$) or uncontrollable intermittent tailshock ($SCI_{shock}$). Initially, we analyzed miRNA expression within the whole spinal cord segment (combined dorsal and ventral spinal cord) at the lesion site at 1 hr following intermittent noxious stimulation. Planned comparisons indicated that there was a significant increase in expression of both miR21 (Student's two-tailed *t*-test, $p_{Unshock}<0.005$ and $p_{Shock}<0.001$) and miR146a (Student's two-tailed *t*-test, $p_{Unshock}<0.05$ and $p_{Shock}<0.005$) following SCI, irrespective of shock or unshock treatment (Figure 18a, b).

#### 4.4.1.2 Multivariate ANOVA and *post hoc* univariate ANOVAs indicated a significant interaction effect of time, treatment, and spinal section on SCI-sensitive miRNA expression

In subsequent experiments, we further microdissected the spinal cord tissue at the injury segment to yield dorsal/sensory and ventral/motor sections in the 24 hrs and 7 days treatment groups to assess spatial (dorsal-ventral) and functionally (sensory-motor)-associated changes in SCI-sensitive miRNA expression. We hypothesized that SCI-induced expression changes of some trauma-sensitive miRNAs would exhibit spatial and functional specificity, and that uncontrollable nociception might exacerbate these changes. Multivariate ANOVA of qRT-PCR data indicated a significant main effect of time (Pillai's Trace Statistic, $F_{(5,33)}=20.888$; $p<0.001$), treatment ($F_{(10,68)}=6.441$; $p<0.001$), and spinal section ($F_{(5,33)}=8.312$; $p<0.001$), and a significant interaction effect

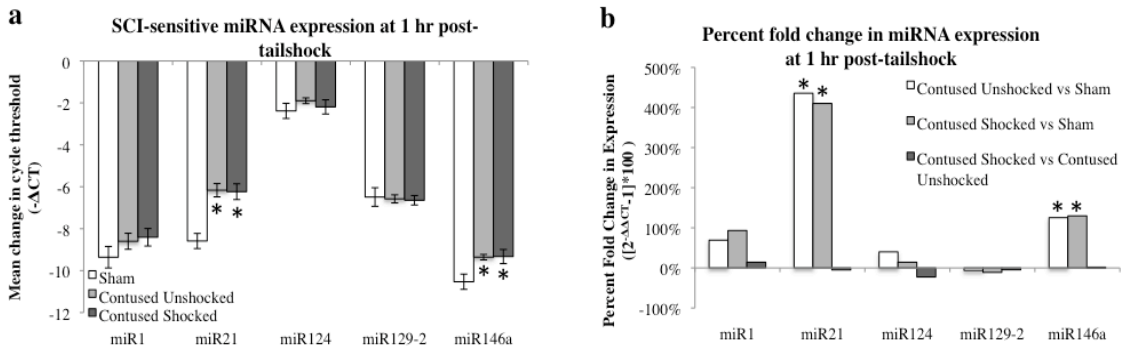


**Figure 18.** Bar graphs depicting qRT-PCR analysis of miRNA expression of miR1, miR21, miR124, miR129-2, and miR146a at the lesion site for sham animals and after unshocked or shock treatment in contused animals at 1 hr following tailshock treatment. (a) The x-axis denotes miRNA of interest, and the y-axis denotes the mean change in cycle threshold, where ΔCT represents the mean difference of miRNA and U6 control ΔCT values. Animals received either a laminectomy only (sham) or a T12-T13 spinal contusion followed by administration of unshock or shock 24 hrs later, and sacrificed at 1 hr following unshock/shock treatment for harvesting of the cords. Data are expressed relative to U6 controls (a value of zero equates to no difference in expression between the miRNA and U6, positive values equate to higher miRNA expression, and negative values vice versa), with asterisks indicating significance (f-LSD) compared with sham controls; *p* values are as indicated in the text. (b) The x-axis denotes miRNA of interest, and the y-axis denotes the baseline-corrected percentage of fold expression change of miRNA using the formula $(2^{-\Delta\Delta CT}-1)*100$, where ΔΔCT represents the mean difference of contused unshocked and sham, contused shocked and sham, or contused shocked and contused unshocked ΔCT values. Data are expressed as a percentage of change (a value of zero equates to no change between surgery conditions), with asterisks indicating significance (f-LSD) compared with sham controls and hash tags indicating significance (f-LSD) compared with contused unshocked controls; *p* values are as indicated in the text.

between both time and treatment ($F_{(10,68)}$=2.592; $p$<0.01), as well as a three-way statistically significant interaction between time, treatment, and spinal section ($F_{(10,68)}$=2.594; $p$<0.01). *Post hoc* univariate ANOVAs indicated a main effect of time on miR1, miR21, miR124, and miR146a ($F_{(1,37)}$=27.562; $p$<0.001, $F_{(1,37)}$=34.516; $p$<0.001, $F_{(1,37)}$=16.025; $p$<0.001, and $F_{(1,37)}$=108.342; $p$<0.001, respectively), a main effect of treatment on miR1, miR21, miR124, and miR129-2 ($F_{(2,37)}$=11.803; $p$<0.001, $F_{(2,37)}$=23.76; $p$<0.001, $F_{(2,37)}$=17.493; $p$<0.001, and $F_{(2,37)}$=14.774; $p$<0.001, respectively), and a main effect of spinal section on miR1 and miR146a ($F_{(1,37)}$=10.58; $p$<0.005 and $F_{(1,37)}$=9.137; $p$<0.005, respectively). There was also a significant interaction effect of time and treatment on miR124 expression ($F_{(2,23)}$=4.866; $p$<0.05), and of time, treatment, and spinal section on miR1, miR129-2, and miR146a ($F_{(2,23)}$=3.68; $p$<0.05, $F_{(2,23)}$=6.31; $p$<0.005, and $F_{(2,23)}$=4.542; $p$<0.05, respectively).

#### 4.4.1.3 Uncontrollable nociception further dysregulated expression of the SCI-sensitive miRNAs miR1, miR124, and miR129-2

In addition, *post hoc* least significant difference (LSD) *t*-tests indicated that miR1, miR124, and miR129-2 expression is significantly decreased following spinal cord trauma, irrespective of exposure to uncontrollable intermittent tailshock ($p_{miR1}$<0.001, $p_{miR124}$<0.001, and $p_{miR129\text{-}2}$<0.001; Figure 19a-d). In contrast, miR21 expression was up-regulated following both no shock exposure and uncontrollable intermittent tailshock ($p_{miR21}$<0.001), and there was no change in the expression of miR146a (Figure 19a-d). In response to uncontrollable intermittent tailshock relative to no shock exposure, *post*

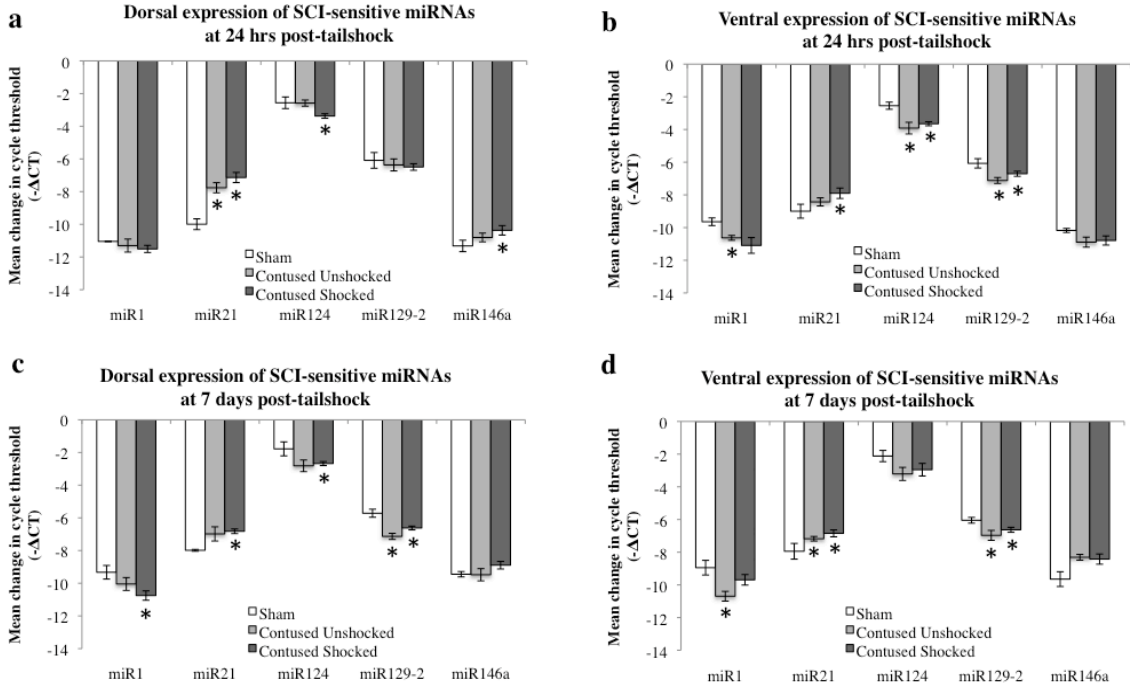


**Figure 19.** Bar graphs depicting qRT-PCR analysis of miRNA expression of miR1, miR21, miR124, miR129-2, and miR146a in dorsal (a, c) and ventral (b, d) sections at the lesion site for sham animals and after unshocked or shock treatment in contused animals at either 24 hrs (a, b) or 7 days (c, d) following tailshock treatment. (a-d) The x-axis denotes miRNA of interest, and the y-axis denotes the mean change in cycle threshold, where ΔCT represents the mean difference of miRNA and U6 control ΔCT values. Animals received either a laminectomy only (sham) or a T12-T13 spinal contusion followed by administration of unshock or shock 24 hrs later, and sacrificed at either 24 hrs or 7 days following unshock/shock treatment for harvesting and spatial sectioning of the cords. Data are expressed relative to U6 controls (a value of zero equates to no difference in expression between the miRNA and U6, positive values equate to higher miRNA expression, and negative values vice versa), with asterisks indicating significance (f-LSD) compared with sham controls; *p* values are as indicated in the text.

*hoc* planned comparisons indicated that there was a significant increase in expression of both miR1 in ventral/motor tissue and miR129-2 in dorsal/sensory tissue at 7 days following $SCI_{unshock}$ or $SCI_{shock}$ treatment (Student's two-tailed *t*-test, $p<0.05$ and $p<0.05$, respectively), and a significant decrease in expression of miR124 in dorsal/sensory tissue at 24 hrs following $SCI_{unshock}$ or $SCI_{shock}$ treatment ($p<0.01$; Figure 20a-d). *Post hoc* planned comparisons also indicated significant spatial changes (dorsal/sensory relative to ventral/motor) in miRNA expression, including decreased expression of both miR1 and miR146a in sham treated subjects at 24 hrs following $SCI_{unshock}$ or $SCI_{shock}$ treatment ($p<0.005$ and $p<0.05$, respectively), increased expression of miR124 in $SCI_{unshock}$ subjects at 24 hrs following $SCI_{unshock}$ or $SCI_{shock}$ treatment ($p<0.01$), decreased expression of miR1 in $SCI_{shock}$ subjects at 7 days following $SCI_{unshock}$ or $SCI_{shock}$ treatment ($p<0.05$), and decreased expression of miR146a in $SCI_{unshock}$ subjects at 7 days following $SCI_{unshock}$ or $SCI_{shock}$ treatment ($p<0.05$; Figure 21a, b).

#### 4.4.1.4 Correlation analyses indicated significant relationships between expression changes within distinct groups of SCI-sensitive miRNAs

Given their dysregulation following both contusion injury and uncontrollable nociception, we also hypothesized that statistical relationships might exist between expression changes of different SCI-sensitive miRNAs, indicative of possible co-regulation. Pearson's product-moment correlations indicated three groups of significant correlations between miRNAs (Fig. 22a, b; Table 2). There were significant correlations between miR1 and miR21, miR124, miR129-2, and miR146a (Pearson's $r=0.28$, $p<0.05$,

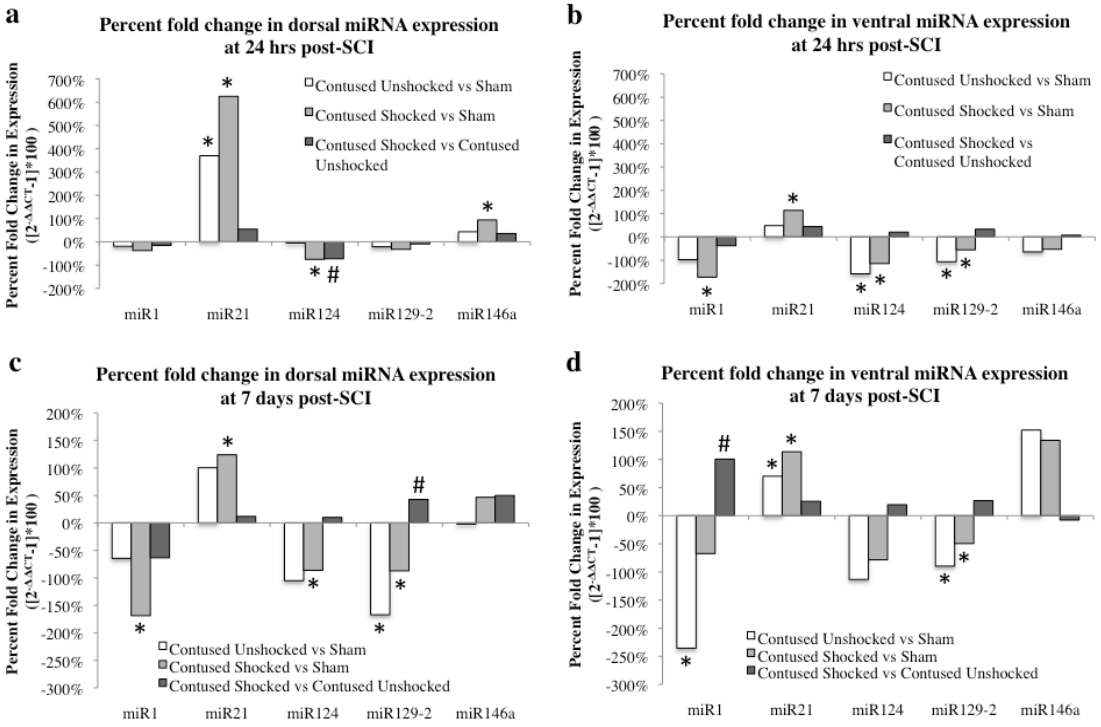


**Figure 20.** Bar graphs depicting qRT-PCR analysis of percent fold change in miRNA expression of miR1, miR21, miR124, miR129-2, and miR146a in dorsal (a, c) and ventral (b, d) sections at the lesion site for sham animals and after unshocked or shock treatment in contused animals at either 24 hrs (a, b) or 7 days (c, d) following tailshock treatment. (a-d) The x-axis denotes miRNA of interest, and the y-axis denotes the baseline-corrected percentage of fold expression change of miRNA using the formula $(2^{-\Delta\Delta CT}-1)*100$, where ΔΔCT represents the mean difference of contused unshocked and sham, contused shocked and sham, or contused shocked and contused unshocked ΔCT values. Data are expressed as a percentage of change (a value of zero equates to no change between surgery conditions), with asterisks indicating significance (f-LSD) compared with sham controls and hash tags indicating significance (f-LSD) compared with contused unshocked controls; *p* values are as indicated in the text.

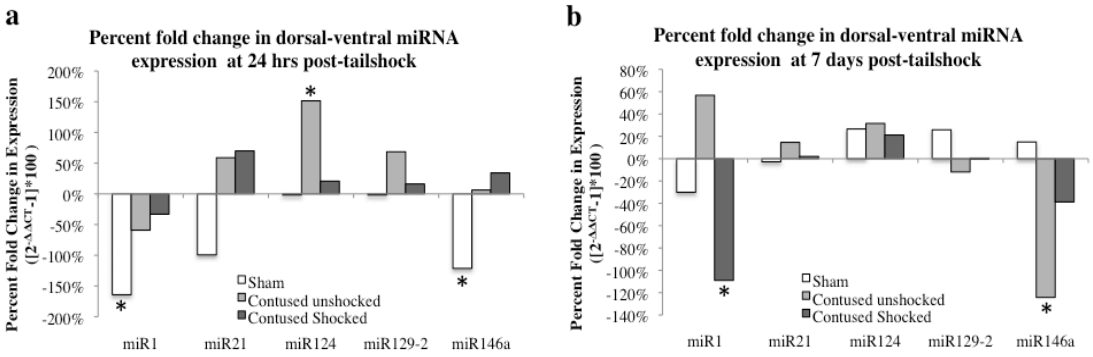


**Figure 21.** Bar graphs depicting qRT-PCR analysis of percent fold change in miRNA expression of miR1, miR21, miR124, miR129-2, and miR146a in dorsal sections relative to ventral at the lesion site for sham animals and after unshocked or shock treatment in contused animals at either 24 hrs (a) or 7 days (b) following tailshock treatment. (a, b) The x-axis denotes miRNA of interest, and the y-axis denotes the baseline-corrected percentage of fold expression change of miRNA using the formula $(2^{-\Delta\Delta CT}-1)*100$, where ΔΔCT represents the mean difference of dorsal and ventral ΔCT values for each treatment (ΔCT represents the mean difference of miRNA and U6 control ΔCT values). Data are expressed as a percentage of change (a value of zero equates to no change between spinal sections), with asterisks indicating significance (f-LSD) compared with ventral expression; *p* values are as indicated in the text.

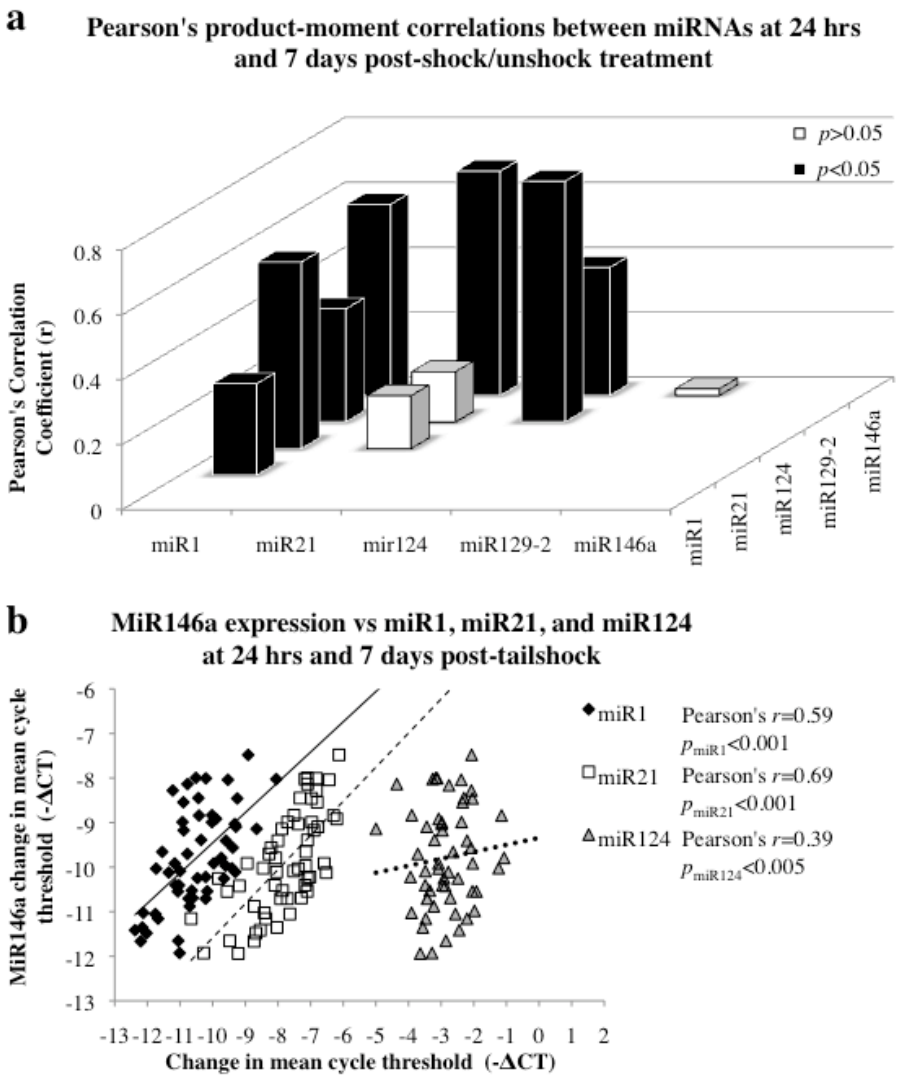


**Figure 22.** Correlation analyses to assess the relationship between miR146a miRNA expression and expression of miR1, miR21, and miR124 following SCI. (a) The x-axis and depth-axis represent the miRNAs of interest, and the y-axis depicts the magnitude of the Pearson's product-moment correlation coefficient, *r*, between corresponding the miRNAs indicated on the x and depth axes. Pearson's correlations indicated 7 statistically significant relationships ($p<0.05$; black bars) and 3 non-significant relationships ($p>0.05$; white bars). (b) The x-axis represents the mean difference in cycle threshold change (-ΔCT) between miRNA expression at both 24 hrs and 7 days following tailshock treatment and U6 controls, and the y-axis depicts the mean difference in cycle threshold change (-ΔCT) between miR146a expression at both 24 hrs and 7 days following tailshock treatment and U6 controls. Pearson's correlations indicated a significant correlation between miR1 (black diamonds), miR21 (white squares), and miR124 (grey triangles), and miR146a (Pearson's $r=0.59$, $P<0.001$, Pearson's $r=0.69$, $P<0.001$, and Pearson's $r=0.39$, $P<0.005$, respectively). Data are represented as the mean change in cycle threshold of miRNA expression relative to U6 controls ($-\Delta CT = CT_{U6} - CT_{miRNA}$).

**Table 2.** Pearson's product-moment correlations for miRNA expression at 24 hrs and 7 days following tailshock treatment. For each correlation between miRNAs given by row and column heading, the Pearson's Correlation Coefficient, *r*, the *p* value based on Student's two-tailed *t*-test, and the sample number, N, are listed in order from top to bottom, respectively. Three main clusters of miRNAs correlate significantly together: miR1 correlates with miR21, miR124, miR129-2, and miR146a, miR124 correlates with miR1, miR129-2, and miR146a, and miR146a correlates with miR1, miR21, and miR124. Single asterisks denote a significance of $p<0.05$, and double asterisks denote a significance of $p<0.01$.

| | | **miR1** | **miR21** | **mir124** | **miR129-2** | **miR146a** |
|---|---|---|---|---|---|---|
| **miR1** | Pearson Correlation | | .282* | .575** | .349** | .589** |
| | Sig. (2-tailed) | | 0.034 | 0.001 | 0.01 | 0.001 |
| | N | | 57 | 54 | 54 | 54 |
| **miR21** | Pearson Correlation | .282* | | 0.163 | -0.155 | .691** |
| | Sig. (2-tailed) | 0.034 | | 0.227 | 0.255 | 0.001 |
| | N | 57 | | 57 | 56 | 57 |
| **mir124** | Pearson Correlation | .575** | 0.163 | | .742** | .394** |
| | Sig. (2-tailed) | 0.001 | 0.227 | | 0.001 | 0.003 |
| | N | 54 | 57 | | 57 | 56 |
| **miR129-2** | Pearson Correlation | .349** | -0.155 | .742** | | 0.021 |
| | Sig. (2-tailed) | 0.01 | 0.255 | 0.001 | | 0.876 |
| | N | 54 | 56 | 57 | | 56 |
| **miR146a** | Pearson Correlation | .589** | .691** | .394** | 0.021 | |
| | Sig. (2-tailed) | 0.001 | 0.001 | 0.003 | 0.876 | |
| | N | 54 | 57 | 56 | 56 | |

Pearson's $r$=0.58, $p$<0.001, Pearson's $r$=0.35, $p$<0.01, and Pearson's $r$=0.59, $p$<0.001, respectively; Fig. 22a), between miR124 and miR1, miR129-2, and miR146a (Pearson's $r$=0.58, $p$<0.001, Pearson's $r$=0.74, $p$<0.001, and Pearson's $r$=0.40, $p$<0.005, respectively), and between miR146a and miR1, miR21, and miR124 (Pearson's $r$=0.59, $p$<0.001, Pearson's $r$=0.69, $p$<0.001, and Pearson's $r$=0.40, $p$<0.005, respectively; Fig. 22b).

*4.4.2 Intermittent shock sensitivity of miRNA target genes*

**4.4.2.1 Uncontrollable nociception had no significant effect on BDNF and IGF-1, mRNA targets of miR1, 1 hr following treatment**

As miR1 is further dysregulated by uncontrollable intermittent tailshock following contusion, we assessed the extent to which changes in miR1 expression corresponded to modulation of its neurotrophin and growth factor mRNA targets. Accordingly, miR1 has been shown to regulate the expression of both BDNF and IGF-1 (Lewis et al., 2003; Yu et al., 2008; Lee et al., 2012; Li et al., 2012). To determine whether uncontrollable intermittent tailshock dysregulates BDNF and IGF-1 mRNAs, their expression was determined by qRT-PCR in sham controls and in response to either no shock exposure or uncontrollable intermittent tailshock following contusion. As with the miRNA expression analysis, we first analyzed miRNA expression in full sections at 1 hr following treatment, and planned comparisons indicated that there was a significant decrease in expression of IGF-1 following contusion, irrespective of uncontrollable

intermittent tailshock (Student's two-tailed *t*-test, $p_{Unshock}<0.01$ and $p_{Shock}<0.005$; Figure 23a, b).

#### 4.4.2.2 Multivariate ANOVA and *post hoc* univariate ANOVAs indicated a significant interaction effect of time and treatment on BDNF and IGF-1 expression

Subsequently, spatial expression (dorsal/sensory-ventral/motor) of BDNF and IGF-1 mRNA was assessed at 24 hrs and 7 days following $SCI_{unshock}$ or $SCI_{shock}$ treatment. Multivariate ANOVA of qRT-PCR data indicated a significant main effect of time (Pillai's Trace Statistic, $F_{(2,51)}=5.198$; $p<0.01$), treatment ($F_{(4,104)}=11.662$; $p<0.001$), and spinal section ($F_{(2,51)}=17.966$; $p<0.001$), and a significant interaction effect between both time and treatment ($F_{(4,104)}=6.29$; $p<0.001$), and treatment and spinal section ($F_{(4,104)}=2.556$; $p<0.05$). *Post hoc* univariate ANOVAs indicated a main effect of time on IGF-1 mRNA ($F_{(1,52)}=9.491$; $p<0.005$), a main effect of treatment on both BDNF and IGF-1 mRNAs ($F_{(2,52)}=10.672$; $p<0.001$ and $F_{(2,52)}=30.133$; $p<0.001$, respectively), and a main effect of spinal section on BDNF mRNA ($F_{(1,52)}=36.314$; $p<0.001$). There was also a significant interaction effect of time and treatment on both BDNF and IGF-1 mRNA expression ($F_{(2,52)}=8.014$; $p<0.001$ and $F_{(2,52)}=7.948$; $p<0.001$, respectively), while BDNF mRNA expression was also significantly altered as a function of the interaction between time and spinal section ($F_{(1,52)}=5.437$; $p<0.05$), treatment and spinal section ($F_{(2,52)}=5.323$; $p<0.01$), and of time, treatment, and spinal section ($F_{(2,52)}=4.028$; $p<0.05$).

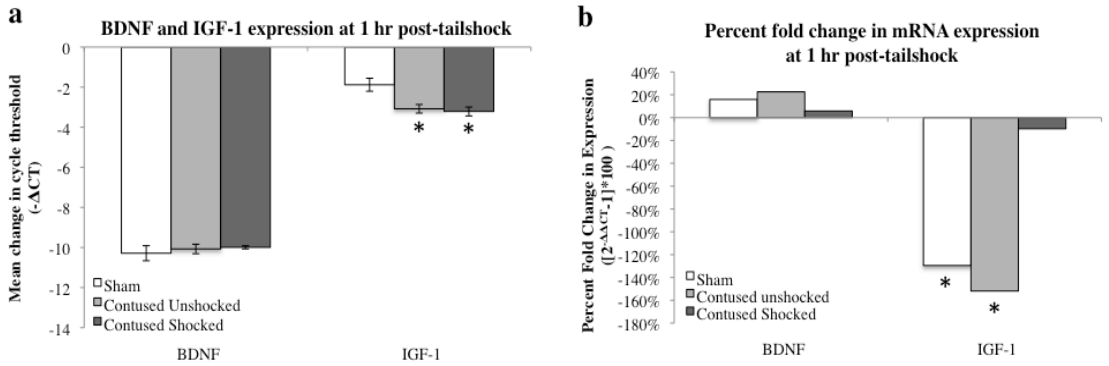


**Figure 23.** Bar graphs depicting qRT-PCR analysis of mRNA expression of BDNF and IGF-1 at the lesion site for sham animals and after unshocked or shock treatment in contused animals at 1 hr following tailshock treatment. (a) The x-axis denotes miRNA of interest, and the y-axis denotes the mean change in cycle threshold, where ΔCT represents the mean difference of mRNA and GAPDH control ΔCT values. Animals received either a laminectomy only (sham) or a T12-T13 spinal contusion followed by administration of unshock or shock 24 hrs later, and sacrificed at 1 hr following unshock/shock treatment for harvesting of the cords. Data are expressed relative to GAPDH controls (a value of zero equates to no difference in expression between the mRNA and GAPDH, positive values equate to higher miRNA expression, and negative values vice versa), with asterisks indicating significance (f-LSD) compared with sham controls; *p* values are as indicated in the text. (b) The x-axis denotes mRNA of interest, and the y-axis denotes the baseline-corrected percentage of fold expression change of mRNA using the formula ($2^{-\Delta\Delta CT}$-1)*100, where ΔΔCT represents the mean difference of contused unshocked and sham, contused shocked and sham, or contused shocked and contused unshocked ΔCT values. Data are expressed as a percentage of change (a value of zero equates to no change between surgery conditions), with asterisks indicating significance (f-LSD) compared with sham controls and hash tags indicating significance (f-LSD) compared with contused unshocked controls; *p* values are as indicated in the text.

#### 4.4.2.3 Uncontrollable nociception exhibited specific spatial and temporal dysregulation of BDNF and IGF-1 mRNA expression

In addition, *post hoc* least significant difference (LSD) *t*-tests indicated that IGF-1 expression was significantly decreased from 24 hrs to 7 days following $SCI_{unshock}$ or $SCI_{shock}$ treatment ($p_{IGF\text{-}1}<0.005$). BDNF mRNA was significantly decreased, while IGF-1 mRNA was significantly increased following spinal cord trauma, irrespective of uncontrollable intermittent tailshock or no shock exposure ($p_{BDNF}<0.001$ and $p_{IGF\text{-}1}<0.001$, respectively; Figure 24a, b). Furthermore, *post hoc* planned comparisons indicated that there was a significant decrease in expression of BDNF in dorsal/sensory tissue of $SCI_{shock}$ subjects relative to $SCI_{unshock}$ at 24 hrs following $SCI_{unshock}$ or $SCI_{shock}$ treatment (Student's two-tailed *t*-test, $p<0.001$), but a significant increase in expression of IGF-1 mRNA in ventral/motor tissue at 7 days following $SCI_{unshock}$ or $SCI_{shock}$ treatment ($p<0.05$; Figure 24c, b). *Post hoc* planned comparisons also indicated significant spatial changes (dorsal/sensory relative to ventral/motor) in mRNA expression, including increased relative dorsal/sensory expression of BDNF in sham, $SCI_{unshock}$, and $SCI_{shock}$ treated subjects at both 24 hrs ($p<0.01$, $p<0.001$, and $p<0.05$, respectively) and 7 days following $SCI_{unshock}$ or $SCI_{shock}$ treatment ($p<0.01$, $p<0.01$, and $p<0.001$, respectively), and increased expression of IGF-1 in $SCI_{shock}$ subjects at 7 days following $SCI_{unshock}$ or $SCI_{shock}$ treatment ($p<0.005$; Figure 25a, b).

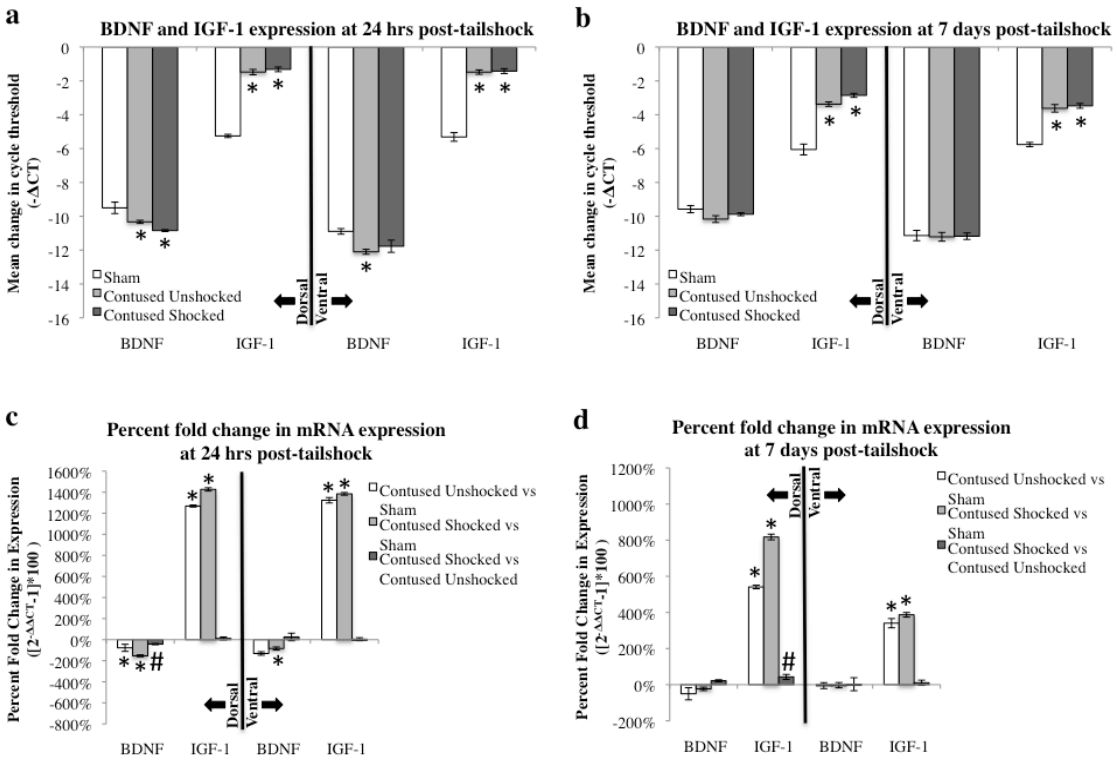


**Figure 24.** Bar graphs depicting qRT-PCR analysis of mRNA expression of BDNF and IGF-1 in dorsal and ventral sections at the lesion site for sham animals and after unshocked or shock treatment in contused animals at either 24 hrs (a, c) or 7 days (b, d) following tailshock treatment. (a, c) The x-axis denotes mRNA of interest, and the y-axis denotes the mean change in cycle threshold, where ΔCT represents the mean difference of mRNA and GAPDH control ΔCT values. Animals received either a laminectomy only (sham) or a T12-T13 spinal contusion followed by administration of unshock or shock 24 hrs later, and sacrificed at either 24 hrs or 7 days following unshock/shock treatment for harvesting and spatial sectioning of the cords. Data are expressed relative to GAPDH controls (a value of zero equates to no difference in expression between the mRNA and GAPDH, positive values equate to higher mRNA expression, and negative values vice versa), with asterisks indicating significance (f-LSD) compared with sham controls; *p* values are as indicated in the text. (b, d) The x-axis denotes mRNA of interest, and the y-axis denotes the baseline-corrected percentage of fold expression change of mRNA using the formula $(2^{-\Delta\Delta CT}-1)*100$, where ΔΔCT represents the mean difference of contused unshocked and sham, contused shocked and sham, or contused shocked and contused unshocked ΔCT values. Data are expressed as a percentage of change (a value of zero equates to no change between surgery conditions), with asterisks indicating significance (f-LSD) compared with sham controls and hash tags indicating significance (f-LSD) compared with contused unshocked controls; *p* values are as indicated in the text.

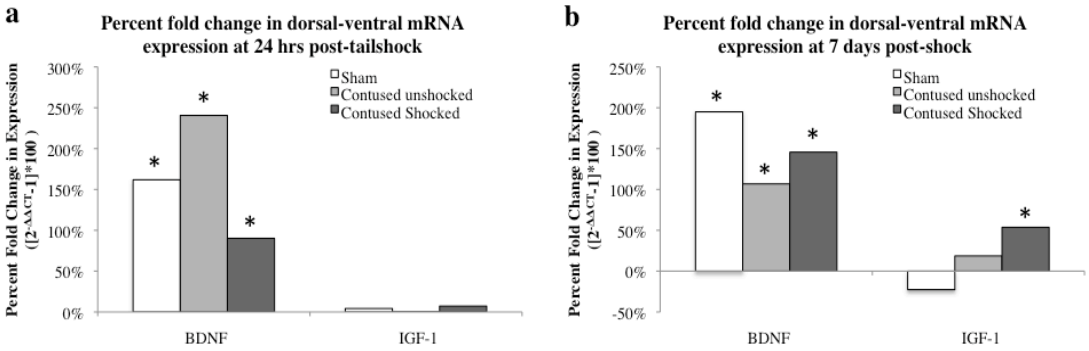


**Figure 25.** Bar graphs depicting qRT-PCR analysis of percent fold change in mRNA expression of BDNF and IGF-1 in dorsal sections relative to ventral at the lesion site for sham animals and after unshocked or shock treatment in contused animals at either 24 hrs (a) or 7 days (b) following tailshock treatment. (a, b) The x-axis denotes mRNA of interest, and the y-axis denotes the baseline-corrected percentage of fold expression change of mRNA using the formula $(2^{-\Delta\Delta CT}-1)*100$, where $\Delta\Delta CT$ represents the mean difference of dorsal and ventral $\Delta CT$ values for each treatment ($\Delta CT$ represents the mean difference of mRNA and GAPDH control $\Delta CT$ values). Data are expressed as a percentage of change (a value of zero equates to no change between spinal sections), with asterisks indicating significance (f-LSD) compared with ventral expression; *p* values are as indicated in the text.

#### 4.4.2.4 Correlation analyses indicated that expression changes of multiple SCI-sensitive miRNAs were associated with changes in BDNF and IGF-1 expression

As BDNF and IGF-1 are mRNA targets of miR1, we hypothesized that a statistical relationship would exist between expression changes in miR1 and that of BDNF and IGF-1. Pearson's product-moment correlations indicated two groups of significant correlations between SCI-sensitive miRNAs, BDNF, and IGF-1. There were significant correlations between BDNF and both miR21 and miR124 (Pearson's $r$=0.33, $p$<0.01 and Pearson's $r$=-0.29, $p$<0.05, respectively), and between IGF-1 and miR1, miR124, miR129-2, and miR146a (Pearson's $r$=0.40, $p$<0.005, Pearson's $r$=0.47, $p$<0.001, and Pearson's $r$=0.42, $p$<0.001, respectively). BDNF and IGF-1 also significantly, but inversely correlated with each other (Pearson's $r$=-0.31, $p$<0.05). Further analysis using stepwise linear regression indicated that the variance in miR21 and miR146a significantly explained the variance in BDNF ($F_{(1,46)}$=4.096; $p$<0.05), and that the variance in miR124, miR21, and miR146a significantly explained the variance in IGF-1 ($F_{(1,46)}$=8.149; $p$<0.01). Interestingly, while miR1 exhibits a significant correlation with IGF-1, the stepwise linear regression model indicated that miR124, miR129-2, and miR146a significantly explains the majority of the variance in IGF-1 independent of miR1.

## 4.5 Discussion

One of the current clinical challenges with mitigating the short and long-term effects of spinal cord injury is managing the uncontrollable nociception that results from

concomitant peripheral tissue damage. It is critical for future efforts to develop therapeutic strategies to attenuate glial activation, cell death, and sensitization of spinal neurons associated with intermittent noxious stimulation in order to inhibit maladaptive spinal plasticity, improve functional recovery, and suppress pain hypersensitivity following SCI with peripheral injuries (Liu et al., 1999; Frei et al., 2000; Beattie et al., 2002; Hains et al., 2003; Xu et al., 2004; Hains and Waxman, 2006; Lampert et al., 2006; Detloff et al., 2008; Kuzhandaivel et al., 2011). As uncontrollable nociception inhibits functional recovery, nociceptive stimuli may directly alter biology within damaged tissue at the injury site. Given their dysregulation following SCI and ability to coordinate the expression of large gene networks, it is possible that miRNAs are involved in the modulation of nociceptive circuitry and prevention of functional recovery resulting from uncontrollable nociception. Therapeutic manipulation of these miRNAs could alleviate the maladaptive effects of noxious stimulation on both the acute and chronic phases of SCI by suppressing activation of glia-mediated inflammation and inhibiting the synaptic remodeling of nociceptive circuitry that results in pain hypersensitivity, increased spasticity, and exacerbation of behavioral deficits.

In the current study, we investigated the regulation of SCI-sensitive miRNAs at the lesion site immediately following uncontrollable intermittent tailshock, and in dorsal and ventral segments at 24 hrs and 7 days after $SCI_{unshock}$ and $SCI_{shock}$ treatment. We found that uncontrollable intermittent tailshock significantly decreased expression of miR124 in dorsal/sensory tissue at 24 hrs post-SCI and significantly induced expression of miR129-2 in dorsal/sensory tissue and miR1 in ventral/motor tissue at 7 days

following $SCI_{unshock}$ and $SCI_{shock}$ treatment. This is the first evidence for the potential involvement of miRNAs and, consequently, miRNA-regulated gene networks, as mediators of uncontrollable nociception's effects on plasticity in the spinal cord, and indicates that peripheral noxious stimulation modulates gene networks and signaling pathways within the lesion site itself. Expression changes in miR1 and miR124, in response to uncontrollable intermittent tailshock, also corresponded to a shift in spatial expression from predominately sensory neural tissue to motor or vise versa, along with miR146a, which was not significantly changed by uncontrollable intermittent tailshock. In addition, changes in expression of miR124 were significantly explained by the variance in expression of miR1, miR129-2, and miR146a, suggesting that these miRNAs may be co-regulated. Collectively, these data suggest that uncontrollable nociception may modulate SCI-sensitive miRNA networks to affect spatially specific alterations to sensorimotor neuro-circuitry and signaling pathways involved in activation of microglia and inflammation at the lesion site. Firstly, miR124 drives neuronal differentiation through a negative feedback loop that inhibits REST-mediated repression of neuronal genes while simultaneously down-regulating non-neuronal genes (Visvanathan et al., 2007). Furthermore, miR124 has been recently shown to promote microglia and macrophage quiescence and inhibit inflammatory nociception (Ponomarev et al., 2011; Willemen et al., 2012; Kynast et al., 2013). Peripheral noxious stimulation led to significant down-regulation of miR124, with further inhibition exacerbating nociceptive behavior and administration of exogenous miR124 mimics attenuating nociception (Kynast et al., 2013). Secondly, MiR1 has been shown to regulate IGF-1, which is

produced by activated microglia in the central nervous system, and inhibition of miR1 is neuroprotective in stroke models (Kerr and Patterson, 2005; Lalancette-Hebert et al., 2007; Yu et al., 2008; Li et al., 2012; Selvamani et al., 2012). Thirdly, the miR129 family maintains cell cycle arrest in post-mitotic neurons through inhibition of G1/S phase-specific regulator cyclin-dependent kinase 6 (CDK6), and aberrant cell cycle entry resulting from suppression of miR129 can result in significant neuronal death (Di Giovanni et al., 2003; Byrnes et al., 2007; Herrup and Yang, 2007; Wu et al., 2010). Finally, miR146a not only plays an important role in innate immune response (Taganov et al., 2006; Nahid et al., 2009; Li et al., 2010a; Li et al., 2010b), but it has also been shown to be a negative feedback regulator of reactive astrocyte-mediated inflammatory response (Iyer et al., 2012).

Interestingly, we observed that although there was initially significant down-regulation of IGF-1 at 1 hr following uncontrollable intermittent tailshock, it was significantly induced in response to contusion at both 24 hrs and 7 days in both dorsal/sensory and ventral/motor tissue, and uncontrollable intermittent tailshock induced additional significant up-regulation at 7 days after $SCI_{unshock}$ and $SCI_{shock}$ treatment in dorsal tissue. Consistent with our previous findings (Garraway et al., 2011), we found that BDNF expression was significantly down-regulated at 24 hrs following uncontrollable intermittent tailshock in both the dorsal and ventral tissue, and additional significant BDNF suppression by uncontrollable intermittent tailshock was confined to the dorsal/sensory section of the spinal cord. We also observed that changes in expression of IGF-1 were significantly explained in a linear regression model by the

variance in miR124, miR21, and miR146a, and that changes in BDNF expression were significantly explained by the variance in miR21 and miR124 expression, suggesting that both BDNF and IGF-1 regulation involves a network of miRNAs. Surprisingly, changes in neither BDNF nor IGF-1 expression was significantly explained by the variance in miR1, despite its sensitivity to uncontrollable intermittent tailshock and microglia-specific involvement in regulating IGF-1 after stroke (Selvamani et al., 2012), and both miR1 and IGF-1 were both significantly up-regulated by uncontrollable nociception, suggesting a dissociation between miRNA and target gene networks following SCI and intermittent noxious stimulation, as have been observed in other models of neural damage (Pappalardo et al., 2013). Regardless, as miR124 suppresses activation of resting microglia and macrophages prior to injury, and both miR21 and miR146a have been shown to negatively regulate astrocyte activation following SCI (Ponomarev et al., 2011; Bhalala et al., 2012; Iyer et al., 2012; Willemen et al., 2012; Kynast et al., 2013), these miRNAs may constitute therapeutic targets for attenuating the maladaptive effects of uncontrollable nociception at the lesion site through inhibition of glial activation. In particular, miR124 is an especially attractive candidate, as it is involved in the regulation of both BDNF and IGF-1, sensitive to uncontrollable intermittent tailshock, and has been shown to inhibit nociceptive behavior associated with neuropathic pain (Kynast et al., 2013). However, because IGF-1 both promotes oligodendrocyte survival after SCI upon up-regulation through leukemia inhibitory factor-mediated activation of microglia (Kerr and Patterson, 2005; Mekhail et al., 2012), and reduces blood-brain barrier permeability and edema through attenuation of nitric

oxide synthase up-regulation upon its topical application prior to and following SCI (Sharma et al., 1997; Nyberg and Sharma, 2002), exogenous IGF-1 and other growth factors may need to be given in conjunction with miRNA treatments to prevent further destabilization of the blood-brain barrier.

## 4.6 Conclusion

Our evidence shows that uncontrollable intermittent noxious stimulation results in a very specific and limited profile of changes in SCI-sensitive miRNA expression within the lesion site in both the acute and chronic phase of injury. Because expression changes are confined to miRNAs, miR1, miR124, and miR129-2, that are involved in the regulation of microglia activation and cell cycle, and miR124 has been shown in other studies to attenuate the microglia activation-driven nociceptive behavior of neuro-inflammatory models of neuropathic pain, trauma-sensitive miRNAs that are further dysregulated by uncontrollable stimulation may serve as therapeutic targets and contribute towards regulation of neuropathic pain through modulation of glial activity. Consequently, it will be interesting to see if miR124, along with miR1 and miR129-2, exhibit similar anti-nociceptive effects in future studies of SCI-based neuropathic pain models.

Additionally, IGF-1 was persistently up-regulated following SCI, induced by uncontrollable intermittent tailshock in dorsal/sensory tissue at 7 days after $SCI_{unshock}$ and $SCI_{shock}$ treatment, and appeared to be either directly or indirectly co-regulated by miR124, miR21, and miR146a, all negative regulators of microglia and astrocyte activation, indicating that dysregulation of this miRNA network may play a role in the

development of neuropathic pain. Furthermore, changes in neither IGF-1 nor BDNF expression exhibited a statistical relationship with changes in miR1 expression, and both IGF-1 and miR1 were up-regulated by uncontrollable nociception, suggesting a dissociation between miRNA and target gene networks following SCI and intermittent noxious stimulation. Collectively, these data suggest that SCI-sensitive miRNAs constitute an important component in response to uncontrollable nociception from peripheral injury, possibly through regulation of microglia and astrocyte activation, and consequently, these miRNAs may constitute therapeutic targets for attenuating neuropathic pain following SCI.

# 5. CONCLUSION

## 5.1 Overview

The experiments in this dissertation were designed to determine the extent of miRNA dysregulation following spinal cord contusion and its implications in neuroinflammation, secondary injury, and neuropathic pain. Our evidence shows that SCI results in a very specific and limited profile of miRNA expression changes that unfold in a coordinated manner following injury, and that these SCI-sensitive miRNAs play an important role in mediating the maladaptive effects of uncontrollable nociception and morphine-induced escalation of pain-sensitivity (Table 3). Changes in miRNA-driven regulation of protein coding gene networks are mostly confined to the lesion site, with minimal adaptations within the surrounding tissue, and both miR129-2 and mir146a exhibit strong potential to be proxy markers for injury severity. MiRNA and cellular marker expression patterns indicated that miRNA dysregulation might play a role in stem cell niche activation and in loss of neuronal identity that might drive neuronal apoptosis and progression of secondary injury. In addition, miRNA dysregulation also plays a role in pain-sensitivity as morphine administration induced up-regulation of miR21 and IL6R expression, which is likely mediated through increased microglia activation, and modulation of miR21 may act as a counter-balance to keep neuroinflammation in check. Uncontrollable nociception modulated expression of SCI-sensitive miRNAs that inhibit cell cycle proteins and microglial activation, along with BDNF and IGF-1, and dysregulation of

**Table 3.** Summary of miRNA expression changes following spinal cord contusion, morphine administration, and uncontrollable nociception. For each miRNA and treatment group given by row and column heading, the direction change of regulation, denoted as either Down, Up, or non-significant (N/S), the baseline-corrected percentage of fold expression change of miRNA using the formula $(2^{-\Delta\Delta CT}-1)*100$, where ΔΔCT represents the mean difference of dorsal and ventral ΔCT values for each treatment (ΔCT represents the mean difference of miRNA and U6 control ΔCT values), and the *p* value based on Student's two-tailed *t*-test, are listed in order from top to bottom, respectively. Bolded treatment groups denote a significance of $p<0.05$.

| | **Treatment** | **Contusion** | | **Morphine** | | **Uncontrolled Shock** | | | | |
|---|---|---|---|---|---|---|---|---|---|---|
| | **Time after treatment** | **4 days** | **14 days** | **2 days** | **15 days** | **1 hr** | **24 hrs** | | **7 days** | |
| | **Spinal section** | **Whole** | **Whole** | **Whole** | **Whole** | **Whole** | **Dorsal** | **Ventral** | **Dorsal** | **Ventral** |
| **miR1** | Regulation | **Down** | **Down** | N/S | N/S | N/S | N/S | N/S | N/S | **Up** |
| | Fold Change | **-409.8%** | **-419.9%** | -7.9% | 36.5% | 14.2% | -15.4% | -38.0% | -63.5% | **100.5%** |
| | *p* value< | **0.05** | **0.04** | 0.69 | 0.34 | 0.72 | 0.65 | 0.38 | 0.16 | **0.03** |
| **miR21** | Regulation | **Up** | **Down** | N/S | **Up** | N/S | N/S | N/S | N/S | N/S |
| | Fold Change | **191.6%** | **-271.4%** | -32.3% | **102.3%** | -5.0% | 54.3% | 44.2% | 11.8% | 25.6% |
| | *p* value< | **0.00** | **0.01** | 0.25 | **0.03** | 0.88 | 0.15 | 0.18 | 0.73 | 0.19 |
| **miR124** | Regulation | N/S | **Down** | N/S | N/S | N/S | **Down** | N/S | N/S | N/S |
| | Fold Change | -81.3% | **-202.0%** | -23.7% | 25.2% | -22.6% | **-72.9%** | 20.5% | 10.1% | 19.5% |
| | *p* value< | 0.19 | **0.02** | 0.36 | 0.52 | 0.40 | **0.01** | 0.49 | 0.70 | 0.62 |
| **miR129-2** | Regulation | **Down** | N/S | N/S | N/S | N/S | N/S | N/S | **Up** | N/S |
| | Fold Change | **-317.0%** | -511.2% | -8.1% | 15.3% | -4.7% | -9.1% | 33.0% | **42.6%** | 26.7% |
| | *p* value< | **0.05** | 0.14 | 0.75 | 0.59 | 0.81 | 0.75 | 0.09 | **0.03** | 0.33 |
| **miR146a** | Regulation | N/S | N/S | N/S | N/S | N/S | N/S | N/S | N/S | N/S |
| | Fold Change | -4.9% | 62.4% | -10.1% | 65.2% | 2.0% | 35.4% | 7.3% | 49.9% | -7.9% |
| | *p* value< | 0.89 | 0.11 | 0.71 | 0.10 | 0.93 | 0.25 | 0.79 | 0.16 | 0.76 |

these miRNAs likely contributes towards the hypersensitivity of spinal neurons that underlies neuropathic pain.

## 5.2 Temporal Expression Patterns of SCI-Sensitive MiRNAs 25 Hours to 14 Days Following Contusion

Analyses of changes in miRNA expression over the entire time course across all three experiments, in response to contusion only, illustrated several interesting trends in SCI-driven modulation of miRNA expression profiles (Figure 26). Quantitative RT-PCR data was compiled for "contusion" groups at each corresponding time point (i.e., contused groups from experiment 1 at 4 and 14 days post-SCI, and contused with no shock exposure treatment groups from experiment 3 at 25 hrs, 2 days, and 8 days post-SCI), and changes in cycle threshold between miRNA and U6 ΔCT values were averaged for all subjects in each treatment group for both dorsal and ventral spinal sections, to approximate whole cord expression at 2 days and 8 days following contusion (24 hrs and 7 days following no shock exposure treatment, respectively). Data from the contused with vehicle treatment groups in experiment 2 were omitted from the analysis due to redundant time points and inconsistent expression as compared to the other groups, most likely due to potential neuroinflammatory effects resulting from vehicle injection and distal nociception from tail-flick testing. Of particular interest, miR21 exhibited significant up-regulation as early as 25 hrs following injury, with significantly increased expression sustained through 8 days after SCI, and expression gradually decreased from peak expression at 25 hrs through 14 days post-SCI, at which point

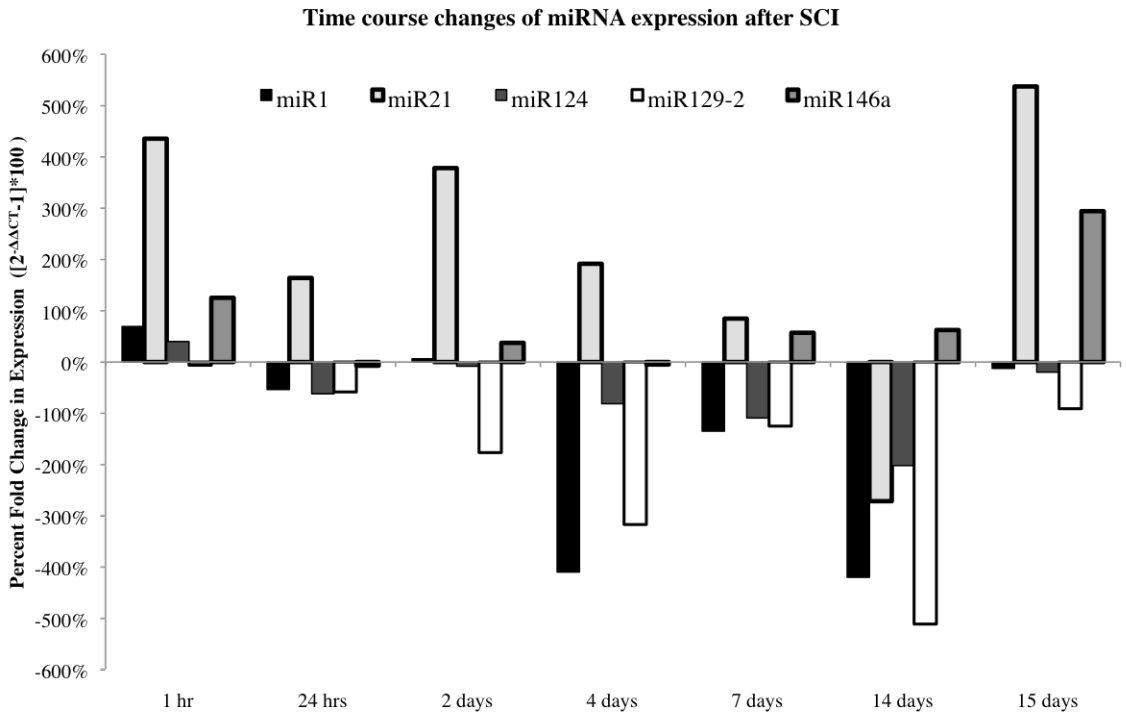


**Figure 26.** Bar graphs depicting qRT-PCR analysis of percent fold change in temporal miRNA expression of miR1, miR21, miR124, miR129-2, and miR146a at the lesion site after contusion and relative to sham controls for 4 and 14 days post-SCI, and after contusion and no shock treatment relative to sham controls at either 25 hrs, 2 days, or 8 days following SCI (1 hr, 24 hrs, and 7 days post-tailshock treatment, respectively). The x-axis denotes time following SCI, and the y-axis denotes the baseline-corrected percentage of fold expression change of miRNA using the formula $(2^{-\Delta\Delta CT}-1)*100$, where $\Delta\Delta CT$ represents the mean difference of dorsal and ventral $\Delta CT$ values for each treatment ($\Delta CT$ represents the mean difference of miRNA and U6 control $\Delta CT$ values). Data are expressed as a percentage of change (a value of zero equates to no change between spinal sections), with asterisks indicating significance (f-LSD) compared with ventral expression; *p* values are as indicated in Section 2.4.1 and Section 4.4.1.

miR21 was significantly down-regulated relative to sham controls. Conversely, miR124 was significantly down-regulated starting at 2 days post-SCI, and expression levels persistently decreased through 14 days following contusion. Given their respective roles in mediating quiescence of microglia and astrocytes (Ponomarev et al., 2011; Bhalala et al., 2012; Willemen et al., 2012), the temporal expression patterns of miR21 and miR124 likely reflect neuroinflammation-driven increases in gliosis at the lesion site.

### 5.3 Commonality of MiRNA Dysregulation in CNS Injury

Importantly, SCI-sensitive miRNAs are also dysregulated following other types of CNS injury, suggesting that there may be specific networks of miRNAs that play major roles in the progression of CNS pathology and that multiple types of CNS injury may share common therapeutic targets. Up-regulation of miR1 and miR124 has been observed within 24 hours of stroke, whereas miR21 and miR146a expression has been shown to be increased, as well as miR124 expression decreased, 7 days after stroke in neural progenitor cells within the subventricular zone (Jeyaseelan et al., 2008; Liu et al., 2010; Liu et al., 2011). Similarly, expression of both miR21 and miR146a is significantly induced after traumatic brain injury, and miR21 closely mirrors the temporal expression pattern observed in SCI, with peak expression at 3 days after injury followed by a gradual reduction back to sham levels of expression by 15 days post-TBI (Lei et al., 2009; Saugstad, 2010; Redell et al., 2011; Thounaojam et al., 2013). As most studies in stroke and TBI have focused on changes that occur with the first 24-72 hrs, it will be interesting to see if future research indicates additional consistencies in miRNA

dysregulation between stroke, TBI, and SCI during both the intermediate and later stages of injury.

### 5.4 Potential of SCI-Sensitive MiRNAs to Regulate Extracellular mRNA Expression and Serve as Biomarkers of Injury Severity

Spinal cord injury-sensitive miRNAs may also play a role in injury progression beyond the cellular compartment and exhibit regulatory effects outside of the lesion site, as miRNAs have been shown to be secreted by cells and both stable and detectable in serum, plasma, and cerebrospinal fluid (Cogswell et al., 2008; Gilad et al., 2008; Mitchell et al., 2008; Michael et al., 2010; Redell et al., 2010). Secreted miRNAs from cells within the lesion site could exert mRNA regulation in nearby cells, thereby directing a coordinated shift in mRNA expression profiles within groups of damaged cell populations as an adaptive response to SCI. In addition, SCI-sensitive miRNAs may serve as biomarkers for injury severity through their detection in blood serum, especially miR129-2 and miR146a, as we found that changes in their expression were predictive of functional deficits 24 hours following SCI. Numerous miRNAs have been shown to be dysregulated in blood plasma following both stroke and TBI, including an over 5-fold decrease in miR146a expression within the first 24 hours of severe TBI in human patients (Jeyaseelan et al., 2008; Liu et al., 2010; Redell et al., 2010). Additionally, a combined assessment of 3 TBI-sensitive miRNAs expressed only in the plasma of TBI patients exhibited substantial diagnostic accuracy (Redell et al., 2010), suggesting that SCI-sensitive miRNAs may also exhibit differential expression in blood plasma

following injury and serve as effective clinical biomarkers. Expression levels of established miRNA biomarkers for injury severity could then be measured in patient blood serum to determine the corresponding expression of key mRNA targets or degree of neuroinflammation within the lesion site, which would allow for metering of potential miRNA therapeutics to carefully optimize dosage to enhance functional recovery.

### 5.5 Potential Role of Distal Nociception after SCI in MiRNA-Target mRNA Network Dissociations and Extracellularly Initiated Regulation of MiRNAs

We also found that expression changes in miR1, miR124, and miR129-2 significantly explained the variance in pain sensitivity following SCI, suggesting that these miRNAs play a role in the regulation of nociceptive signaling pathways and that distal nociception likely modulates their expression. In addition, models of acute and neuropathic pain also result in dissociation between expression of both miR21 and miR1 and regulation of their mRNA targets. Concurrent up-regulation of miR21 and IL6R following morphine administration and of miR1 and IGF-1 following uncontrollable nociception lends further evidence that distal nociceptive stimulation can regulate expression changes in SCI-sensitive miRNAs within the lesion site. This regulation is likely a result of damaged neuronal circuitry at the lesion site being incapable of properly responding to distal nociceptive signaling in the form of neurotransmitter release, leading to accumulation of excitatory neurotransmitters and exacerbated activation of nearby microglia and astrocytes. Increased extracellular signaling and binding of surface receptors can activate multiple signaling pathways capable of regulating specific miRNA

expression. For example, ethanol has been shown to selectively suppress miR21 expression in neural stem cells through activation of $GABA_A$ receptor-dependent mechanisms (Sathyan et al., 2007). Activation of these receptor mediated intracellular signaling pathways can trigger phosphorylation cascades with the capacity to modulate multiple aspects of miRNA biogenesis. Specifically, activation of the mitogen-activated protein kinase (MAPk) pathway has been shown to lead to phosphorylation of a component of the Drosha/DGCR8 pri-miRNA processing complex, RNA helicase P68/DDX5 (Hong et al., 2013). In addition, MAPk can modulate activity of the RISC complex through phosphorylation of the Argonaute 2 protein at a serine residue, thereby preventing its localization with processing bodies, or at a tyrosine residue within the RNA binding region that reduces binding of miRNAs and, consequently, their ability to inhibit translation (Zeng et al., 2008; Rudel et al., 2011). Similar regulation of Argonaute protein phosphorylation may contribute to the dissociations in miRNA and mRNA target networks following SCI and distal nociception, as phosphorylation within specific sites of the RNA binding region may alter protein folding in a functionally selective manner. The modulated RNA binding region could reduce binding of a majority of miRNAs, while allowing for a few specific miRNAs to maintain the same binding affinity with reduced interference from competing miRNAs. Distal nociception-induced dissociations could occur both from highly expressed miRNAs being unable to form stable complexes with RISC, allowing mRNA target translation to occur with reduced inhibition (i.e., up-regulation of both miRNA and mRNA target expression), and from lower expressed miRNAs being preferentially loaded onto RISC in the presence of

reduced binding competition, yielding increased inhibition of mRNA targets without the need for a corresponding increase in initial miRNA expression. Furthermore, increased activation of phosphorylation signaling pathways can also lead to increased activation or inactivation of transcription factors that either directly or indirectly regulate transcriptional expression of miRNAs, which could synergistically enhance these miRNA-mRNA target dissociations following SCI and distal nociception.

## 5.6 Future Directions

While these SCI-sensitive miRNAs hold potential as therapeutic targets, additional studies are needed to determine their ability to improve functional recovery, mitigate neuropathic pain, and block the maladaptive effects of morphine administration. *In vivo* studies examining the effects of exogenous administration of individual SCI-sensitive miRNA mimics and anti-miRNAs following SCI could indicate the regulatory effects of specific miRNAs on functional behavior and, in conjunction with the use of gene and miRNA microarrays, immunofluorescence, and *in situ* hybridization, could elucidate their specific effects on SCI pathology-associated gene networks, inflammation, apoptosis, and glial activation in the damaged spinal cord. The increased understanding of miRNA function on the SCI microenvironment would allow for more effective development of therapeutics by indicating which combinations of different miRNA mimics and anti-miRNAs could be the most effective at minimizing secondary injury, promoting regeneration within the lesion site, improving functional recovery, and attenuating neuropathic pain. In addition, analysis of global gene expression changes

due to miRNA manipulations could also indicate important factors that are beneficial to injury mitigation, such as BDNF and IGF-1, but adversely impacted by miRNA treatments. Correspondingly, exogenous administration of these compromised factors to the lesion site, in addition to selected miRNA mimics and anti-miRNAs, could optimize the effectiveness of miRNA therapeutics by mitigating potential maladaptive regulation. For example, miR124 is a promising candidate for preventing neuropathic pain, as it is sensitive to uncontrollable nociception, suppresses activation of resting microglia and macrophages prior to injury, and has been shown to inhibit nociceptive behavior associated with peripheral noxious stimulation (Ponomarev et al., 2011; Willemen et al., 2012; Kynast et al., 2013). However, because miR124 plays a role in IGF-1 regulation, which is beneficial following SCI through promotion of oligodendrocytes survival and restoration of the blood-spinal cord barrier (Sharma et al., 1997; Nyberg and Sharma, 2002; Kerr and Patterson, 2005; Mekhail et al., 2012), IGF-1 may need to be included with miR124 administration to maximize effectiveness. Consequently, thorough analyses of the regulatory and physiological effects of *in vivo* miRNA manipulation following contusion injury, uncontrollable nociception, and morphine administration could uncover novel therapeutic strategies to substantially improve functional outcomes and prevent neuropathic pain in human patients.

# REFERENCES


Albrecht PJ, Dahl JP, Stoltzfus OK, Levenson R, Levison SW (2002) Ciliary neurotrophic factor activates spinal cord astrocytes, stimulating their production and release of fibroblast growth factor-2, to increase motor neuron survival. Exp Neurol 173:46-62.

Allen SJ, Dawbarn D (2006) Clinical relevance of the neurotrophins and their receptors. Clin Sci (Lond) 110:175-191.

Alvarez-Garcia I, Miska EA (2005) MicroRNA functions in animal development and human disease. Development 132:4653-4662.

Anderson KD (2004) Targeting recovery: priorities of the spinal cord-injured population. J Neurotrauma 21:1371-1383.

Ankeny DP, Popovich PG (2009) Mechanisms and implications of adaptive immune responses after traumatic spinal cord injury. Neuroscience 158:1112-1121.

Ashburner M, Ball CA, Blake JA, Botstein D, Butler H, Cherry JM, Davis AP, Dolinski K, Dwight SS, Eppig JT, Harris MA, Hill DP, Issel-Tarver L, Kasarskis A, Lewis S, Matese JC, Richardson JE, Ringwald M, Rubin GM, Sherlock G (2000) Gene ontology: tool for the unification of biology. The Gene Ontology Consortium. Nat Genet 25:25-29.

Bains M, Hall ED (2012) Antioxidant therapies in traumatic brain and spinal cord injury. Biochim Biophys Acta 1822:675-684.

Balami JS, Chen RL, Grunwald IQ, Buchan AM (2011) Neurological complications of acute ischaemic stroke. Lancet Neurol 10:357-371.

Balasingam V, Tejada-Berges T, Wright E, Bouckova R, Yong VW (1994) Reactive astrogliosis in the neonatal mouse brain and its modulation by cytokines. J Neurosci 14:846-856.

Barbacid M (1994) The Trk family of neurotrophin receptors. J Neurobiol 25:1386-1403.

Bareyre FM, Schwab ME (2003) Inflammation, degeneration and regeneration in the injured spinal cord: insights from DNA microarrays. Trends Neurosci 26:555-563.

Barnabe-Heider F, Frisen J (2008) Stem cells for spinal cord repair. Cell Stem Cell 3:16-24.

Barone FC, Arvin B, White RF, Miller A, Webb CL, Willette RN, Lysko PG, Feuerstein GZ (1997) Tumor necrosis factor-alpha. A mediator of focal ischemic brain injury. Stroke 28:1233-1244.

Bartholdi D, Schwab ME (1997) Expression of pro-inflammatory cytokine and chemokine mRNA upon experimental spinal cord injury in mouse: an in situ hybridization study. Eur J Neurosci 9:1422-1438.

Basso DM, Beattie MS, Bresnahan JC (1995) A sensitive and reliable locomotor rating scale for open field testing in rats. J Neurotrauma 12:1-21.

Beattie MS, Hermann GE, Rogers RC, Bresnahan JC (2002) Cell death in models of spinal cord injury. Prog Brain Res 137:37-47.

Beck T, Lindholm D, Castren E, Wree A (1994) Brain-derived neurotrophic factor protects against ischemic cell damage in rat hippocampus. J Cereb Blood Flow Metab 14:689-692.

Beilharz EJ, Russo VC, Butler G, Baker NL, Connor B, Sirimanne ES, Dragunow M, Werther GA, Gluckman PD, Williams CE, Scheepens A (1998) Co-ordinated and cellular specific induction of the components of the IGF/IGFBP axis in the rat brain following hypoxic-ischemic injury. Brain Res Mol Brain Res 59:119-134.

Benowitz LI, Popovich PG (2011) Inflammation and axon regeneration. Curr Opin Neurol 24:577-583.

Benveniste EN (1998) Cytokine actions in the central nervous system. Cytokine Growth Factor Rev 9:259-275.

Bethea JR, Dietrich WD (2002) Targeting the host inflammatory response in traumatic spinal cord injury. Curr Opin Neurol 15:355-360.

Bethea JR, Nagashima H, Acosta MC, Briceno C, Gomez F, Marcillo AE, Loor K, Green J, Dietrich WD (1999) Systemically administered interleukin-10 reduces tumor necrosis factor-alpha production and significantly improves functional recovery following traumatic spinal cord injury in rats. J Neurotrauma 16:851-863.

Bhalala OG, Pan L, Sahni V, McGuire TL, Gruner K, Tourtellotte WG, Kessler JA (2012) microRNA-21 regulates astrocytic response following spinal cord injury. J Neurosci 32:17935-17947.

Bhaumik D, Scott GK, Schokrpur S, Patil CK, Orjalo AV, Rodier F, Lithgow GJ, Campisi J (2009) MicroRNAs miR-146a/b negatively modulate the senescence-associated inflammatory mediators IL-6 and IL-8. Aging (Albany NY) 1:402-411.

Bilgen M, Dogan B, Narayana PA (2002) In vivo assessment of blood-spinal cord barrier permeability: serial dynamic contrast enhanced MRI of spinal cord injury. Magn Reson Imaging 20:337-341.

Blaha GR, Raghupathi R, Saatman KE, McIntosh TK (2000) Brain-derived neurotrophic factor administration after traumatic brain injury in the rat does not protect against behavioral or histological deficits. Neuroscience 99:483-493.

Blight AR (1994) Effects of silica on the outcome from experimental spinal cord injury: implication of macrophages in secondary tissue damage. Neuroscience 60:263-273.

Bonita R (1992) Epidemiology of stroke. Lancet 339:342-344.

Boswell K, Menaker J, Falcone R (2013) An Update on Spinal Cord Injury: Epidemiology, Diagnosis, and Treatment for the Emergency Physician. Trauma reports 14:1-11.

Boutin H, LeFeuvre RA, Horai R, Asano M, Iwakura Y, Rothwell NJ (2001) Role of IL-1alpha and IL-1beta in ischemic brain damage. J Neurosci 21:5528-5534.

Boyce VS, Tumolo M, Fischer I, Murray M, Lemay MA (2007) Neurotrophic factors promote and enhance locomotor recovery in untrained spinalized cats. J Neurophysiol 98:1988-1996.

Brambilla R, Bracchi-Ricard V, Hu WH, Frydel B, Bramwell A, Karmally S, Green EJ, Bethea JR (2005) Inhibition of astroglial nuclear factor kappaB reduces inflammation and improves functional recovery after spinal cord injury. J Exp Med 202:145-156.

Brennecke J, Stark A, Russell RB, Cohen SM (2005) Principles of microRNA-target recognition. PLoS Biol 3:e85.

Brenneman DE, Hill JM, Glazner GW, Gozes I, Phillips TW (1995) Interleukin-1 alpha and vasoactive intestinal peptide: enigmatic regulation of neuronal survival. Int J Dev Neurosci 13:187-200.

Breving K, Esquela-Kerscher A (2010) The complexities of microRNA regulation: mirandering around the rules. Int J Biochem Cell Biol 42:1316-1329.

Brown AK, Woller SA, Moreno G, Grau JW, Hook MA (2011) Exercise therapy and recovery after SCI: evidence that shows early intervention improves recovery of function. Spinal Cord 49:623-628.

Bruce AJ, Boling W, Kindy MS, Peschon J, Kraemer PJ, Carpenter MK, Holtsberg FW, Mattson MP (1996) Altered neuronal and microglial responses to excitotoxic and ischemic brain injury in mice lacking TNF receptors. Nat Med 2:788-794.

Busch SA, Silver J (2007) The role of extracellular matrix in CNS regeneration. Curr Opin Neurobiol 17:120-127.

Bushati N, Cohen SM (2007) microRNA functions. Annu Rev Cell Dev Biol 23:175-205.

Buttini M, Sauter A, Boddeke HW (1994) Induction of interleukin-1 beta mRNA after focal cerebral ischaemia in the rat. Brain Res Mol Brain Res 23:126-134.

Bye N, Habgood MD, Callaway JK, Malakooti N, Potter A, Kossmann T, Morganti-Kossmann MC (2007) Transient neuroprotection by minocycline following traumatic brain injury is associated with attenuated microglial activation but no changes in cell apoptosis or neutrophil infiltration. Exp Neurol 204:220-233.

Byrnes KR, Stoica BA, Fricke S, Di Giovanni S, Faden AI (2007) Cell cycle activation contributes to post-mitotic cell death and secondary damage after spinal cord injury. Brain 130:2977-2992.

Cao Y, Gunn AJ, Bennet L, Wu D, George S, Gluckman PD, Shao XM, Guan J (2003) Insulin-like growth factor (IGF)-1 suppresses oligodendrocyte caspase-3 activation and increases glial proliferation after ischemia in near-term fetal sheep. J Cereb Blood Flow Metab 23:739-747.

Castillo J, Rodriguez I (2004) Biochemical changes and inflammatory response as markers for brain ischaemia: molecular markers of diagnostic utility and prognosis in human clinical practice. Cerebrovasc Dis 17 Suppl 1:7-18.

Chen JF, Mandel EM, Thomson JM, Wu Q, Callis TE, Hammond SM, Conlon FL, Wang DZ (2006) The role of microRNA-1 and microRNA-133 in skeletal muscle proliferation and differentiation. Nat Genet 38:228-233.

Cheng B, Mattson MP (1994) NT-3 and BDNF protect CNS neurons against metabolic/excitotoxic insults. Brain Res 640:56-67.

Chiang CS, Stalder A, Samimi A, Campbell IL (1994) Reactive gliosis as a consequence of interleukin-6 expression in the brain: studies in transgenic mice. Dev Neurosci 16:212-221.

Chodobski A, Zink BJ, Szmydynger-Chodobska J (2011) Blood-brain barrier pathophysiology in traumatic brain injury. Transl Stroke Res 2:492-516.

Christensen MD, Hulsebosch CE (1997) Chronic central pain after spinal cord injury. J Neurotrauma 14:517-537.

Chung IY, Benveniste EN (1990) Tumor necrosis factor-alpha production by astrocytes. Induction by lipopolysaccharide, IFN-gamma, and IL-1 beta. J Immunol 144:2999-3007.

Clausen BH, Lambertsen KL, Babcock AA, Holm TH, Dagnaes-Hansen F, Finsen B (2008) Interleukin-1beta and tumor necrosis factor-alpha are expressed by different subsets of microglia and macrophages after ischemic stroke in mice. J Neuroinflammation 5:46.

Cogswell JP, Ward J, Taylor IA, Waters M, Shi Y, Cannon B, Kelnar K, Kemppainen J, Brown D, Chen C, Prinjha RK, Richardson JC, Saunders AM, Roses AD, Richards CA (2008) Identification of miRNA changes in Alzheimer's disease brain and CSF yields putative biomarkers and insights into disease pathways. J Alzheimers Dis 14:27-41.

Constantini S, Young W (1994) The effects of methylprednisolone and the ganglioside GM1 on acute spinal cord injury in rats. J Neurosurg 80:97-111.

Conti A, Miscusi M, Cardali S, Germano A, Suzuki H, Cuzzocrea S, Tomasello F (2007) Nitric oxide in the injured spinal cord: synthases cross-talk, oxidative stress and inflammation. Brain Res Rev 54:205-218.

Corsten MF, Miranda R, Kasmieh R, Krichevsky AM, Weissleder R, Shah K (2007) MicroRNA-21 knockdown disrupts glioma growth in vivo and displays synergistic cytotoxicity with neural precursor cell delivered S-TRAIL in human gliomas. Cancer Res 67:8994-9000.

Cripps RA, Lee BB, Wing P, Weerts E, Mackay J, Brown D (2011) A global map for traumatic spinal cord injury epidemiology: towards a living data repository for injury prevention. Spinal Cord 49:493-501.

Crown ED, Ferguson AR, Joynes RL, Grau JW (2002) Instrumental learning within the spinal cord. II. Evidence for central mediation. Physiol Behav 77:259-267.

Cui Y, Chen Y, Zhi JL, Guo RX, Feng JQ, Chen PX (2006) Activation of p38 mitogen-activated protein kinase in spinal microglia mediates morphine antinociceptive tolerance. Brain Res 1069:235-243.

D'Ercole AJ, Ye P, Calikoglu AS, Gutierrez-Ospina G (1996) The role of the insulin-like growth factors in the central nervous system. Mol Neurobiol 13:227-255.

Das M, Mohapatra S, Mohapatra SS (2012) New perspectives on central and peripheral immune responses to acute traumatic brain injury. J Neuroinflammation 9:236.

Dave RS, Khalili K (2010) Morphine treatment of human monocyte-derived macrophages induces differential miRNA and protein expression: impact on

inflammation and oxidative stress in the central nervous system. J Cell Biochem 110:834-845.

Davies CA, Loddick SA, Toulmond S, Stroemer RP, Hunt J, Rothwell NJ (1999) The progression and topographic distribution of interleukin-1beta expression after permanent middle cerebral artery occlusion in the rat. J Cereb Blood Flow Metab 19:87-98.

De Biase A, Knoblach SM, Di Giovanni S, Fan C, Molon A, Hoffman EP, Faden AI (2005) Gene expression profiling of experimental traumatic spinal cord injury as a function of distance from impact site and injury severity. Physiol Genomics 22:368-381.

Demediuk P, Saunders RD, Anderson DK, Means ED, Horrocks LA (1987) Early membrane lipid changes in laminectomized and traumatized cat spinal cord. Neurochem Pathol 7:79-89.

Dennis G, Jr., Sherman BT, Hosack DA, Yang J, Gao W, Lane HC, Lempicki RA (2003) DAVID: Database for Annotation, Visualization, and Integrated Discovery. Genome Biol 4:P3.

Detloff MR, Fisher LC, McGaughy V, Longbrake EE, Popovich PG, Basso DM (2008) Remote activation of microglia and pro-inflammatory cytokines predict the onset and severity of below-level neuropathic pain after spinal cord injury in rats. Exp Neurol 212:337-347.

DeVivo MJ (1997) Causes and costs of spinal cord injury in the United States. Spinal Cord 35:809-813.

Dharap A, Bowen K, Place R, Li LC, Vemuganti R (2009) Transient focal ischemia induces extensive temporal changes in rat cerebral microRNAome. J Cereb Blood Flow Metab 29:675-687.

Di Giovanni S, Knoblach SM, Brandoli C, Aden SA, Hoffman EP, Faden AI (2003) Gene profiling in spinal cord injury shows role of cell cycle in neuronal death. Ann Neurol 53:454-468.

Dluzniewska J, Sarnowska A, Beresewicz M, Johnson I, Srai SK, Ramesh B, Goldspink G, Gorecki DC, Zablocka B (2005) A strong neuroprotective effect of the autonomous C-terminal peptide of IGF-1 Ec (MGF) in brain ischemia. FASEB J 19:1896-1898.

Doench JG, Sharp PA (2004) Specificity of microRNA target selection in translational repression. Genes Dev 18:504-511.

Donnan GA, Fisher M, Macleod M, Davis SM (2008) Stroke. Lancet (London, England) 371:1612-1623.

Du T, Zamore PD (2005) microPrimer: the biogenesis and function of microRNA. Development 132:4645-4652.

Dweep H, Sticht C, Pandey P, Gretz N (2011) miRWalk--database: prediction of possible miRNA binding sites by "walking" the genes of three genomes. J Biomed Inform 44:839-847.

Dworkin RH, Backonja M, Rowbotham MC, Allen RR, Argoff CR, Bennett GJ, Bushnell MC, Farrar JT, Galer BS, Haythornthwaite JA, Hewitt DJ, Loeser JD, Max MB, Saltarelli M, Schmader KE, Stein C, Thompson D, Turk DC, Wallace

MS, Watkins LR, Weinstein SM (2003) Advances in neuropathic pain: diagnosis, mechanisms, and treatment recommendations. Arch Neurol 60:1524-1534.

Elkabes S, DiCicco-Bloom EM, Black IB (1996) Brain microglia/macrophages express neurotrophins that selectively regulate microglial proliferation and function. J Neurosci 16:2508-2521.

Faulkner JR, Herrmann JE, Woo MJ, Tansey KE, Doan NB, Sofroniew MV (2004) Reactive astrocytes protect tissue and preserve function after spinal cord injury. J Neurosci 24:2143-2155.

Feigin VL, Barker-Collo S, Krishnamurthi R, Theadom A, Starkey N (2010) Epidemiology of ischaemic stroke and traumatic brain injury. Best Pract Res Clin Anaesthesiol 24:485-494.

Ferguson AR, Bolding KA, Huie JR, Hook MA, Santillano DR, Miranda RC, Grau JW (2008) Group I metabotropic glutamate receptors control metaplasticity of spinal cord learning through a protein kinase C-dependent mechanism. J Neurosci 28:11939-11949.

Ferguson AR, Crown ED, Grau JW (2006) Nociceptive plasticity inhibits adaptive learning in the spinal cord. Neuroscience 141:421-431.

Fichtlscherer S, Zeiher AM, Dimmeler S (2011) Circulating microRNAs: biomarkers or mediators of cardiovascular diseases? Arterioscler Thromb Vasc Biol 31:2383-2390.

Figlewicz DA, Gremo F, Innocenti GM (1988) Differential expression of neurofilament subunits in the developing corpus callosum. Brain Res 470:181-189.

Filipowicz W, Bhattacharyya SN, Sonenberg N (2008) Mechanisms of post-transcriptional regulation by microRNAs: are the answers in sight? Nat Rev Genet 9:102-114.

Fitch MT, Doller C, Combs CK, Landreth GE, Silver J (1999) Cellular and molecular mechanisms of glial scarring and progressive cavitation: in vivo and in vitro analysis of inflammation-induced secondary injury after CNS trauma. J Neurosci 19:8182-8198.

Frankel LB, Christoffersen NR, Jacobsen A, Lindow M, Krogh A, Lund AH (2008) Programmed cell death 4 (PDCD4) is an important functional target of the microRNA miR-21 in breast cancer cells. J Biol Chem 283:1026-1033.

Frei E, Klusman I, Schnell L, Schwab ME (2000) Reactions of oligodendrocytes to spinal cord injury: cell survival and myelin repair. Exp Neurol 163:373-380.

Frisen J, Verge VM, Cullheim S, Persson H, Fried K, Middlemas DS, Hunter T, Hokfelt T, Risling M (1992) Increased levels of trkB mRNA and trkB protein-like immunoreactivity in the injured rat and cat spinal cord. Proc Natl Acad Sci U S A 89:11282-11286.

Garraway SM, Petruska JC, Mendell LM (2003) BDNF sensitizes the response of lamina II neurons to high threshold primary afferent inputs. Eur J Neurosci 18:2467-2476.

Garraway SM, Turtle JD, Huie JR, Lee KH, Hook MA, Woller SA, Grau JW (2011) Intermittent noxious stimulation following spinal cord contusion injury impairs

locomotor recovery and reduces spinal brain-derived neurotrophic factor-tropomyosin-receptor kinase signaling in adult rats. Neuroscience 199:86-102.

Ghajar J (2000) Traumatic brain injury. Lancet 356:923-929.

Ghirnikar RS, Lee YL, Eng LF (1998) Inflammation in traumatic brain injury: role of cytokines and chemokines. Neurochem Res 23:329-340.

Gilad S, Meiri E, Yogev Y, Benjamin S, Lebanony D, Yerushalmi N, Benjamin H, Kushnir M, Cholakh H, Melamed N, Bentwich Z, Hod M, Goren Y, Chajut A (2008) Serum microRNAs are promising novel biomarkers. PLoS One 3:e3148.

Gilyarov AV (2008) Nestin in central nervous system cells. Neurosci Behav Physiol 38:165-169.

Giulian D, Robertson C (1990) Inhibition of mononuclear phagocytes reduces ischemic injury in the spinal cord. Ann Neurol 27:33-42.

Gomes-Leal W, Corkill DJ, Freire MA, Picanco-Diniz CW, Perry VH (2004) Astrocytosis, microglia activation, oligodendrocyte degeneration, and pyknosis following acute spinal cord injury. Exp Neurol 190:456-467.

Gomez-Pinilla F, Huie JR, Ying Z, Ferguson AR, Crown ED, Baumbauer KM, Edgerton VR, Grau JW (2007) BDNF and learning: Evidence that instrumental training promotes learning within the spinal cord by up-regulating BDNF expression. Neuroscience 148:893-906.

Gorgey AS, Gater DR (2012) Insulin growth factors may explain relationship between spasticity and skeletal muscle size in men with spinal cord injury. J Rehabil Res Dev 49:373-380.

Grau JW, Crown ED, Ferguson AR, Washburn SN, Hook MA, Miranda RC (2006) Instrumental learning within the spinal cord: underlying mechanisms and implications for recovery after injury. Behav Cogn Neurosci Rev 5:191-239.

Grau JW, Washburn SN, Hook MA, Ferguson AR, Crown ED, Garcia G, Bolding KA, Miranda RC (2004) Uncontrollable stimulation undermines recovery after spinal cord injury. J Neurotrauma 21:1795-1817.

Grimson A, Farh KK, Johnston WK, Garrett-Engele P, Lim LP, Bartel DP (2007) MicroRNA targeting specificity in mammals: determinants beyond seed pairing. Mol Cell 27:91-105.

Gris P, Tighe A, Levin D, Sharma R, Brown A (2007) Transcriptional regulation of scar gene expression in primary astrocytes. Glia 55:1145-1155.

Gruner JA (1992) A monitored contusion model of spinal cord injury in the rat. J Neurotrauma 9:123-126; discussion 126-128.

Guan J, Miller OT, Waugh KM, McCarthy DC, Gluckman PD (2001) Insulin-like growth factor-1 improves somatosensory function and reduces the extent of cortical infarction and ongoing neuronal loss after hypoxia-ischemia in rats. Neuroscience 105:299-306.

Gul H, Yildiz O, Dogrul A, Yesilyurt O, Isimer A (2000) The interaction between IL-1beta and morphine: possible mechanism of the deficiency of morphine-induced analgesia in diabetic mice. Pain 89:39-45.

Hains BC, Klein JP, Saab CY, Craner MJ, Black JA, Waxman SG (2003) Upregulation of sodium channel Nav1.3 and functional involvement in neuronal

hyperexcitability associated with central neuropathic pain after spinal cord injury. J Neurosci 23:8881-8892.

Hains BC, Waxman SG (2006) Activated microglia contribute to the maintenance of chronic pain after spinal cord injury. J Neurosci 26:4308-4317.

He L, Hannon GJ (2004) MicroRNAs: small RNAs with a big role in gene regulation. Nat Rev Genet 5:522-531.

Hebert SS, De Strooper B (2009) Alterations of the microRNA network cause neurodegenerative disease. Trends Neurosci 32:199-206.

Hebert SS, Horre K, Nicolai L, Papadopoulou AS, Mandemakers W, Silahtaroglu AN, Kauppinen S, Delacourte A, De Strooper B (2008) Loss of microRNA cluster miR-29a/b-1 in sporadic Alzheimer's disease correlates with increased BACE1/beta-secretase expression. Proc Natl Acad Sci U S A 105:6415-6420.

Hernandez G, Vazquez-Pianzola P (2005) Functional diversity of the eukaryotic translation initiation factors belonging to eIF4 families. Mech Dev 122:865-876.

Herrup K, Yang Y (2007) Cell cycle regulation in the postmitotic neuron: oxymoron or new biology? Nat Rev Neurosci 8:368-378.

Hicks RR, Martin VB, Zhang L, Seroogy KB (1999) Mild experimental brain injury differentially alters the expression of neurotrophin and neurotrophin receptor mRNAs in the hippocampus. Exp Neurol 160:469-478.

Hicks RR, Numan S, Dhillon HS, Prasad MR, Seroogy KB (1997) Alterations in BDNF and NT-3 mRNAs in rat hippocampus after experimental brain trauma. Brain Res Mol Brain Res 48:401-406.

Hofer M, Pagliusi SR, Hohn A, Leibrock J, Barde YA (1990) Regional distribution of brain-derived neurotrophic factor mRNA in the adult mouse brain. EMBO J 9:2459-2464.

Hong S, Noh H, Chen H, Padia R, Pan ZK, Su SB, Jing Q, Ding HF, Huang S (2013) Signaling by p38 MAPK stimulates nuclear localization of the microprocessor component p68 for processing of selected primary microRNAs. Sci Signal 6:ra16.

Hook MA, Liu GT, Washburn SN, Ferguson AR, Bopp AC, Huie JR, Grau JW (2007) The impact of morphine after a spinal cord injury. Behav Brain Res 179:281-293.

Hook MA, Moreno G, Woller S, Puga D, Hoy K, Jr., Balden R, Grau JW (2009) Intrathecal morphine attenuates recovery of function after a spinal cord injury. J Neurotrauma 26:741-752.

Hook MA, Washburn SN, Moreno G, Woller SA, Puga D, Lee KH, Grau JW (2011) An IL-1 receptor antagonist blocks a morphine-induced attenuation of locomotor recovery after spinal cord injury. Brain Behav Immun 25:349-359.

Horky LL, Galimi F, Gage FH, Horner PJ (2006) Fate of endogenous stem/progenitor cells following spinal cord injury. J Comp Neurol 498:525-538.

Huang da W, Sherman BT, Lempicki RA (2009) Systematic and integrative analysis of large gene lists using DAVID bioinformatics resources. Nat Protoc 4:44-57.

Hwang IK, Yoo KY, Park SK, An SJ, Lee JY, Choi SY, Kang JH, Kwon YG, Kang TC, Won MH (2004) Expression and changes of endogenous insulin-like growth

factor-1 in neurons and glia in the gerbil hippocampus and dentate gyrus after ischemic insult. Neurochem Int 45:149-156.

Inoue A, Ikoma K, Morioka N, Kumagai K, Hashimoto T, Hide I, Nakata Y (1999) Interleukin-1beta induces substance P release from primary afferent neurons through the cyclooxygenase-2 system. J Neurochem 73:2206-2213.

Ivey KN, Muth A, Arnold J, King FW, Yeh RF, Fish JE, Hsiao EC, Schwartz RJ, Conklin BR, Bernstein HS, Srivastava D (2008) MicroRNA regulation of cell lineages in mouse and human embryonic stem cells. Cell Stem Cell 2:219-229.

Iyer A, Zurolo E, Prabowo A, Fluiter K, Spliet WG, van Rijen PC, Gorter JA, Aronica E (2012) MicroRNA-146a: a key regulator of astrocyte-mediated inflammatory response. PLoS One 7:e44789.

Jackson AB, Dijkers M, Devivo MJ, Poczatek RB (2004) A demographic profile of new traumatic spinal cord injuries: change and stability over 30 years. Arch Phys Med Rehabil 85:1740-1748.

Jakeman LB, Wei P, Guan Z, Stokes BT (1998) Brain-derived neurotrophic factor stimulates hindlimb stepping and sprouting of cholinergic fibers after spinal cord injury. Exp Neurol 154:170-184.

Jakob P, Landmesser U (2012) Role of microRNAs in stem/progenitor cells and cardiovascular repair. Cardiovasc Res 93:614-622.

Jeyaseelan K, Lim KY, Armugam A (2008) MicroRNA expression in the blood and brain of rats subjected to transient focal ischemia by middle cerebral artery occlusion. Stroke 39:959-966.

Ji RR, Kohno T, Moore KA, Woolf CJ (2003) Central sensitization and LTP: do pain and memory share similar mechanisms? Trends Neurosci 26:696-705.

Jin Z, Liu L, Bian W, Chen Y, Xu G, Cheng L, Jing N (2009) Different transcription factors regulate nestin gene expression during P19 cell neural differentiation and central nervous system development. J Biol Chem 284:8160-8173.

John GR, Chen L, Rivieccio MA, Melendez-Vasquez CV, Hartley A, Brosnan CF (2004) Interleukin-1beta induces a reactive astroglial phenotype via deactivation of the Rho GTPase-Rock axis. J Neurosci 24:2837-2845.

Johnnidis JB, Harris MH, Wheeler RT, Stehling-Sun S, Lam MH, Kirak O, Brummelkamp TR, Fleming MD, Camargo FD (2008) Regulation of progenitor cell proliferation and granulocyte function by microRNA-223. Nature 451:1125-1129.

Johnston IN, Milligan ED, Wieseler-Frank J, Frank MG, Zapata V, Campisi J, Langer S, Martin D, Green P, Fleshner M, Leinwand L, Maier SF, Watkins LR (2004) A role for proinflammatory cytokines and fractalkine in analgesia, tolerance, and subsequent pain facilitation induced by chronic intrathecal morphine. J Neurosci 24:7353-7365.

Jordan J, Segura T, Brea D, Galindo M, Castillo J (2008) Inflammation as Therapeutic Objective in Stroke. Current pharmaceutical design 14:3549-3564.

Kahles T, Brandes RP (2012) NADPH oxidases as therapeutic targets in ischemic stroke. Cell Mol Life Sci 69:2345-2363.

Karimi-Abdolrezaee S, Billakanti R (2012) Reactive astrogliosis after spinal cord injury-beneficial and detrimental effects. Mol Neurobiol 46:251-264.

Karimi-Abdolrezaee S, Eftekharpour E, Wang J, Morshead CM, Fehlings MG (2006) Delayed transplantation of adult neural precursor cells promotes remyelination and functional neurological recovery after spinal cord injury. J Neurosci 26:3377-3389.

Karimi-Abdolrezaee S, Eftekharpour E, Wang J, Schut D, Fehlings MG (2010) Synergistic effects of transplanted adult neural stem/progenitor cells, chondroitinase, and growth factors promote functional repair and plasticity of the chronically injured spinal cord. J Neurosci 30:1657-1676.

Kaur C, Ling EA (2008) Blood brain barrier in hypoxic-ischemic conditions. Curr Neurovasc Res 5:71-81.

Kazanis I, Giannakopoulou M, Philippidis H, Stylianopoulou F (2004) Alterations in IGF-I, BDNF and NT-3 levels following experimental brain trauma and the effect of IGF-I administration. Exp Neurol 186:221-234.

Kerr BJ, Bradbury EJ, Bennett DL, Trivedi PM, Dassan P, French J, Shelton DB, McMahon SB, Thompson SW (1999) Brain-derived neurotrophic factor modulates nociceptive sensory inputs and NMDA-evoked responses in the rat spinal cord. J Neurosci 19:5138-5148.

Kerr BJ, Patterson PH (2005) Leukemia inhibitory factor promotes oligodendrocyte survival after spinal cord injury. Glia 51:73-79.

Kharazmi A, Nielsen H, Rechnitzer C, Bendtzen K (1989) Interleukin 6 primes human neutrophil and monocyte oxidative burst response. Immunol Lett 21:177-184.

Khatri R, McKinney AM, Swenson B, Janardhan V (2012) Blood-brain barrier, reperfusion injury, and hemorrhagic transformation in acute ischemic stroke. Neurology 79:S52-57.

Kim GM, Xu J, Song SK, Yan P, Ku G, Xu XM, Hsu CY (2001) Tumor necrosis factor receptor deletion reduces nuclear factor-kappaB activation, cellular inhibitor of apoptosis protein 2 expression, and functional recovery after traumatic spinal cord injury. J Neurosci 21:6617-6625.

Kim J, Inoue K, Ishii J, Vanti WB, Voronov SV, Murchison E, Hannon G, Abeliovich A (2007) A MicroRNA feedback circuit in midbrain dopamine neurons. Science 317:1220-1224.

Kindy MS (1993) Inhibition of tyrosine phosphorylation prevents delayed neuronal death following cerebral ischemia. J Cereb Blood Flow Metab 13:372-377.

Kossmann T, Hans VH, Imhof HG, Stocker R, Grob P, Trentz O, Morganti-Kossmann C (1995) Intrathecal and serum interleukin-6 and the acute-phase response in patients with severe traumatic brain injuries. Shock 4:311-317.

Krichevsky AM, Gabriely G (2009) miR-21: a small multi-faceted RNA. J Cell Mol Med 13:39-53.

Kulik T, Kusano Y, Aronhime S, Sandler AL, Winn HR (2008) Regulation of cerebral vasculature in normal and ischemic brain. Neuropharmacology 55:281-288.

Kumar S, Selim MH, Caplan LR (2010) Medical complications after stroke. Lancet Neurol 9:105-118.

Kusuda R, Cadetti F, Ravanelli MI, Sousa TA, Zanon S, De Lucca FL, Lucas G (2011) Differential expression of microRNAs in mouse pain models. Mol Pain 7:17.

Kuzhandaivel A, Nistri A, Mazzone GL, Mladinic M (2011) Molecular mechanisms underlying cell death in spinal networks in relation to locomotor activity after acute injury in vitro. Front Cell Neurosci 5:9.

Kynast KL, Russe OQ, Moser CV, Geisslinger G, Niederberger E (2013) Modulation of central nervous system-specific microRNA-124a alters the inflammatory response in the formalin test in mice. Pain 154:368-376.

Lagace DC, Whitman MC, Noonan MA, Ables JL, DeCarolis NA, Arguello AA, Donovan MH, Fischer SJ, Farnbauch LA, Beech RD, DiLeone RJ, Greer CA, Mandyam CD, Eisch AJ (2007) Dynamic contribution of nestin-expressing stem cells to adult neurogenesis. J Neurosci 27:12623-12629.

Lai AY, Todd KG (2006) Microglia in cerebral ischemia: molecular actions and interactions. Can J Physiol Pharmacol 84:49-59.

Lalancette-Hebert M, Gowing G, Simard A, Weng YC, Kriz J (2007) Selective ablation of proliferating microglial cells exacerbates ischemic injury in the brain. J Neurosci 27:2596-2605.

Lambertsen KL, Biber K, Finsen B (2012) Inflammatory cytokines in experimental and human stroke. J Cereb Blood Flow Metab 32:1677-1698.

Lambertsen KL, Meldgaard M, Ladeby R, Finsen B (2005) A quantitative study of microglial-macrophage synthesis of tumor necrosis factor during acute and late focal cerebral ischemia in mice. J Cereb Blood Flow Metab 25:119-135.

Lampert A, Hains BC, Waxman SG (2006) Upregulation of persistent and ramp sodium current in dorsal horn neurons after spinal cord injury. Exp Brain Res 174:660-666.

Langlois J, Rutland Brown W, Wald M (2006) The epidemiology and impact of traumatic brain injury: a brief overview. The journal of head trauma rehabilitation 21:375-378.

Lee CT, Risom T, Strauss WM (2007) Evolutionary conservation of microRNA regulatory circuits: an examination of microRNA gene complexity and conserved microRNA-target interactions through metazoan phylogeny. DNA Cell Biol 26:209-218.

Lee ST, Chu K, Jung KH, Kim JH, Huh JY, Yoon H, Park DK, Lim JY, Kim JM, Jeon D, Ryu H, Lee SK, Kim M, Roh JK (2012) miR-206 regulates brain-derived neurotrophic factor in Alzheimer disease model. Ann Neurol 72:269-277.

Lee TH, Kato H, Chen ST, Kogure K, Itoyama Y (2002) Expression disparity of brain-derived neurotrophic factor immunoreactivity and mRNA in ischemic hippocampal neurons. Neuroreport 13:2271-2275.

Lehrmann E, Kiefer R, Christensen T, Toyka KV, Zimmer J, Diemer NH, Hartung HP, Finsen B (1998) Microglia and macrophages are major sources of locally

produced transforming growth factor-beta1 after transient middle cerebral artery occlusion in rats. Glia 24:437-448.

Lei P, Li Y, Chen X, Yang S, Zhang J (2009) Microarray based analysis of microRNA expression in rat cerebral cortex after traumatic brain injury. Brain Res 1284:191-201.

Lewis BP, Burge CB, Bartel DP (2005) Conserved seed pairing, often flanked by adenosines, indicates that thousands of human genes are microRNA targets. Cell 120:15-20.

Lewis BP, Shih IH, Jones-Rhoades MW, Bartel DP, Burge CB (2003) Prediction of mammalian microRNA targets. Cell 115:787-798.

Li G, Luna C, Qiu J, Epstein DL, Gonzalez P (2010a) Modulation of inflammatory markers by miR-146a during replicative senescence in trabecular meshwork cells. Invest Ophthalmol Vis Sci 51:2976-2985.

Li L, Chen XP, Li YJ (2010b) MicroRNA-146a and human disease. Scand J Immunol 71:227-231.

Li LC, Okino ST, Zhao H, Pookot D, Place RF, Urakami S, Enokida H, Dahiya R (2006) Small dsRNAs induce transcriptional activation in human cells. Proc Natl Acad Sci U S A 103:17337-17342.

Li Q, Stephenson D (2002) Postischemic administration of basic fibroblast growth factor improves sensorimotor function and reduces infarct size following permanent focal cerebral ischemia in the rat. Exp Neurol 177:531-537.

Li Q, Verma IM (2002) NF-kappaB regulation in the immune system. Nat Rev Immunol 2:725-734.

Li Y, Shelat H, Geng YJ (2012) IGF-1 prevents oxidative stress induced-apoptosis in induced pluripotent stem cells which is mediated by microRNA-1. Biochem Biophys Res Commun 426:615-619.

Liberto CM, Albrecht PJ, Herx LM, Yong VW, Levison SW (2004) Pro-regenerative properties of cytokine-activated astrocytes. J Neurochem 89:1092-1100.

Lindvall O, Kokaia Z, Bengzon J, Elmer E, Kokaia M (1994) Neurotrophins and brain insults. Trends Neurosci 17:490-496.

Liu D, Xu GY, Pan E, McAdoo DJ (1999) Neurotoxicity of glutamate at the concentration released upon spinal cord injury. Neuroscience 93:1383-1389.

Liu DZ, Tian Y, Ander BP, Xu H, Stamova BS, Zhan X, Turner RJ, Jickling G, Sharp FR (2010) Brain and blood microRNA expression profiling of ischemic stroke, intracerebral hemorrhage, and kainate seizures. J Cereb Blood Flow Metab 30:92-101.

Liu NK, Wang XF, Lu QB, Xu XM (2009) Altered microRNA expression following traumatic spinal cord injury. Exp Neurol 219:424-429.

Liu XF, Fawcett JR, Thorne RG, Frey WH, 2nd (2001) Non-invasive intranasal insulin-like growth factor-I reduces infarct volume and improves neurologic function in rats following middle cerebral artery occlusion. Neurosci Lett 308:91-94.

Liu XS, Chopp M, Zhang RL, Tao T, Wang XL, Kassis H, Hozeska-Solgot A, Zhang L, Chen C, Zhang ZG (2011) MicroRNA profiling in subventricular zone after

stroke: MiR-124a regulates proliferation of neural progenitor cells through Notch signaling pathway. PLoS One 6:e23461.

Loddick SA, Rothwell NJ (1996) Neuroprotective effects of human recombinant interleukin-1 receptor antagonist in focal cerebral ischaemia in the rat. J Cereb Blood Flow Metab 16:932-940.

Loffler D, Brocke-Heidrich K, Pfeifer G, Stocsits C, Hackermuller J, Kretzschmar AK, Burger R, Gramatzki M, Blumert C, Bauer K, Cvijic H, Ullmann AK, Stadler PF, Horn F (2007) Interleukin-6 dependent survival of multiple myeloma cells involves the Stat3-mediated induction of microRNA-21 through a highly conserved enhancer. Blood 110:1330-1333.

Lopez AD, Mathers CD, Ezzati M, Jamison DT, Murray CJ (2006) Global and regional burden of disease and risk factors, 2001: systematic analysis of population health data. Lancet 367:1747-1757.

Loscher CJ, Hokamp K, Wilson JH, Li T, Humphries P, Farrar GJ, Palfi A (2008) A common microRNA signature in mouse models of retinal degeneration. Exp Eye Res 87:529-534.

Madathil SK, Evans HN, Saatman KE (2010) Temporal and regional changes in IGF-1/IGF-1R signaling in the mouse brain after traumatic brain injury. J Neurotrauma 27:95-107.

Mason JL, Suzuki K, Chaplin DD, Matsushima GK (2001) Interleukin-1beta promotes repair of the CNS. J Neurosci 21:7046-7052.

McCarberg B (2004) Contemporary management of chronic pain disorders. J Fam Pract 53:S11-22.

McKeon RJ, Hoke A, Silver J (1995) Injury-induced proteoglycans inhibit the potential for laminin-mediated axon growth on astrocytic scars. Exp Neurol 136:32-43.

McTigue DM, Horner PJ, Stokes BT, Gage FH (1998) Neurotrophin-3 and brain-derived neurotrophic factor induce oligodendrocyte proliferation and myelination of regenerating axons in the contused adult rat spinal cord. J Neurosci 18:5354-5365.

Meakin SO, Shooter EM (1992) The nerve growth factor family of receptors. Trends Neurosci 15:323-331.

Mekhail M, Almazan G, Tabrizian M (2012) Oligodendrocyte-protection and remyelination post-spinal cord injuries: a review. Prog Neurobiol 96:322-339.

Mellios N, Huang HS, Grigorenko A, Rogaev E, Akbarian S (2008) A set of differentially expressed miRNAs, including miR-30a-5p, act as post-transcriptional inhibitors of BDNF in prefrontal cortex. Hum Mol Genet 17:3030-3042.

Michael A, Bajracharya SD, Yuen PS, Zhou H, Star RA, Illei GG, Alevizos I (2010) Exosomes from human saliva as a source of microRNA biomarkers. Oral Dis 16:34-38.

Mishima T, Mizuguchi Y, Kawahigashi Y, Takizawa T (2007) RT-PCR-based analysis of microRNA (miR-1 and -124) expression in mouse CNS. Brain Res 1131:37-43.

Mitchell PS, Parkin RK, Kroh EM, Fritz BR, Wyman SK, Pogosova-Agadjanyan EL, Peterson A, Noteboom J, O'Briant KC, Allen A, Lin DW, Urban N, Drescher CW, Knudsen BS, Stirewalt DL, Gentleman R, Vessella RL, Nelson PS, Martin DB, Tewari M (2008) Circulating microRNAs as stable blood-based markers for cancer detection. Proc Natl Acad Sci U S A 105:10513-10518.

Miwa T, Furukawa S, Nakajima K, Furukawa Y, Kohsaka S (1997) Lipopolysaccharide enhances synthesis of brain-derived neurotrophic factor in cultured rat microglia. J Neurosci Res 50:1023-1029.

Moschos SA, Williams AE, Perry MM, Birrell MA, Belvisi MG, Lindsay MA (2007) Expression profiling in vivo demonstrates rapid changes in lung microRNA levels following lipopolysaccharide-induced inflammation but not in the anti-inflammatory action of glucocorticoids. BMC Genomics 8:240.

Mukaino M, Nakamura M, Yamada O, Okada S, Morikawa S, Renault-Mihara F, Iwanami A, Ikegami T, Ohsugi Y, Tsuji O, Katoh H, Matsuzaki Y, Toyama Y, Liu M, Okano H (2010) Anti-IL-6-receptor antibody promotes repair of spinal cord injury by inducing microglia-dominant inflammation. Exp Neurol 224:403-414.

Murray CJ, Lopez AD (1997) Global mortality, disability, and the contribution of risk factors: Global Burden of Disease Study. Lancet 349:1436-1442.

Nahid MA, Pauley KM, Satoh M, Chan EK (2009) miR-146a is critical for endotoxin-induced tolerance: implication in innate immunity. J Biol Chem 284:34590-34599.

Nakamura M, Okada S, Toyama Y, Okano H (2005) Role of IL-6 in spinal cord injury in a mouse model. Clin Rev Allergy Immunol 28:197-204.

Nakanishi K, Nakasa T, Tanaka N, Ishikawa M, Yamada K, Yamasaki K, Kamei N, Izumi B, Adachi N, Miyaki S, Asahara H, Ochi M (2010) Responses of microRNAs 124a and 223 following spinal cord injury in mice. Spinal Cord 48:192-196.

Nakasa T, Miyaki S, Okubo A, Hashimoto M, Nishida K, Ochi M, Asahara H (2008) Expression of microRNA-146 in rheumatoid arthritis synovial tissue. Arthritis Rheum 58:1284-1292.

Nawashiro H, Tasaki K, Ruetzler CA, Hallenbeck JM (1997) TNF-alpha pretreatment induces protective effects against focal cerebral ischemia in mice. J Cereb Blood Flow Metab 17:483-490.

Nesic O, Svrakic NM, Xu GY, McAdoo D, Westlund KN, Hulsebosch CE, Ye Z, Galante A, Soteropoulos P, Tolias P, Young W, Hart RP, Perez-Polo JR (2002) DNA microarray analysis of the contused spinal cord: effect of NMDA receptor inhibition. J Neurosci Res 68:406-423.

Nesic O, Xu GY, McAdoo D, High KW, Hulsebosch C, Perez-Pol R (2001) IL-1 receptor antagonist prevents apoptosis and caspase-3 activation after spinal cord injury. J Neurotrauma 18:947-956.

Nielsen CB, Shomron N, Sandberg R, Hornstein E, Kitzman J, Burge CB (2007) Determinants of targeting by endogenous and exogenous microRNAs and siRNAs. RNA 13:1894-1910.

Nieto-Sampedro M, Lewis ER, Cotman CW, Manthorpe M, Skaper SD, Barbin G, Longo FM, Varon S (1982) Brain injury causes a time-dependent increase in neuronotrophic activity at the lesion site. Science 217:860-861.

Noble LJ, Wrathall JR (1988) Blood-spinal cord barrier disruption proximal to a spinal cord transection in the rat: time course and pathways associated with protein leakage. Exp Neurol 99:567-578.

Noble LJ, Wrathall JR (1989) Distribution and time course of protein extravasation in the rat spinal cord after contusive injury. Brain Res 482:57-66.

Nolan RT (1969) Traumatic oedema of the spinal cord. Br Med J 1:710.

Norris JG, Tang LP, Sparacio SM, Benveniste EN (1994) Signal transduction pathways mediating astrocyte IL-6 induction by IL-1 beta and tumor necrosis factor-alpha. J Immunol 152:841-850.

Novikova L, Novikov L, Kellerth JO (1996) Brain-derived neurotrophic factor reduces necrotic zone and supports neuronal survival after spinal cord hemisection in adult rats. Neurosci Lett 220:203-206.

Numakawa T, Richards M, Adachi N, Kishi S, Kunugi H, Hashido K (2011) MicroRNA function and neurotrophin BDNF. Neurochem Int 59:551-558.

Nyberg F, Sharma HS (2002) Repeated topical application of growth hormone attenuates blood-spinal cord barrier permeability and edema formation following spinal cord injury: an experimental study in the rat using Evans blue, ([125])I-sodium and lanthanum tracers. Amino Acids 23:231-239.

O'Connell RM, Taganov KD, Boldin MP, Cheng G, Baltimore D (2007) MicroRNA-155 is induced during the macrophage inflammatory response. Proc Natl Acad Sci U S A 104:1604-1609.

Okada S, Nakamura M, Mikami Y, Shimazaki T, Mihara M, Ohsugi Y, Iwamoto Y, Yoshizaki K, Kishimoto T, Toyama Y, Okano H (2004) Blockade of interleukin-6 receptor suppresses reactive astrogliosis and ameliorates functional recovery in experimental spinal cord injury. J Neurosci Res 76:265-276.

Oudega M (2012) Molecular and cellular mechanisms underlying the role of blood vessels in spinal cord injury and repair. Cell Tissue Res 349:269-288.

Pan W, Kastin AJ (2008) Cytokine transport across the injured blood-spinal cord barrier. Curr Pharm Des 14:1620-1624.

Pappalardo DL, Balaraman S, Sathyan P, Carter ES, Chen WJ, Miranda RC (2013) Suppression and epigenetic regulation of miR-9 contributes to ethanol teratology: evidence from zebrafish and murine fetal neural stem cell models. Alcohol Clin Exp Res (in press).

Patterson SL, Abel T, Deuel TA, Martin KC, Rose JC, Kandel ER (1996) Recombinant BDNF rescues deficits in basal synaptic transmission and hippocampal LTP in BDNF knockout mice. Neuron 16:1137-1145.

Pedersen I, David M (2008) MicroRNAs in the immune response. Cytokine 43:391-394.

Penkowa M, Camats J, Hadberg H, Quintana A, Rojas S, Giralt M, Molinero A, Campbell IL, Hidalgo J (2003) Astrocyte-targeted expression of interleukin-6

protects the central nervous system during neuroglial degeneration induced by 6-aminonicotinamide. J Neurosci Res 73:481-496.

Penkowa M, Giralt M, Carrasco J, Hadberg H, Hidalgo J (2000) Impaired inflammatory response and increased oxidative stress and neurodegeneration after brain injury in interleukin-6-deficient mice. Glia 32:271-285.

Perry VH (1998) A revised view of the central nervous system microenvironment and major histocompatibility complex class II antigen presentation. J Neuroimmunol 90:113-121.

Peters L, Meister G (2007) Argonaute proteins: mediators of RNA silencing. Mol Cell 26:611-623.

Ponomarev ED, Veremeyko T, Barteneva N, Krichevsky AM, Weiner HL (2011) MicroRNA-124 promotes microglia quiescence and suppresses EAE by deactivating macrophages via the C/EBP-alpha-PU.1 pathway. Nat Med 17:64-70.

Popovich PG, Guan Z, McGaughy V, Fisher L, Hickey WF, Basso DM (2002) The neuropathological and behavioral consequences of intraspinal microglial/macrophage activation. J Neuropathol Exp Neurol 61:623-633.

Prow NA, Irani DN (2008) The inflammatory cytokine, interleukin-1 beta, mediates loss of astroglial glutamate transport and drives excitotoxic motor neuron injury in the spinal cord during acute viral encephalomyelitis. J Neurochem 105:1276-1286.

Raghavendra V, Rutkowski MD, DeLeo JA (2002) The role of spinal neuroimmune activation in morphine tolerance/hyperalgesia in neuropathic and sham-operated rats. J Neurosci 22:9980-9989.

Rana TM (2007) Illuminating the silence: understanding the structure and function of small RNAs. Nat Rev Mol Cell Biol 8:23-36.

Redell JB, Liu Y, Dash PK (2009) Traumatic brain injury alters expression of hippocampal microRNAs: potential regulators of multiple pathophysiological processes. J Neurosci Res 87:1435-1448.

Redell JB, Moore AN, Ward NH, 3rd, Hergenroeder GW, Dash PK (2010) Human traumatic brain injury alters plasma microRNA levels. J Neurotrauma 27:2147-2156.

Redell JB, Zhao J, Dash PK (2011) Altered expression of miRNA-21 and its targets in the hippocampus after traumatic brain injury. J Neurosci Res 89:212-221.

Ridet JL, Malhotra SK, Privat A, Gage FH (1997) Reactive astrocytes: cellular and molecular cues to biological function. Trends Neurosci 20:570-577.

Rink C, Khanna S (2011) MicroRNA in ischemic stroke etiology and pathology. Physiol Genomics 43:521-528.

Rodriguez-Baeza A, Reina-de la Torre F, Poca A, Marti M, Garnacho A (2003) Morphological features in human cortical brain microvessels after head injury: a three-dimensional and immunocytochemical study. Anat Rec A Discov Mol Cell Evol Biol 273:583-593.

Roy S, Sen CK (2011) MiRNA in innate immune responses: novel players in wound inflammation. Physiol Genomics 43:557-565.

Rudel S, Wang Y, Lenobel R, Korner R, Hsiao HH, Urlaub H, Patel D, Meister G (2011) Phosphorylation of human Argonaute proteins affects small RNA binding. Nucleic Acids Res 39:2330-2343.

Ryan MM, Ryan B, Kyrke-Smith M, Logan B, Tate WP, Abraham WC, Williams JM (2012) Temporal profiling of gene networks associated with the late phase of long-term potentiation in vivo. PLoS One 7:e40538.

Saatman KE, Feeko KJ, Pape RL, Raghupathi R (2006) Differential behavioral and histopathological responses to graded cortical impact injury in mice. J Neurotrauma 23:1241-1253.

Sanchez Mejia RO, Ona VO, Li M, Friedlander RM (2001) Minocycline reduces traumatic brain injury-mediated caspase-1 activation, tissue damage, and neurological dysfunction. Neurosurgery 48:1393-1399; discussion 1399-1401.

Sandberg Nordqvist AC, von Holst H, Holmin S, Sara VR, Bellander BM, Schalling M (1996) Increase of insulin-like growth factor (IGF)-1, IGF binding protein-2 and -4 mRNAs following cerebral contusion. Brain Res Mol Brain Res 38:285-293.

Sandoval KE, Witt KA (2008) Blood-brain barrier tight junction permeability and ischemic stroke. Neurobiol Dis 32:200-219.

Sathyan P, Golden HB, Miranda RC (2007) Competing interactions between micro-RNAs determine neural progenitor survival and proliferation after ethanol

exposure: evidence from an ex vivo model of the fetal cerebral cortical neuroepithelium. J Neurosci 27:8546-8557.

Saugstad JA (2010) MicroRNAs as effectors of brain function with roles in ischemia and injury, neuroprotection, and neurodegeneration. J Cereb Blood Flow Metab 30:1564-1576.

Sawada M, Suzumura A, Marunouchi T (1995) Cytokine network in the central nervous system and its roles in growth and differentiation of glial and neuronal cells. Int J Dev Neurosci 13:253-264.

Schabitz WR, Schwab S, Spranger M, Hacke W (1997) Intraventricular brain-derived neurotrophic factor reduces infarct size after focal cerebral ischemia in rats. J Cereb Blood Flow Metab 17:500-506.

Scherbel U, Raghupathi R, Nakamura M, Saatman KE, Trojanowski JQ, Neugebauer E, Marino MW, McIntosh TK (1999) Differential acute and chronic responses of tumor necrosis factor-deficient mice to experimental brain injury. Proc Natl Acad Sci U S A 96:8721-8726.

Schoknecht K, Shalev H (2012) Blood-brain barrier dysfunction in brain diseases: clinical experience. Epilepsia 53 Suppl 6:7-13.

Scholz J, Woolf CJ (2007) The neuropathic pain triad: neurons, immune cells and glia. Nat Neurosci 10:1361-1368.

Schwab ME, Bartholdi D (1996) Degeneration and regeneration of axons in the lesioned spinal cord. Physiol Rev 76:319-370.

Segal JL (2005) Immunoactivation and altered intercellular communication mediate the pathophysiology of spinal cord injury. Pharmacotherapy 25:145-156.

Selvamani A, Sathyan P, Miranda RC, Sohrabji F (2012) An antagomir to microRNA Let7f promotes neuroprotection in an ischemic stroke model. PLoS One 7:e32662.

Sharma HS (2005a) Neuroprotective effects of neurotrophins and melanocortins in spinal cord injury: an experimental study in the rat using pharmacological and morphological approaches. Ann N Y Acad Sci 1053:407-421.

Sharma HS (2005b) Pathophysiology of blood-spinal cord barrier in traumatic injury and repair. Curr Pharm Des 11:1353-1389.

Sharma HS (2006) Post-traumatic application of brain-derived neurotrophic factor and glia-derived neurotrophic factor on the rat spinal cord enhances neuroprotection and improves motor function. Acta Neurochir Suppl 96:329-334.

Sharma HS (2007a) Neurotrophic factors in combination: a possible new therapeutic strategy to influence pathophysiology of spinal cord injury and repair mechanisms. Curr Pharm Des 13:1841-1874.

Sharma HS (2007b) A select combination of neurotrophins enhances neuroprotection and functional recovery following spinal cord injury. Ann N Y Acad Sci 1122:95-111.

Sharma HS (2008) New perspectives for the treatment options in spinal cord injury. Expert Opin Pharmacother 9:2773-2800.

Sharma HS (2010) A combination of tumor necrosis factor-alpha and neuronal nitric oxide synthase antibodies applied topically over the traumatized spinal cord enhances neuroprotection and functional recovery in the rat. Ann N Y Acad Sci 1199:175-185.

Sharma HS (2011) Early microvascular reactions and blood-spinal cord barrier disruption are instrumental in pathophysiology of spinal cord injury and repair: novel therapeutic strategies including nanowired drug delivery to enhance neuroprotection. J Neural Transm 118:155-176.

Sharma HS, Nyberg F, Gordh T, Alm P, Westman J (1997) Topical application of insulin like growth factor-1 reduces edema and upregulation of neuronal nitric oxide synthase following trauma to the rat spinal cord. Acta Neurochir Suppl 70:130-133.

Sharma HS, Nyberg F, Gordh T, Alm P, Westman J (2000a) Neurotrophic factors influence upregulation of constitutive isoform of heme oxygenase and cellular stress response in the spinal cord following trauma. An experimental study using immunohistochemistry in the rat. Amino Acids 19:351-361.

Sharma HS, Nyberg F, Westman J, Alm P, Gordh T, Lindholm D (1998) Brain derived neurotrophic factor and insulin like growth factor-1 attenuate upregulation of nitric oxide synthase and cell injury following trauma to the spinal cord. An immunohistochemical study in the rat. Amino Acids 14:121-129.

Sharma HS, Olsson Y, Cervos-Navarro J (1993a) Early perifocal cell changes and edema in traumatic injury of the spinal cord are reduced by indomethacin, an

inhibitor of prostaglandin synthesis. Experimental study in the rat. Acta Neuropathol 85:145-153.

Sharma HS, Olsson Y, Cervos-Navarro J (1993b) p-Chlorophenylalanine, a serotonin synthesis inhibitor, reduces the response of glial fibrillary acidic protein induced by trauma to the spinal cord. An immunohistochemical investigation in the rat. Acta Neuropathol 86:422-427.

Sharma HS, Olsson Y, Nyberg F, Dey PK (1993c) Prostaglandins modulate alterations of microvascular permeability, blood flow, edema and serotonin levels following spinal cord injury: an experimental study in the rat. Neuroscience 57:443-449.

Sharma HS, Olsson Y, Persson S, Nyberg F (1995) Trauma-induced opening of the the blood-spinal cord barrier is reduced by indomethacin, an inhibitor of prostaglandin biosynthesis. Experimental observations in the rat using [131I]-sodium, Evans blue and lanthanum as tracers. Restor Neurol Neurosci 7:207-215.

Sharma HS, Westman J, Gordh T, Alm P (2000b) Topical application of brain derived neurotrophic factor influences upregulation of constitutive isoform of heme oxygenase in the spinal cord following trauma an experimental study using immunohistochemistry in the rat. Acta Neurochir Suppl 76:365-369.

Sharma HS, Winkler T, Stalberg E, Gordh T, Alm P, Westman J (2003) Topical application of TNF-alpha antiserum attenuates spinal cord trauma induced edema formation, microvascular permeability disturbances and cell injury in the rat. Acta Neurochir Suppl 86:407-413.

Shigeno T, Mima T, Takakura K, Graham DI, Kato G, Hashimoto Y, Furukawa S (1991) Amelioration of delayed neuronal death in the hippocampus by nerve growth factor. J Neurosci 11:2914-2919.

Shimojo M, Nakajima K, Takei N, Hamanoue M, Kohsaka S (1991) Production of basic fibroblast growth factor in cultured rat brain microglia. Neurosci Lett 123:229-231.

Shlosberg D, Benifla M, Kaufer D, Friedman A (2010) Blood-brain barrier breakdown as a therapeutic target in traumatic brain injury. Nat Rev Neurol 6:393-403.

Shohami E, Gallily R, Mechoulam R, Bass R, Ben-Hur T (1997) Cytokine production in the brain following closed head injury: dexanabinol (HU-211) is a novel TNF-alpha inhibitor and an effective neuroprotectant. J Neuroimmunol 72:169-177.

Siddall PJ, Loeser JD (2001) Pain following spinal cord injury. Spinal Cord 39:63-73.

Siebert JR, Osterhout DJ (2011) The inhibitory effects of chondroitin sulfate proteoglycans on oligodendrocytes. J Neurochem 119:176-188.

Siebert JR, Stelzner DJ, Osterhout DJ (2011) Chondroitinase treatment following spinal contusion injury increases migration of oligodendrocyte progenitor cells. Exp Neurol 231:19-29.

Silver J, Miller JH (2004) Regeneration beyond the glial scar. Nat Rev Neurosci 5:146-156.

Sinson G, Voddi M, McIntosh TK (1995) Nerve growth factor administration attenuates cognitive but not neurobehavioral motor dysfunction or hippocampal cell loss following fluid-percussion brain injury in rats. J Neurochem 65:2209-2216.

Skaper SD, Walsh FS (1998) Neurotrophic molecules: strategies for designing effective therapeutic molecules in neurodegeneration. Mol Cell Neurosci 12:179-193.

Slot KB, Berge E, Sandercock P, Lewis SC, Dorman P, Dennis M (2009) Causes of death by level of dependency at 6 months after ischemic stroke in 3 large cohorts. Stroke 40:1585-1589.

Sluka KA, Rees H, Chen PS, Tsuruoka M, Willis WD (1997) Capsaicin-induced sensitization of primate spinothalamic tract cells is prevented by a protein kinase C inhibitor. Brain Res 772:82-86.

Smith C (2013) Review: the long-term consequences of microglial activation following acute traumatic brain injury. Neuropathol Appl Neurobiol 39:35-44.

Smith CJ, Emsley HC, Gavin CM, Georgiou RF, Vail A, Barberan EM, del Zoppo GJ, Hallenbeck JM, Rothwell NJ, Hopkins SJ, Tyrrell PJ (2004) Peak plasma interleukin-6 and other peripheral markers of inflammation in the first week of ischaemic stroke correlate with brain infarct volume, stroke severity and long-term outcome. BMC Neurol 4:2.

Smith JA, Das A, Ray SK, Banik NL (2012) Role of pro-inflammatory cytokines released from microglia in neurodegenerative diseases. Brain Res Bull 87:10-20.

Sofroniew MV (2005) Reactive astrocytes in neural repair and protection. Neuroscientist 11:400-407.

Sofroniew MV (2009) Molecular dissection of reactive astrogliosis and glial scar formation. Trends Neurosci 32:638-647.

Song P, Zhao ZQ (2001) The involvement of glial cells in the development of morphine tolerance. Neurosci Res 39:281-286.

Sosin DM, Sniezek JE, Thurman DJ (1996) Incidence of mild and moderate brain injury in the United States, 1991. Brain Inj 10:47-54.

Stahlhut C, Suarez Y, Lu J, Mishima Y, Giraldez AJ (2012) miR-1 and miR-206 regulate angiogenesis by modulating VegfA expression in zebrafish. Development 139:4356-4365.

Stefani G, Slack FJ (2008) Small non-coding RNAs in animal development. Nat Rev Mol Cell Biol 9:219-230.

Stellwagen D, Beattie EC, Seo JY, Malenka RC (2005) Differential regulation of AMPA receptor and GABA receptor trafficking by tumor necrosis factor-alpha. J Neurosci 25:3219-3228.

Streit WJ, Semple-Rowland SL, Hurley SD, Miller RC, Popovich PG, Stokes BT (1998) Cytokine mRNA profiles in contused spinal cord and axotomized facial nucleus suggest a beneficial role for inflammation and gliosis. Exp Neurol 152:74-87.

Strickland ER, Hook MA, Balaraman S, Huie JR, Grau JW, Miranda RC (2011) MicroRNA dysregulation following spinal cord contusion: implications for neural plasticity and repair. Neuroscience 186:146-160.

Sudo K, Takahashi E, Nakamura Y (1995) Isolation and mapping of the human EIF4A2 gene homologous to the murine protein synthesis initiation factor 4A-II gene Eif4a2. Cytogenet Cell Genet 71:385-388.

Sullivan PG, Bruce-Keller AJ, Rabchevsky AG, Christakos S, Clair DK, Mattson MP, Scheff SW (1999) Exacerbation of damage and altered NF-kappaB activation in mice lacking tumor necrosis factor receptors after traumatic brain injury. J Neurosci 19:6248-6256.

Suzuki S, Tanaka K, Nogawa S, Nagata E, Ito D, Dembo T, Fukuuchi Y (1999) Temporal profile and cellular localization of interleukin-6 protein after focal cerebral ischemia in rats. J Cereb Blood Flow Metab 19:1256-1262.

Suzuki S, Tanaka K, Suzuki N (2009) Ambivalent aspects of interleukin-6 in cerebral ischemia: inflammatory versus neurotrophic aspects. J Cereb Blood Flow Metab 29:464-479.

Szabo I, Chen XH, Xin L, Adler MW, Howard OM, Oppenheim JJ, Rogers TJ (2002) Heterologous desensitization of opioid receptors by chemokines inhibits chemotaxis and enhances the perception of pain. Proc Natl Acad Sci U S A 99:10276-10281.

Taganov KD, Boldin MP, Chang KJ, Baltimore D (2006) NF-kappaB-dependent induction of microRNA miR-146, an inhibitor targeted to signaling proteins of innate immune responses. Proc Natl Acad Sci U S A 103:12481-12486.

Tai YH, Wang YH, Wang JJ, Tao PL, Tung CS, Wong CS (2006) Amitriptyline suppresses neuroinflammation and up-regulates glutamate transporters in morphine-tolerant rats. Pain 124:77-86.

Tan JR, Koo YX, Kaur P, Liu F, Armugam A, Wong PT, Jeyaseelan K (2011) microRNAs in stroke pathogenesis. Curr Mol Med 11:76-92.

Thounaojam MC, Kaushik DK, Basu A (2013) MicroRNAs in the Brain: It's Regulatory Role in Neuroinflammation. Mol Neurobiol 47:1034-1044.

Tili E, Michaille JJ, Cimino A, Costinean S, Dumitru CD, Adair B, Fabbri M, Alder H, Liu CG, Calin GA, Croce CM (2007) Modulation of miR-155 and miR-125b levels following lipopolysaccharide/TNF-alpha stimulation and their possible roles in regulating the response to endotoxin shock. J Immunol 179:5082-5089.

Touzani O, Boutin H, LeFeuvre R, Parker L, Miller A, Luheshi G, Rothwell N (2002) Interleukin-1 influences ischemic brain damage in the mouse independently of the interleukin-1 type I receptor. J Neurosci 22:38-43.

Tsitsiou E, Lindsay MA (2009) microRNAs and the immune response. Curr Opin Pharmacol 9:514-520.

Tsukahara T, Yonekawa Y, Tanaka K, Ohara O, Wantanabe S, Kimura T, Nishijima T, Taniguchi T (1994) The role of brain-derived neurotrophic factor in transient forebrain ischemia in the rat brain. Neurosurgery 34:323-331; discussion 331.

Uchida K, Baba H, Maezawa Y, Furukawa S, Furusawa N, Imura S (1998) Histological investigation of spinal cord lesions in the spinal hyperostotic mouse (twy/twy): morphological changes in anterior horn cells and immunoreactivity to neurotropic factors. J Neurol 245:781-793.

Visvanathan J, Lee S, Lee B, Lee JW, Lee SK (2007) The microRNA miR-124 antagonizes the anti-neural REST/SCP1 pathway during embryonic CNS development. Genes Dev 21:744-749.

Viviani B, Bartesaghi S, Gardoni F, Vezzani A, Behrens MM, Bartfai T, Binaglia M, Corsini E, Di Luca M, Galli CL, Marinovich M (2003) Interleukin-1beta enhances NMDA receptor-mediated intracellular calcium increase through activation of the Src family of kinases. J Neurosci 23:8692-8700.

Wang XF, Huang LD, Yu PP, Hu JG, Yin L, Wang L, Xu XM, Lu PH (2006) Upregulation of type I interleukin-1 receptor after traumatic spinal cord injury in adult rats. Acta Neuropathol 111:220-228.

Washburn SN, Patton BC, Ferguson AR, Hudson KL, Grau JW (2007) Exposure to intermittent nociceptive stimulation under pentobarbital anesthesia disrupts spinal cord function in rats. Psychopharmacology (Berl) 192:243-252.

Watkins LR, Hutchinson MR, Johnston IN, Maier SF (2005) Glia: novel counter-regulators of opioid analgesia. Trends Neurosci 28:661-669.

Watkins LR, Hutchinson MR, Ledeboer A, Wieseler-Frank J, Milligan ED, Maier SF (2007) Norman Cousins Lecture. Glia as the "bad guys": implications for improving clinical pain control and the clinical utility of opioids. Brain Behav Immun 21:131-146.

Widerstrom-Noga EG, Turk DC (2003) Types and effectiveness of treatments used by people with chronic pain associated with spinal cord injuries: influence of pain and psychosocial characteristics. Spinal Cord 41:600-609.

Wiessner C, Gehrmann J, Lindholm D, Topper R, Kreutzberg GW, Hossmann KA (1993) Expression of transforming growth factor-beta 1 and interleukin-1 beta

mRNA in rat brain following transient forebrain ischemia. Acta Neuropathol 86:439-446.

Wildburger R, Zarkovic N, Leb G, Borovic S, Zarkovic K, Tatzber F (2001) Post-traumatic changes in insulin-like growth factor type 1 and growth hormone in patients with bone fractures and traumatic brain injury. Wien Klin Wochenschr 113:119-126.

Willemen HL, Huo XJ, Mao-Ying QL, Zijlstra J, Heijnen CJ, Kavelaars A (2012) MicroRNA-124 as a novel treatment for persistent hyperalgesia. J Neuroinflammation 9:143.

Williams AE, Perry MM, Moschos SA, Larner-Svensson HM, Lindsay MA (2008) Role of miRNA-146a in the regulation of the innate immune response and cancer. Biochem Soc Trans 36:1211-1215.

Williams AH, Liu N, van Rooij E, Olson EN (2009) MicroRNA control of muscle development and disease. Curr Opin Cell Biol 21:461-469.

Woolf CJ, Wall PD (1986) Relative effectiveness of C primary afferent fibers of different origins in evoking a prolonged facilitation of the flexor reflex in the rat. J Neurosci 6:1433-1442.

Wu D (2005) Neuroprotection in experimental stroke with targeted neurotrophins. NeuroRx 2:120-128.

Wu J, Qian J, Li C, Kwok L, Cheng F, Liu P, Perdomo C, Kotton D, Vaziri C, Anderlind C, Spira A, Cardoso WV, Lu J (2010) miR-129 regulates cell proliferation by downregulating Cdk6 expression. Cell Cycle 9:1809-1818.

Xing Z, Gauldie J, Cox G, Baumann H, Jordana M, Lei XF, Achong MK (1998) IL-6 is an antiinflammatory cytokine required for controlling local or systemic acute inflammatory responses. J Clin Invest 101:311-320.

Xu GY, Hughes MG, Ye Z, Hulsebosch CE, McAdoo DJ (2004) Concentrations of glutamate released following spinal cord injury kill oligodendrocytes in the spinal cord. Exp Neurol 187:329-336.

Xu T, Zhu Y, Wei QK, Yuan Y, Zhou F, Ge YY, Yang JR, Su H, Zhuang SM (2008) A functional polymorphism in the miR-146a gene is associated with the risk for hepatocellular carcinoma. Carcinogenesis 29:2126-2131.

Xu XM, Guenard V, Kleitman N, Aebischer P, Bunge MB (1995) A combination of BDNF and NT-3 promotes supraspinal axonal regeneration into Schwann cell grafts in adult rat thoracic spinal cord. Exp Neurol 134:261-272.

Yamamoto Y, Gaynor RB (2001) Role of the NF-kappaB pathway in the pathogenesis of human disease states. Curr Mol Med 1:287-296.

Yamasaki Y, Matsuura N, Shozuhara H, Onodera H, Itoyama Y, Kogure K (1995) Interleukin-1 as a pathogenetic mediator of ischemic brain damage in rats. Stroke 26:676-680; discussion 681.

Yan Q, Elliott J, Snider WD (1992) Brain-derived neurotrophic factor rescues spinal motor neurons from axotomy-induced cell death. Nature 360:753-755.

Yang GY, Gong C, Qin Z, Ye W, Mao Y, Bertz AL (1998) Inhibition of TNFalpha attenuates infarct volume and ICAM-1 expression in ischemic mouse brain. Neuroreport 9:2131-2134.

Yang L, Zhang FX, Huang F, Lu YJ, Li GD, Bao L, Xiao HS, Zhang X (2004) Peripheral nerve injury induces trans-synaptic modification of channels, receptors and signal pathways in rat dorsal spinal cord. Eur J Neurosci 19:871-883.

Yu XY, Song YH, Geng YJ, Lin QX, Shan ZX, Lin SG, Li Y (2008) Glucose induces apoptosis of cardiomyocytes via microRNA-1 and IGF-1. Biochem Biophys Res Commun 376:548-552.

Yunta M, Nieto-Diaz M, Esteban FJ, Caballero-Lopez M, Navarro-Ruiz R, Reigada D, Pita-Thomas DW, del Aguila A, Munoz-Galdeano T, Maza RM (2012) MicroRNA dysregulation in the spinal cord following traumatic injury. PLoS One 7:e34534.

Zaheer A, Yorek MA, Lim R (2001) Effects of glia maturation factor overexpression in primary astrocytes on MAP kinase activation, transcription factor activation, and neurotrophin secretion. Neurochem Res 26:1293-1299.

Zamore PD, Haley B (2005) Ribo-gnome: the big world of small RNAs. Science 309:1519-1524.

Zeng Y, Sankala H, Zhang X, Graves PR (2008) Phosphorylation of Argonaute 2 at serine-387 facilitates its localization to processing bodies. Biochem J 413:429-436.

Zhang X, Luhrs KJ, Ryff KA, Malik WT, Driscoll MJ, Culver B (2009) Suppression of nuclear factor kappa B ameliorates astrogliosis but not amyloid burden in APPswe/PS1dE9 mice. Neuroscience 161:53-58.

Zhu Y, Roth-Eichhorn S, Braun N, Culmsee C, Rami A, Krieglstein J (2000) The expression of transforming growth factor-beta1 (TGF-beta1) in hippocampal neurons: a temporary upregulated protein level after transient forebrain ischemia in the rat. Brain Res 866:286-298.

Ziebell JM, Morganti-Kossmann MC (2010) Involvement of pro- and anti-inflammatory cytokines and chemokines in the pathophysiology of traumatic brain injury. Neurotherapeutics 7:22-30.